

**A COMPUTATIONAL STUDY ON THE
STRUCTURES OF PROTONATED PEPTIDES**

**A Thesis Submitted to
the Graduate School of Engineering and Science of
İzmir Institute of Technology
in Partial Fulfillment of the Requirements for the Degree of**

DOCTOR OF PHILOSOPHY

in Chemistry

**by
Sıla KARACA**

**July 2014
İZMİR**

We approve the thesis of **Sıla KARACA**

Examining Committee Members:

Prof.Dr. Ersin YURTSEVER
Department of Chemistry, Koç University

Prof.Dr. Talat YALÇIN
Department of Chemistry, İzmir Institute of Technology

Prof.Dr. Nuran ELMACI IRMAK
Department of Chemistry, İzmir Institute of Technology

Assoc.Prof.Dr. Armağan KINAL
Department of Chemistry, Ege University

Prof.Dr. Levent ARTOK
Department of Chemistry, İzmir Institute of Technology

14 July 2014

Prof.Dr. Nuran ELMACI IRMAK
Supervisor, Department of Chemistry
İzmir Institute of Technology

Prof.Dr. Ahmet Emin EROĞLU
Head of the Department of Chemistry

Prof.Dr. R. Tuğrul SENGER
Dean of the Graduate School of
Engineering and Sciences

ACKNOWLEDGEMENT

First of all, I would like to express my deepest gratitude to my advisor Prof.Dr. Nuran Elmaci for her guidance, motivation and understanding. I have learned so many things from her both in academic and a personal life for ten years. I thank for everthing.

I would also like to special thanks to Prof.Dr. Talat Yalçın for his contributions, useful suggestions, and constructive comments on my thesis study and also thanks for helping me to understand the experimental part of this study.

I am also sincerely grateful to my thesis progressing committee member Prof. Dr. Ersin Yurtsever for his productive discussions and constructive advices. I also thank my defense committee members Prof.Dr. Levent Artok and Assoc.Prof.Dr. Armağan Kınal. Also I thank Seckin Boz for the molecular dynamic calculations. And I thank to Deniz Akkoç for writing the program to analyses the results easily.

I would like to express my special thanks to Ahmet Emin Atik for helping and give his best suggestions for this study. Also I thank my friends, İbrahim Karaman, Çağdaş Taşoğlu, Melda Güray and Özge Görgün.

I would like to thank State Planning Organization (DPT) for the funding of Biological Mass Spectrometry and Proteomics Facility located at chemistry department at İzmir Institute of Technology.

For financial support, I am pleased to acknowledge the Scientific and Technological Research Council of Turkey (TÜBİTAK) for research project (project no: 111T935). And also thanks to TUBITAK ULAKBİM, High Performance and Grid Computing Center (TRUBA Resources) for the numerical calculations reported in this work.

I would also like to thank my lovely family Arife Karaca, Aysel Çermikli, Gönül Karaca Ucer and Necmir Ucer for supporting and encouraging me throughout all my life.

Finally, and most importantly, I would like to special thanks to my wife Şenay Yalçın Karaca for her love, support, understanding and patience. Lastly, very special thanks go to my lovely son Aras Toprak Karaca.

ABSTRACT

A COMPUTATIONAL STUDY ON THE STRUCTURES OF PROTONATED PEPTIDES

The reliable protein identification can be achieved by the knowledge of the structures and fragmentation mechanisms of gas-phase peptide fragment ions. Depending on the size and variety of amino acids in the peptide sequence, the probable structures of *b*-type fragments have been proposed as an acylium, a diketopiperazine, and an oxazolone structures. Recently, a macrocyclic structure has also been reported in the literature for larger *b* ions (b_4 and greater). The macrocyclic structure is one of the problems for determining the correct sequence of peptides because original primary peptide structure is lost. Another problem is the unclear structure of the fragment ions depending on the peptide size and type. In such cases, the databases which are used with the MS/MS results will be insufficient to identify peptide/protein.

In this thesis, the structures of peptide b_n^+ ions having different size and type with a sequence of XAAAA, AAXAA and AAAAX (where A is Ala and X is Asn, Asp, Leu, Phe, Tyr or Cys) have been analyzed by using computational methods. The results showed that, the macrocyclic structure is more favorable than linear oxazolone structure for all b_5^+ ions studied in this work. The proton prefers to be on the oxygen atoms in the macrocycle while it likes to be on the nitrogen atom for the corresponding linear isomer. However, histidine containing b_5^+ ions do not obey this observation, for those, proton always is found on the nitrogen on the side chain of histidine. There is no significant position effect of amino acid residue for those b_5^+ ions, the energies of the most of the linear isomers with different position are very similar.

Additionally, the proton affinity calculations have also been carried out to explain intensities of PX (where P is Pro and X is Ala, Phe, Asp, Trp or His) and AAAA fragment ions in the mass spectra. The results demonstrated that the mass spectrum consist of both PX and AAAA fragments were in competition with each other, this is explained by the proton affinity calculations.

ÖZET

PROTONLANMIŞ PEPTİTLERİN YAPILARI ÜZERİNE HESAPSAL BİR ÇALIŞMA

Güvenilir protein tanımlanması gaz-fazı peptit iyonlarının yapılarının ve parçalanma mekanizmalarının bilinmesi ile elde edilir. Peptit dizilimindeki amino asitlerin çeşitliliğine ve peptitin boyutuna bağlı olarak b iyonlarının muhtemel yapısı asilyum, diketopeparazin ve okzazon olarak önerilmiştir. Son yıllarda büyük b iyonları (b_4 ve büyük b iyonları) için makrohalkalı yapı da rapor edilmiştir. Makrohalkalı yapı, peptitlerin doğru dizilimlerinin bulunmasında sorunlardan biridir, çünkü başlangıç peptit sekansı kaybolmaktadır. Diğer problem ise, peptitlerin çeşidine ve büyüklüğüne göre parçalanma iyonlarının yapılarının bilinmemesidir. Bu gibi durumlarda, MS/MS sonuçları ile kullanılan veritabanları peptit/proteinlerin tanımlanmasında yetersiz kalmaktadır.

Bu tezde, farklı boyutlardaki ve çeşitli amino asit içeren XAAAA, AAXAA, AAAAX (A harfi Ala ve X harfi ise Asn, Asp, Leu, Phe, Tyr veya Cys) peptitlerin b_n^+ iyonlarının yapıları, hesaplamalı metotlar kullanılarak analiz edilmiştir. Sonuçlar göstermektedir ki, bu çalışmadaki tüm b_5^+ iyonları için makrohalkalı yapı lineer okzazon yapısına göre daha çok tercih edilen bir yapıdır. Proton makrohalkada oksijen atomunu tercih ederken, lineer izomerde ise azot atomu üzerindedir. Fakat, histidin içeren b_5^+ iyonları bu gözlemi desteklememektedir, proton her zaman histidinin yan zincirindeki azot atomuna bağlıdır. b_5^+ iyonları için aminoasitlerin pozisyon etkileri kayda değer olmadığı gözlemlendi ve çoğu pozisyonu farklı amino asit bulunan lineer izomerlerin enerjileri birbirlerine çok yakındır.

Ek olarak, kütle spektrumundaki PX (P harfi Pro ve X harfi ise Ala, Phe, Asp, Trp veya His) ve AAAA iyonlarının şiddetlerini açıklayabilmek için proton ilgisi hesaplamaları yapılmıştır. Sonuçlar göstermektedir ki, PX ve AAAA iyonlarını içeren kütle spektrumunda iyon şiddetleri yarış halindedir ve bu durum proton ilgisi hesaplamaları ile açıklanabilmektedir.

TABLE OF CONTENTS

LIST OF FIGURES	ix
LIST OF TABLES.....	xii
CHAPTER 1. INTRODUCTION	1
1.1. Proteins and Amino Acids	1
1.2. The Amino Acid Sequence	4
1.3. Mass Spectrometry.....	5
1.4. Nomenclature of the Peptide Fragments.....	7
1.5. Literature Studies	8
1.5.1. b_2 ions	8
1.5.2. b_4 ions and b_5 ions	11
1.6. Aim of the Study.....	14
CHAPTER 2. COMPUTATIONAL METHODS.....	15
2.1. Ab-initio Methods.....	16
2.2. Semi-empirical Methods.....	16
2.3. Density Functional Theory (DFT)	17
2.4. Molecular Mechanics.....	18
2.5. Molecular Dynamics.....	18
2.6. Principal Coordinates Analysis Method	20
2.7. Overview of the Thesis	22
CHAPTER 3. COMPUTATIONAL METHOD VALIDATION.....	23
3.1. The b_2^+ ions.....	23
3.1.1. b_2^+ (Gly-Gly).....	24
3.1.2. b_2^+ (Ala-Ala).....	26
3.1.3. b_2^+ (Ala-Gly).....	27
3.1.4. b_2^+ (His-Ala).....	28
3.1.5. b_2^+ (Ala-His).....	30
3.1.6. Conclusions of the b_2^+ ions.....	31

3.2. The b_4^+ and b_5^+ ions	33
3.2.1. The b_4^+ ions of HAAA, AHAA, AAHA and AAAH	34
3.2.2. The b_5^+ ions of GGGGG	36
3.2.3. The b_5^+ ions of HAAAA, AAHAA, and AAAAH	38
3.2.4. The b_5^+ ions of YAGFL	40
3.2.5. Conclusions of the b_4^+ and b_5^+ ions	41
CHAPTER 4. AMINO ACID AND POSITION EFFECT ON THE STRUCTURES OF b_5 IONS.....	42
4.1. Introduction.....	42
4.1.1. Computational Details	43
4.1.2. Mass Spectrometry Details	45
4.2. The b_5^+ ions of NAAAA, AANAA, AAAAN isomers.....	46
4.3. The b_5^+ ions of DAAAA, AADAA, AAAAD isomers.....	52
4.4. The b_5^+ ions of LAAAA, AALAA, AAAAL isomers	58
4.5. The b_5^+ ions of FAAAA, AAFAA, AAAAF isomers.....	63
4.6. The b_5^+ ions of YAAAA, AAYAA, AAAAY isomers.....	66
4.7. The b_5^+ ions of CAAAA, AACAA, AAAAC isomers	69
4.8. The Conformational Analyses of the b_5 ions	72
4.9. The Geometry and Charge Analyses of the most favorable b_5 ions	74
CHAPTER 5. The b_5 and b_7 of HISTIDINE CONTAINING PEPTIDES	81
5.1. The b_5^+ ions of HAAAA, AAHAA, AAAAH isomers.....	81
5.2. The b_7^+ ions of HAAAAAA, AAAHAAA, AAAAAAH isomers	85
5.3. Analysis of the b_5^+ and b_7^+ ions of histidine containing peptides	89
CHAPTER 6. EFFECT OF PROTON AFFINITY ON THE FRAGMENTATION REACTIONS OF N-TERMINAL PROLINE CONTAINING HEXAPEPTIDES	90
6.1. Introduction.....	90
6.1.1. Computational Details	92
6.1.2. Mass Spectrometry Details	93
6.2. The b_4^+ ions of AAAA	94
6.3. The b_2^+ ions of PA	95

6.4. The b_2^+ ions of PF	96
6.5. The b_2^+ ions of PD	97
6.6. The b_2^+ ions of PW	98
6.7. The b_2^+ ions of PH	99
6.8. The Conformational Analysis of the b_2 ions of PX	101
6.9. Proton Affinities of the b ions.....	101
CHAPTER 7. CONCLUSION.....	106
REFERENCES	108

LIST OF FIGURES

<u>Figure</u>	<u>Page</u>
Figure 1.1. The general structure of amino acids	1
Figure 1.2. Twenty different amino acids commonly found in proteins	2
Figure 1.3 Formation of a peptide	3
Figure 1.4. Schematic representation of peptide chain	4
Figure 1.5. Main components of a mass spectrometer	5
Figure 1.6. The nomenclature of peptide fragment ions	7
Figure 1.7. The main possible structures of b_2^+ ions	8
Figure 1.8. Cyclization pathway of b_5^+ ion [12]	11
Figure 1.9. Comparison of CID mass spectra of b_5^+ ions derived from permuted isomers of YAGFL-NH ₂ and cyclo-YAGFL [11].....	12
Figure 2.1. A schematic diagram of a) a low temperature b) a high temperature simulation [29].....	20
Figure 3.1. General neutral structure of b_2 ions of oxazolone and diketopiperazine.....	23
Figure 3.2. The lowest energy structures of b_2^+ ion of GG.....	24
Figure 3.3. The lowest-energy structures of b_2^+ ion of AA	26
Figure 3.4. The lowest energy conformers of b_2^+ ion of AG.....	27
Figure 3.5. The lowest-energy conformers of b_2^+ ion of HA.....	29
Figure 3.6. The lowest-energy conformers of b_2^+ ion of AH.....	30
Figure 3.7. General macrocycle mechanism of the b_5^+ ions	33
Figure 3.8. The structures and energies of b_5^+ ions of GGGGG isomers	38
Figure 3.9. The structures and energies of b_5^+ ions of YAGFL isomers	40
Figure 4.1. The structures of alanine, leucine, asparagine, aspartic acid, phenylalanine, tyrosine and cysteine	42
Figure 4.2. The general structures of linear oxazolone of neutral b_5 ions	44
Figure 4.3. The general structure of macrocycle of neutral b_5 ion	44
Figure 4.4. The macrocyclic structures of oxygen protonated conformers of NA ₄	48
Figure 4.5. The linear structures of nitrogen protonated conformers of NA ₄	49
Figure 4.6. The macrocycle structures of nitrogen protonated conformers of NA ₄	50
Figure 4.7. Comparison of the CID mass spectra of b_5 ions of NAAAAAA-NH ₂ , AANAAAA-NH ₂ , and AAAANAA-NH ₂	51

Figure 4.8. The macrocyclic structures of oxygen protonated conformers of DA ₄	54
Figure 4.9. The linear structures of nitrogen protonated conformers of DA ₄	55
Figure 4.10. The macrocycle structures of nitrogen protonated conformers of DA ₄	56
Figure 4.11. Comparison of the CID mass spectra of <i>b</i> ₅ ions of DAAAAAA-NH ₂ , AADAAAA-NH ₂ and AAAADAA-NH ₂	57
Figure 4.12. The macrocyclic structures of oxygen protonated conformers of LA ₄	60
Figure 4.13. The linear structures of nitrogen protonated conformers of LA ₄	61
Figure 4.14. The macrocycle structures of nitrogen protonated conformers of LA ₄	62
Figure 4.15. The macro-cyclic structures of oxygen protonated conformers of FA ₄	64
Figure 4.16. The linear structures of nitrogen protonated conformers of FA ₄	65
Figure 4.17. The macrocyclic structures of oxygen protonated conformers of YA ₄	67
Figure 4.18. The linear structures of nitrogen protonated conformers of YA ₄	68
Figure 4.19. The macrocyclic structures of oxygen protonated conformers of CA ₄	70
Figure 4.20. The linear structures of nitrogen protonated conformers of CA ₄	71
Figure 4.21. Relative Energy (E+ZPE) of protonated oxygen macrocycle and linear of <i>b</i> ₅ ⁺ ions	72
Figure 4.22. The general structure of macrocycle of neutral <i>b</i> ₅ ions.....	74
Figure 4.23. The average bond lengths (Å) of the macrocycle isomers	75
Figure 4.24. The most stable structures of the <i>b</i> ₅ ⁺ ions	77
Figure 4.25. The general structure of the proton cycle.....	78
Figure 4.26. The NBO charged with color of the proton cycles of <i>b</i> ₅ ⁺ ions	80
Figure 5.1. The macrocyclic structures of oxygen protonated conformers of HA ₄	83
Figure 5.2. The linear structures of nitrogen protonated conformers of HA ₄	84
Figure 5.3. The macro-cyclic structures of oxygen protonated conformers of HA ₆	87
Figure 5.4. The linear structures of nitrogen protonated conformers of HA ₆	88
Figure 5.5. The relative ZPE corrected energies of the linear protonated <i>b</i> ₅ ⁺ and <i>b</i> ₇ ⁺ histidine isomers	89
Figure 6.1. The neutral oxazolone and diketopiperazine structures of the <i>b</i> ₂ ions of PX.....	92
Figure 6.2. The structures of proline, alanine, phenylalanine, aspartic acid, tryptophan and histidine.....	93
Figure 6.3. The favorable conformers of <i>b</i> ₄ ion of AAAA.....	94
Figure 6.4. The favorable conformers of <i>b</i> ₂ ion of PA	95
Figure 6.5. The favorable conformers of <i>b</i> ₂ ion of PF	96

Figure 6.6. The favorable conformers of b_2 ion of PD	97
Figure 6.7. The favorable conformers of b_2 ion of PW	98
Figure 6.8. The favorable conformers of b_2 ion of PH	99
Figure 6.9. The calculated DFT proton affinities of diketopiperazine and oxazolone structures of b_2^+ ions of PX	102
Figure 6.10. The experimental proton affinity of single amino acids and calculated DFT proton affinity b_2^+ ions of PX	103
Figure 6.11. Comparison of the CID mass spectra of b_6 ions of PXAAAA-NH ₂	104
Figure 6.12. CID mass spectra of peak intensities ratio ($\ln (PX/AAAA)$) vs the calculated proton affinities of the PX ions	105

LIST OF TABLES

<u>Table</u>	<u>Page</u>
Table 1.1. Abbreviations for amino acids.....	3
Table 3.1. The ZPE corrected energies of b_2^+ ion of GG	24
Table 3.2. Energy difference diketo_op and oxa_np of GG with different level of theory	25
Table 3.3. The ZPE corrected energies of b_2^+ ions of AA.....	26
Table 3.4. Energy difference diketo_op and oxa_np of AA with different level of theory	27
Table 3.5. Relative enthalpy and free energy changes (in kj/mol) of the lowest energy conformers of b_2 ions of AG.....	28
Table 3.6. Relative enthalpy and free energy changes (in kj/mol) of the lowest energy conformers of b_2 ions of HA.....	29
Table 3.7. Relative enthalpy and free energy changes (in kj/mol) of the lowest energy conformers of b_2 ions of AH.....	30
Table 3.8. The relative energy, enthalpy and gibbs energy differences (in kcal/mol) between oxazolone and diketopiperazine structures of the GG, AA, AG, HA and AH.....	32
Table 3.9. The energies of b_4^+ ions of HA_3 isomers	35
Table 3.10. The 10 lowest energy conformers of b_5^+ fragment of GGGGG isomers at the DFT/B3LYP/6-31+G(d,p) level of theory.....	37
Table 3.11. The energies of b_5^+ ions of HA_4 isomers	39
Table 4.1. Nomenclature of Protonated Conformers.....	45
Table 4.2. The electronic (E) and ZPE corrected energies of b_5^+ ions of NA_4	47
Table 4.3. The electronic (E) and ZPE corrected energies of b_5^+ ions of DA_4	52
Table 4.4. The electronic (E) and ZPE corrected energies of b_5^+ ions of LA_4	58
Table 4.5. The electronic (E) and ZPE corrected energies of b_5^+ ions of FA_4	63
Table 4.6. The electronic (E) and ZPE corrected energies of b_5^+ ions of YA_4	66
Table 4.7. The electronic (E) and ZPE corrected energies of b_5^+ ions of CA_4	69
Table 4.8. The bond lengths (in Å) of protonated b_5^+ ions	74
Table 4.9. The NBO charges of the b_5^+ ions.....	76
Table 4.10. The bond lengths (in Å) and angles of the proton cycles of b_5^+ ions	78

Table 4.11. The NBO charges of the proton cycles of b_5^+ ions	79
Table 5.1. The electronic (E) and ZPE corrected energies of b_5^+ ions of HA_4	82
Table 5.2. The electronic (E) and ZPE corrected energies of b_5^+ ions of HA_6	85
Table 6.1 Proton affinity of the natural amino acids	91
Table 6.2. The energies and zero point corrected energies (E+ZPE) of b ions of AAA, AAAA and PX	100
Table 6.3. The DFT proton affinities of the diketopiperazine and oxazolone structures of b_2^+ ions of PX.....	102

*Dedicated to;
my lovely son Aras Toprak KARACA*

CHAPTER 1

INTRODUCTION

1.1. Proteins and Amino Acids

Proteins are biological macromolecules which have diverse functions in living cells. Up to date more than 100,000 different proteins have been determined. They are responsible for the structure and the function of the cells such as enzymatic catalyst, transport of the molecules, cell responses, protection and defense, source of energy etc. [1].

In a general point of view, the proteins are the long chains of polymers composed of amino acids. Amino acids are building blocks of proteins and composed of a central carbon atom (α -carbon), a hydrogen atom, an amine group ($-\text{NH}_2$), a carboxyl group ($-\text{COOH}$) and a side-chain, R. (Figure 1.1).

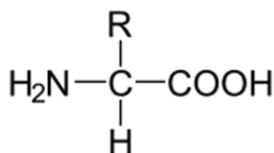


Figure 1.1. The general structure of amino acids

The side chains of the amino acids, which have designated with R, reflects different sizes, shapes, hydrogen bonding capabilities, charge distributions. These properties enable proteins to have a unique chemical and physical property. There are 20 different natural amino acids commonly found in proteins and their structures are displayed in Figure 1.2.

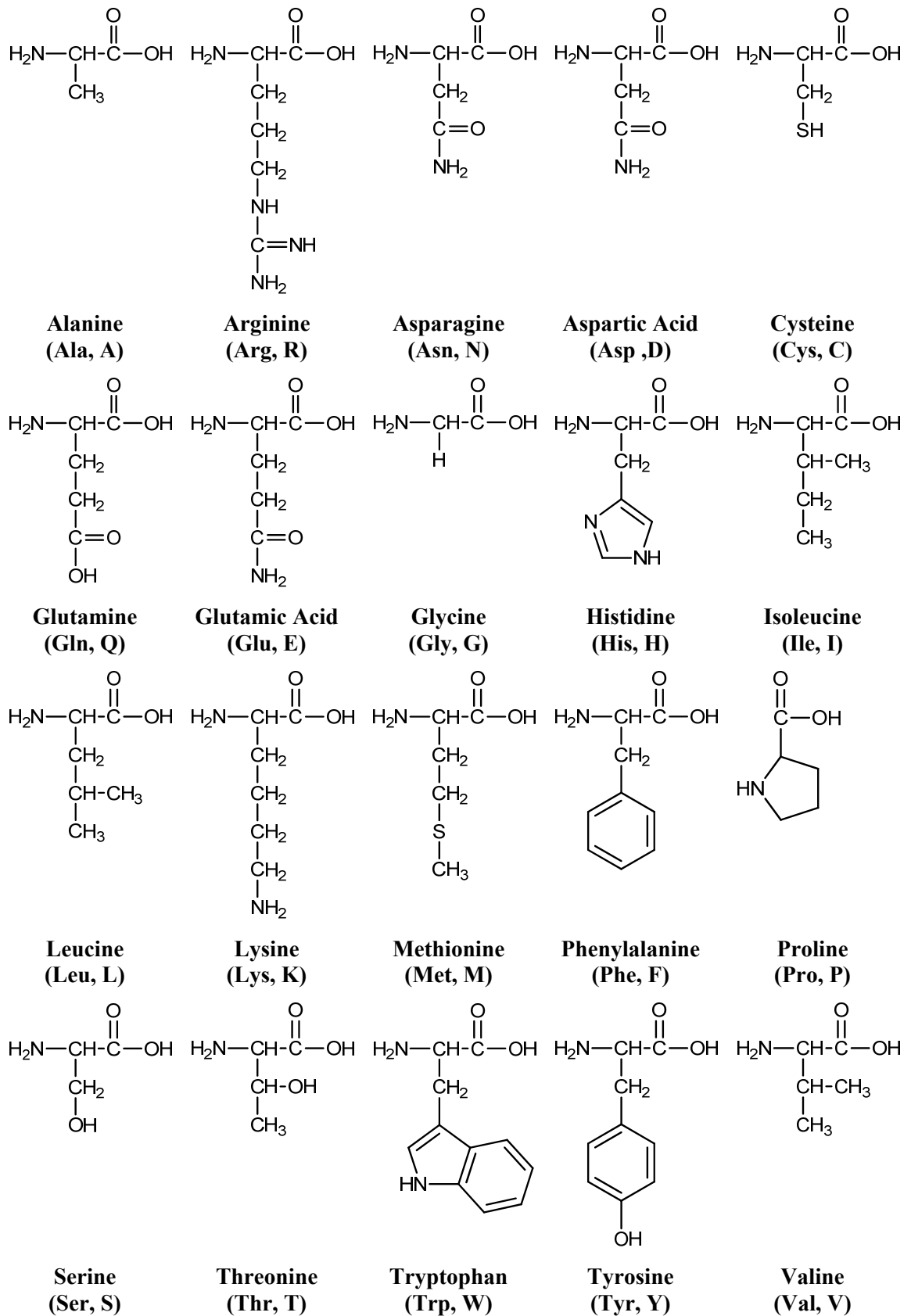


Figure 1.2. Twenty different amino acids commonly found in proteins

Each amino acid residue is demonstrated by either three or one-letter codes, and presented in (Table 1.1).

Table 1.1. Abbreviations for amino acids

Amino acid	Three-letter abbreviation	One-letter abbreviation
Alanine	Ala	A
Arginine	Arg	R
Asparagine	Asn	N
Aspartic Acid	Asp	D
Cysteine	Cys	C
Glutamine	Gln	Q
Glutamic Acid	Glu	E
Glycine	Gly	G
Histidine	His	H
Isoleucine	Ile	I
Leucine	Leu	L
Lysine	Lys	K
Methionine	Met	M
Phenylalanine	Phe	F
Proline	Pro	P
Serine	Ser	S
Threonine	Thr	T
Tryptophan	Trp	W
Tyrosine	Tyr	Y
Valine	Val	V

Amino acids are linked to each other with the carboxyl group of the one amino acid to the amine group of other amino acid by an amide bonds. During linkage, dehydration reaction occurs and water molecule is released (Figure 1.3).

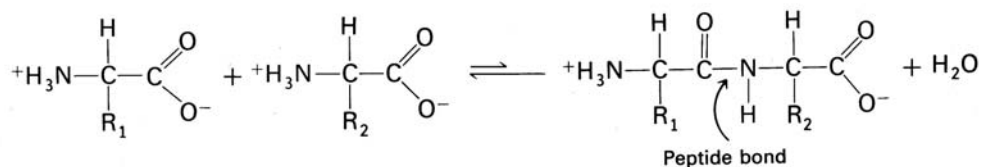


Figure 1.3 Formation of a peptide

There are two ends in the peptide chain length. One of them is the amino group (-NH₂) which is called N-terminal, while the other end is the carboxyl group (-COOH), referred to C-terminal (Figure 1.4). A peptide consists of two or more amino acid

residues which are joined with a covalent bond (30-40 amino acids) to form polypeptide chains. Proteins contain more than one polypeptide (50-2,000 amino acids). Generally, the molecular weights of proteins are between 5,500 and 220,000 amu (1 atomic mass unit (amu) equals to the 1 Dalton (D) [2].

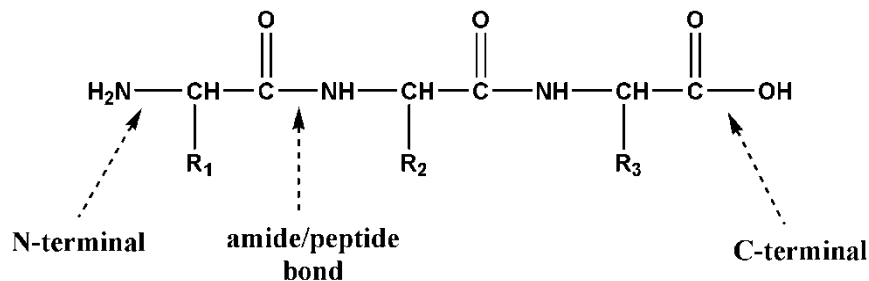


Figure 1.4. Schematic representation of peptide chain

1.2. The Amino Acid Sequence

The sequence of the amino acids can be determined from the primary structure of the protein and the sequence determines functions of proteins. Therefore, the elucidation of amino acid sequence of proteins is essential to describe its biological activities. The first amino acid sequence has been found (insulin, a protein hormone) by Frederick Sanger in 1953. With this study, he demonstrated that the protein has specific amino acid sequence. This result is turning point in the biochemistry [2]. The structure of protein is divided into four categories and these structures are well defined in the following

- **Primary Structure:** It is the linear amino acid sequence of the protein.
- **Secondary Structure:** It represents the formation of repeated structural patterns (e.g. α -helix, β -sheet) mediated by local folding of the amino acid chain.
- **Tertiary Structure:** It shows the three-dimensional structure due to the folding of whole protein.
- **Quaternary Structure:** It refers the interactions of two or more polypeptide subunits to form a larger protein complex in space.

The protein sequencing had been previously accomplished with the Edman degradation method but this technique has its own troublesome. After 1990, with the

development of soft ionization techniques such as; fast-atom bombardment (FAB), electrospray ionization (ESI), matrix-assisted laser-desorption ionization (MALDI), the determination of the molecular masses as well as the sequence of peptides and proteins by mass spectrometry became routine [3]. In order to elucidate the peptide sequence, the tandem mass spectrometry (MS/MS) coupled with collision induced dissociation (CID) has become widely applicable technique to peptide/protein sequencing.

1.3. Mass Spectrometry

Mass spectrometry (MS) is an analytical instrument which measures the mass-to-charge ratio (m/z) of the components in the sample. It has been widely used in chemistry, biology, material science, physics, nuclear science etc. to detect unknown compounds, to clarify the structure and chemical properties of the compounds since 1900s. It is a powerful technique because of its ultrahigh detection sensitivity, short detection time, very low detection limit (about 10^{-12} g), practicable all elements and all kinds of molecules (volatile-nonvolatile, polar-nonpolar, solid-liquid-gas, etc) of the compounds.

The mass spectrometer consist of three components; an ion source, a mass analyzer and a detector (Figure 1.5). These components are operated under high vacuum conditions.

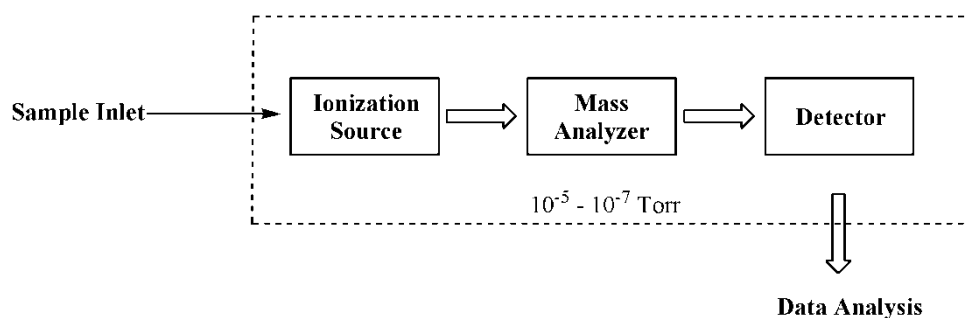


Figure 1.5. Main components of a mass spectrometer

In the ionization source, the analyte molecules are converted into its ions either gaining or losing a proton(s). Ionization techniques are divided into two categories, namely hard ionization and soft ionization. If the analyte molecule is kept intact during the ionization process, this method is called soft ionization. On the contrary, the analyte molecule undergoes extensive fragmentation via ionization with hard ionization

method. Some of the ionization techniques are listed below where only electron impact is classified as a hard ionization and all others can be accepted as soft ionization methods.

- Electron Impact (EI)
- Chemical Ionization (CI)
- Fast Atom Bombardment (FAB)
- Plasma Desorption (PD)
- Field Desorption (FD)
- Electrospray Ionization (ESI)
- Matrix Assisted Laser Desorption ionization (MALDI)

In the mass analyzer, the protonated/deprotonated analyte ions are separated based on their mass-to-charge ratios. An electric or magnetic field is applied to differentiate the ions with different m/z values. The mostly commonly used mass analyzers are:

- Quadrupole (Q)
- Ion-Trap (IT)
- Time-of-Flight (TOF)
- Fourier Transform-Ion Cyclotron Resonance (FT-ICR)

In the detector, the separated ions are collected and converted into a current signal. The commonly used detectors are;

- Faraday Cup
- Electron Multiplier
- Microchannel Plate

1.4. Nomenclature of the Peptide Fragments

The accepted nomenclature for fragment ions was first proposed by Roepstorff and Fohlman and subsequently modified by Biemann [4, 5]. Upon dissociation, if the charge is resided on the N-terminal side, the fragment ions are named as either *a*, *b* or *c*. On the other hand, if the charge is retained on the C-terminal side, the ions are called either *x*, *y* or *z*. A subscript shows the number of residues in the fragment.

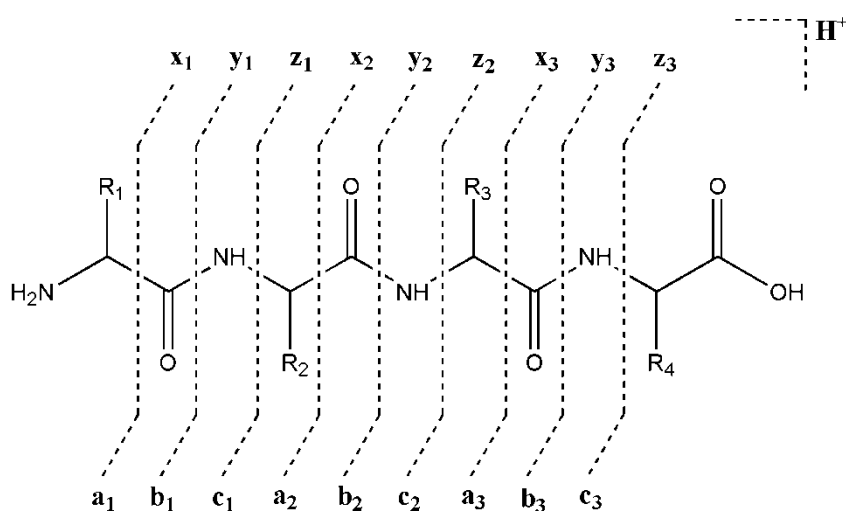


Figure 1.6. The nomenclature of peptide fragment ions

Under low-energy CID conditions, protonated peptides primarily undergo amide bond cleavage to form a series of informative N-terminal *b* and *a* ions and/or C-terminal *y* ions [4, 5]. These sequence ions are used to deduce the primary peptide sequence. The structures of *y* ions have been known to be truncated peptides or protonated C-terminal amino acids [6, 7]. However, considerable effort has been devoted to the understanding the gas-phase structures of *b* ions [7-10]. An acylium ion structure was firstly assigned for *b* ions [4, 5]. However, extensive studies by Harrison and Yalcin showed that the five-membered oxazolone ring structure at the C-terminal end is the most stable for small *b_n* (*n*=2-4) ions [8, 9]. In some cases, a third probable structure was also appeared in the literature, known as diketopiperazine (six-membered ring) by nucleophilic attack of N-terminal nitrogen atom to the carbonyl carbon of the protonated amide bond [7]. Recently, a macrocyclic structure which is another probable structure for *b_n* (*n* ≥ 4) ions were also proposed Harrison and co-workers [11, 12].

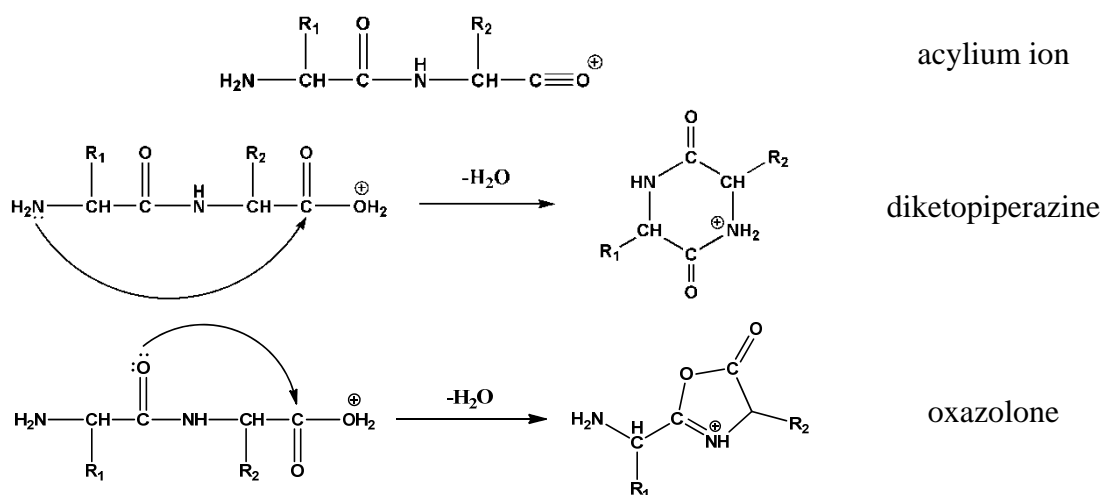


Figure 1.7. The main possible structures of b_2^+ ions

1.5. Literature Studies

In the last two decades, the structure of b ions have been explored by extensive numerous methods namely, tandem mass spectrometry (MS/MS), hydrogen-deuterium exchange (HDX) and infrared-multiphoton dissociation (IRMPD) experiments. In addition, the computational calculations have been performed to support experimental findings and further improvement.

1.5.1. b_2 ions

There are many combined experimental and theoretical studies on protonated peptides in the literature. Wesdemiotis et al. proposed the structure of the b_2 ion of the Ala-Ala was different from the protonated diketopiperazine in 1993 [13]. This observation was also reported for the structure of b_2 ions Gly-Gly [14] and Gly-Pro [15] in 1994.

In a later work, Yalcin et al showed that mass spectra of Leu-Gly and Gly-Leu were different from cyclo-Leu-Gly (diketopiperazine) in 1995 [9]. This work was the first study for the experimental evidence of the oxazolone structure of a b_2 ion. They also showed that the acyclic acylium isomer is 1.49 eV (34.4 kcal/mol) higher energy than the protonated oxazolone structure by theoretical calculations with HF/6-31G** level of theory. Afterward, Paizs et al. supported this observation by finding acylium isomer $HC(O)-NH-CH_2-C(O)^+$ is about 30 kcal/mol higher in energy than the oxazolone isomer (33.3 kcal/mol at the HF and 32.2 kcal/mol at the MP2 level) [10].

Rodriguez et al. investigated the theoretical calculation of the isomers of b_2^+ of Gly-Gly such as protonated oxazolone and diketopiperazine structures [16]. They examined the energies of the structures and detected the preferred sites of protonation. In the calculations, structure optimizations were performed with DFT/B3LYP/6-31++G(d,p) level of theory. According to their results, Nitrogen-protonated oxazolone structure is 12.7 kcal/mol more stable than the Nitrogen-protonated diketopiperazine isomer. On the other hand, Oxygen-protonated diketopiperazine structure is 1.3 kcal/mol more stable than the Nitrogen-protonated oxazolone. This study also showed that protonation site is also important for the structures.

Mostly studies have showed that the b_2^+ fragment of the peptides have the oxazolone structure. On the other hand, O'Hair group have studied both experimentally and theoretically on the different type of peptide b_2^+ ions containing arginine, histidine, lysine, methionine, asparagine, glutamine and serine [17]. They have declared that the b_2^+ fragment of the basic peptides arginine, histidine and lysine side chain structures were thermodynamically more stable than the oxazolone structures. And also O'Hair et al. demonstrated that the b_2^+ ions of HG and GH have the similar spectra of the diketopiperazine structure of GH [18]. The experimental and theoretical calculations were agree with the side-chain protonated diketopiperazine of GH is the most stable one.

Later, the Wysocki group investigated the HA peptide in 2009 [19]. The IRMPD spectra of b_2^+ ion of HAAAA and the protonated cyclic-HA were compared to the calculated IR of the protonated diketopiperazine and oxazolone isomer which were carried out DFT/B3LYP/6-311++G(d,p) level of theory. As a consequence, b_2^+ ion of HA was a mixture of both diketopiperazine and oxazolone structures. This study is the first spectroscopic proof of diketopiperazine and oxazolone isomers of b_2^+ ions are mixtures. And also calculations showed that oxazolone structure is about 85 kJ/mol higher energy than the diketopiperazine.

In an another study, Polfer et al. have studied on the series of Glycine b fragment ions, from b_2 to b_8 to examine the effect of peptide fragment size on the cyclization [20]. At first the input structures were optimized with DFT methods and electrostatic potential were calculated with HF method by Gaussian03. After that, the obtained geometry and charges were imported to AMBER program, and then a conformational search using simulated annealing was done. Finally, the energies of the last structures were calculated with DFT/B3LYP/6-31G+(d,p) level of theory. They

showed that the b_2^+ ion of oxygen-protonated diketopiperazine is 7.6 kJ/mol more stable than the nitrogen-protonated oxazolone structure. However according to comparison of the experimental and theoretical IR spectrum, the spectrum of the Nitrogen-protonated oxazolone is similar to the b_2^+ fragment in spite of its being higher energetic.

Quantum chemical and experimental study of the b_2^+ ion from the protonated tri-alanine was performed by Oomens et al. [21]. They used infrared multiple photon dissociation (IRMPD) spectroscopy to identify the b_2 ions. The experimental IR spectra of b_2^+ fragment of AAAH and cyclo-Ala-Ala were compared and it was concluded that their spectra were different from each other. DFT /B3LYP/6-311+G(d,p) calculations were also performed for determining the structures. They showed that the diketopiperazine structure is 2.36 kcal/mol more stable than the oxazolone and the IRMPD spectra of b_2^+ ion and calculated spectra of nitrogen-protonated oxazolone structure were almost same.

Wysocki et al. have investigated the b_2^+ ions of the AG both experimentally and theoretically [22]. The geometry optimization and frequency calculations have been done at the B3LYP/6-311++G(d,p) level of theory. The IRMPD spectra and quantum chemical calculations indicated that cyclo AG was a diketopiperazine and the b_2^+ fragment of AGG was an oxazolone structure.

Very recently, Paizs and Maitre groups have demonstrated that b_2 fragment from doubly protonated tryptic model peptide YIGSR has ring protonated oxazolone structure illuminated by IRMPD spectra [23]. The quantum chemical calculations showed that oxygen protonated diketopiperazine is more stable than the oxazolone structures by the B3LYP/6-31+G(d,p) level of theory.

In another recent study, Wysocki and co-workers have been studied both experimentally and theoretically to elucidate the b_2 ions structure (diketopiperazine or oxazolone) from histidine analogue containing peptides [24]. They reported that the position of side chain nitrogen atom of the basic amino acid residue is important parameter for diketopiperazine formation. The authors also concluded that the b_2 ion of only KA formed diketopiperazine structure while HA shows a mixture of diketopiperazine and oxazolone structure. The relative energy order of the b_2 ion of KA is diketopiperazine (0.0), oxazolone (77.5 kJ/mol), side chain ring (86.3 kJ/mol) has been found of the B3LYP /6-311++G(d,p) level of theory.

In 2012 the formation of b_2 ion diketopiperazine structure in the presence of arginine residue has been well studied by Polfer et al. [25]. The position of arginine

residue is important for the formation competition between diketopiperazine and oxazolone structures. They demonstrated that Arg-Gly has the oxazolone structure whereas Gly-Arg adopts only diketopiperazine structure with quantum chemical calculations and IRMPD experiments.

1.5.2. b_4 ions and b_5 ions

The spectroscopic (IRMPD) and theoretical (DFT) investigation of the b_4 fragment from the Tyr-Gly-Gly-Phe-Leu (YGGFL) have been explored by Polfer et al.[26]. The IRMPD and B3LYP/6-31+G(d,p) results showed that only oxazolone and cyclic isomers are possible for b_4 ion. The N-terminal protonated oxazolone is 16.9 kJ/mol more stable than the protonated cyclic one.

An experimental and theoretical study of the fragmentation of the b_5 ion derived from protonated H-Tyr-Ala-Gly-Phe-Leu-NH₂ (YAGFL-NH₂) has been published by Harrison et al in 2006 [12]. The total energies and zero-point energies were calculated of B3LYP/6-31+G(d,p) and B3LYP/6-31G(d) levels of theory, respectively. They showed that the cyclization pathway illustrated in Figure 1.8 has a low energy barrier to form cyclic structure. The authors found that the breakdown graph for the b_5 ion and protonated cyclo-YAGFL were almost same. This result was the proof of the cyclization (b-type sequence scrambling) of the b_5 ion.

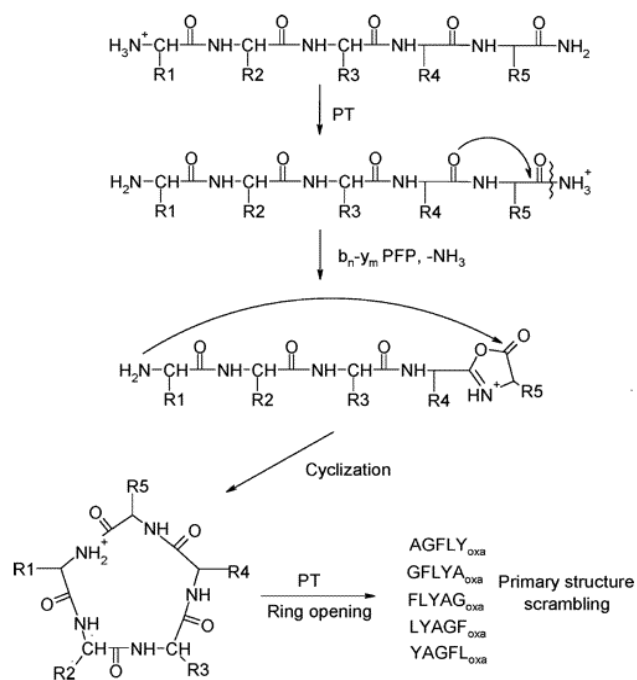


Figure 1.8. Cyclization pathway of b_5^+ ion [12]

Afterwards Harrison, Paizs and co-workers have investigated the fragmentation pathways of b fragments of YAGFL-NH₂, AGFLY-NH₂, GFLYA-NH₂, FLYAG-NH₂, and LYAGF-NH₂ using collision-induced dissociation (CID), the molecular dynamics simulations and DFT calculations [11]. They showed that the b₅ fragments of series of permuted YAGFL isomers and protonated cyclo-YAGFL have essentially identical spectra Figure 1.9. In addition to that the computational results support the cyclization-reopening mechanism. The protonated cyclo-YAGFL isomer is between 6.9 kcal/mol and 9.9 kcal/mol more stable than the linear b₅ isomers (YAGFL_{oxa}, AGFLY_{oxa}, GFLYA_{oxa}, FLYAG_{oxa}, and LYAGF_{oxa}).

The elimination of Tyr (-163 u), Leu (-113 u) and Ala(-71 u) from b₅ ion (m/z 552) can only be explained by cyclization followed by ring-opening process of original YAGFL_{oxa}. Ring opening at the F-L amide bond (to form LYAGF_{oxa}) is not favored when compared to the Y-L, Y-A and A-G amide bonds. For that reason the elimination of Phe (-147 u) from b₅ ion was not detected in the MS/MS spectra. On the otherhand, the cleavage of F-G amide bond (to form FLYAG_{oxa}) is completely inhibited, that is why Gly (-57 u) was not observed in the MS/MS spectra of permuted isomers.

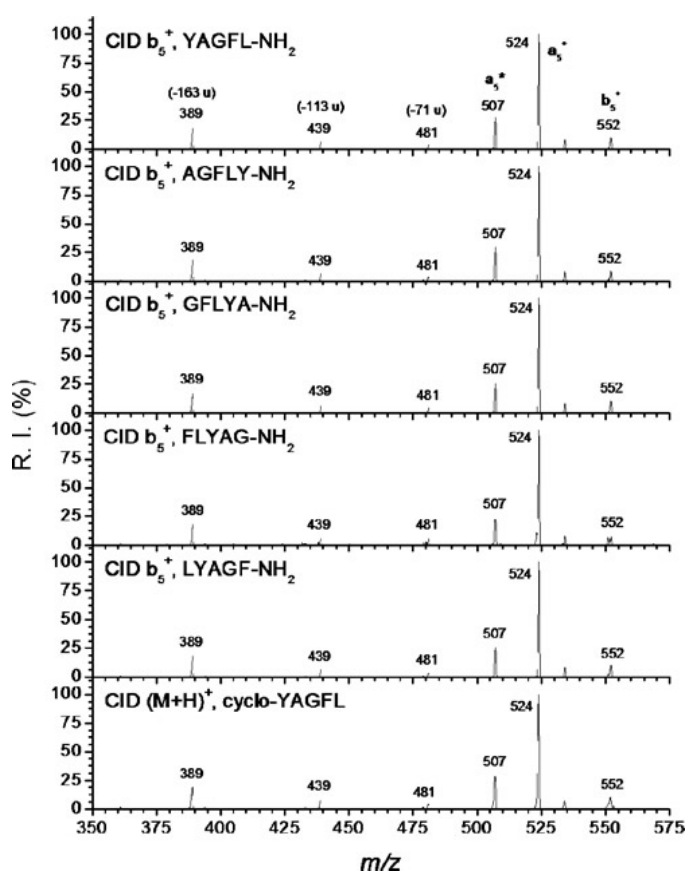


Figure 1.9. Comparison of CID mass spectra of b₅⁺ ions derived from permuted isomers of YAGFL-NH₂ and cyclo-YAGFL [11]

In another study, the b_5 ions of the protonated G_5R have been examined by IRMPD spectroscopy and DFT calculations by Erlekam et al.[27]. The relative energy order (given in kcal/mol) was determined for the macrocyclic isomer in which the protonation at amide oxygen (0.0), oxazolone ring nitrogen (8.9), N-terminal amino oxazolone (12.2) and macrocyclic isomer at amide (13.9) at the DFT/B3LYP/6-31+G(d,p) level of theory. Consequently, the macrocyclic isomer protonated at the amide oxygen is 8.9 kcal/mol is more favorable than the linear oxazolone ring protonated isomer. Furthermore, the theoretical spectra of cyclic peptide is more similar to the experimental spectra than the calculated the oxazolone structures. The results of the experimental and theoretical spectra have showed that the b_5 ion of G_5R has a macrocyclic structure.

The effect of the strongly basic histidine (His) residue on the cyclization of b_n ions using the experimental 'isomeric peptide' method and DFT calculations on the macrocyclic and open b_n structures and their isomerization reactions have been studied by Bythell et al.[28]. If the His residue is close to the N-terminal position, no clear evidence for cyclization. If the His residue gets closer to the C-terminal position sequence scrambling is observed. So the position of the His residue is important for the macro-cyclization of b_5 ions.

1.6. Aim of the Study

The macro-cyclic structure is a problem for determining the amino acid sequence of a peptide. After the formation of the macrocycle, reopening of that ring from different sites is also possible and that cause to lose the sequence data of the original peptide. The databases of software which are used to identify peptide sequence with the MS/MS results will be insufficient. These databases must be improved by the detailed and comprehensive studies of the gas phase fragmentations of protonated peptides. This will lead to get reliable results for the proteomic researches.

The aim of this study is to explore the fragmentation pathways of small peptides. For that purpose, the structures of b_n^+ ions; XAAAA, AAXAA, AAAAX (where A is Ala and X is Asn, Asp, Leu, Phe, Tyr or Cys) have been investigated by using computational chemical methods. The b_5^+ ions which consist of nonpolar Alanine (Ala, A), Leucine (Leu, L), Phenylalanine (Phe, F), polar Tyrosine (Tyr, Y), Cysteine (Cys, C), Asparagine (Asn, N), and acidic Aspartic Acid (Asp, D) have been considered to investigate the the amino acid effect on the production of macrocycles. The effect of proton position and size of ions have also been analyzed. In addition, positional effect of histidine for b_7^+ ion on the macrocycle structure have been studied. Furthermore, the proton affinity calculations have been carried out to explain intensities of PX (where P is Pro, X is Ala; Phe; Asp; Trp or His) and AAAA peaks in the mass spectra.

CHAPTER 2

COMPUTATIONAL METHODS

Computational chemistry is a branch of chemistry; that investigates the chemical structures and generates data by using principle of the physical laws and solving them with mathematical methods by the help of computers. This branch of chemistry spreads rapidly by every passing day as a result of increasing of the computer skills, obtaining the accurate results from computational calculations and also decreasing the expense of the computer prices. Furthermore, almost all branches of science begin to deal with the computational chemistry. Consequently, the collaboration between theory and experiment rises in the researches.

The computational chemistry can calculate and identify the properties of chemical systems such as; molecular structures and energies of ground and excited state, reaction pathways and mechanisms, molecular orbitals, bond lengths and angles, atomic charges, dipole moments, vibrational frequencies and spectroscopic properties etc. Hence, with the help of the computational chemistry, chemical reactions and problems can be understood easily, eliminate the time consuming, providing low cost without the synthesizing new molecules, and obtaining information without doing the experiments.

There are different types of theory in the computational chemistry such as; ab-initio calculations, semi-empirical methods, density functional theory, molecular mechanics and molecular dynamics. The brief explanations of these methods were given in the following sections. The details of these theories can be obtained from the most popular computational chemistry books [29-34].

2.1. Ab-initio Methods

The term ab-initio is Latin, means “from the beginning”. It calculates the properties of a system from first principles with no experimental parameters in their equations. Ab-initio calculations use the laws of quantum mechanics with solving the Schrödinger equation (2.1) for molecules.

$$H\Psi = E\Psi \quad (2.1)$$

where;

E= energy of the system,

Ψ = wavefunction

H=Hamiltonian operator

However, exact solutions of the Schrödinger equation cannot be solved analitically for any atom/molecule except hydrogen atom due to the electron-electron interactions. Thus, mathematical approximations have been done to solve the equation. The common ab-initio calculation is a Hartree-Fock (HF) method. Electron-electron repulsion is taken an average of the repulsion. So, this is the disadvantage of the HF method because of the not including the electron correlation. Some of corrected HF methods are Møller–Plesset perturbation theory (MPn, where n is the order), configuration interaction (CI), coupled cluster theory (CC) etc.[34]. Moreover, these methods need powerful computers and large computational cost. On the other hand, ab-initio calculations give reliable results for the small molecules.

2.2. Semi-empirical Methods

Semi-empirical methods are also depending on the solution of Schrödinger equation as the ab-initio methods. It is computationally less expensive and much faster method than the ab-initio calculation due to the making more approximations. Instead of solving the some integrals, experimental results have been used for the calculations. The results of these methods are mixing between theory and experiment. [32]. And also the core electrons are not used in these calculations. With these methods fewer properties of the molecules can be found and also the results may not reliable [34]. For instance, if

the parameterization is different from the calculated molecule, the results may be incorrect. On the other hand, semi-empirical calculations give accurate results for the many organic molecules. The common semi-empirical methods are AM1, PM3, SAM1, INDO, MNDO, MINDO, ZINDO etc.

2.3. Density Functional Theory (DFT)

Density functional theory (DFT) is based on the solution of Schrödinger equation as ab-initio and semi-empirical calculations. The main difference between DFT and others is; the electron density function (ρ) is used in DFT rather than a wave function. In 1964, Hohenberg and Kohn stated that the ground state electronic energy can be determined by electron density function. After that, the use of DFT in computational chemistry was provided by Kohn and Sham. The electron correlation was included in this method. The electronic energy is defined as [35] ;

$$E = E^T + E^V + E^J + E^{XC} \quad (2.2)$$

where;

E^T = kinetic energy term

E^V = potential energy of nuclear-electron attraction and repulsion of nuclei term

E^J = electron-electron repulsion term

E^{XC} = exchange correlation term

E^{XC} divided to exchange (E^X) correlation and (E^C) parts.

$$E^{XC} = E^X + E^C \quad (2.3)$$

Density functionals were categorized in various sections. One of them is the $X\alpha$, the simplest one, electron exchange term is in the formula, but electron correlation term is not. The other and more complex one is the gradient-corrected methods (such as BLYP, PW91) that use the electron density and its gradient. In addition, hybrid functionals (such as B3LYP, B3P86) are the combination of HF functionals and other

methods Hybrid functionals gives more accurate results than the gradient-corrected methods [34].

DFT computational time is faster than the HF methods with good results. Thus, DFT has been used very popular for the calculations because of the agreement of the experimental results.

2.4. Molecular Mechanics

Molecular Mechanics (MM) is based on the classical physics instead of quantum mechanics. The wave functions or electron density are not used in this method. The energy of the molecules can be described from the bond stretching, bond bending, torsions, van der Waals forces, electrostatic interactions and hydrogen bonding [34]. The energy can be found in the following formula.

$$E = E_{\text{bond}} + E_{\text{angle}} + E_{\text{torsion}} + E_{\text{electrostatic}} + E_{\text{van der Waals}} \quad (2.4)$$

The force fields are used to describe the potential energy of the system. Most of the force fields are needed to parameterize depend on the type of molecules. Generally, parameterization is done from experimental and ab-initio calculations results. Common used force fields are Amber, Charmm, Gromos, MMFF etc.

This method especially is used to conformational analyses. It is also faster than the other methods. And also it is applicable for the very large molecules. On the other hand, this method could not be used for the molecular properties depend on the electronic effects. Moreover, molecular mechanics could not be used to identify the new structures and conformations of molecules outside the range of parameterization.

2.5. Molecular Dynamics

Molecular dynamics (MD) simulation is time-dependent processes to study structural and thermodynamic properties of molecules which based on Newton's second law or the equation of motion. The trajectories of atom and molecules are found out the by numerically solving the Newton's equations.

In the MD, firstly, the forces (F) act on each the atoms (m, mass) after it starts to accelerate (a) and gains velocity (v) then it changes its position (x) in a given time (t) step and they are calculated by using force fields.

In the following formulas, the motion of a particle in one dimension has been considered.

$$F = ma \quad a = \frac{\Delta v}{\Delta t} \quad v = \frac{\Delta x}{\Delta t} \quad (2.5)$$

The initial position (x_1) and velocity (v_1) and final positions (x_2) and velocity (v_2) of the atom then $\Delta x = x_2 - x_1$ and $\Delta v = v_2 - v_1$ [36].

The MD is a deterministic technique. If the positions and velocities of molecules are known, the state of the system can be determined at any time interval in the future or the past.

$$x_2 = x_1 + v_1 \Delta t \quad v_2 = v_1 + a_1 \Delta t = v_1 + \frac{F_1}{m} \Delta t \quad (2.6)$$

Furthermore, the force (F) can be determined by the gradient of the potential energy (V) with respect to the position (x) of atom.

$$F = -\frac{dV}{dx} \quad (2.7)$$

The final velocity can be found out from the potential energy

$$v_2 = v_1 - m^{-1} \frac{dV(x)}{dx} \Delta t \quad (2.8)$$

The following formula expresses the relationship between temperature (T) and velocity (v) of the system (where, k=Boltzmann constant) [36]:

$$\frac{1}{2} m v^2 = \frac{1}{2} k T \quad (2.9)$$

In the conformational analysis in MD, the different molecular conformations can be obtained by changing heat. If the temperature of system is low, the molecules cannot overcome energy barrier so, a few conformers will be obtained by the MD. On the other hand, at the high temperatures, the molecules become more flexible by gaining energy and then they easily overcome the energy barrier. Hence, more conformers will be obtained by MD simulations [29].

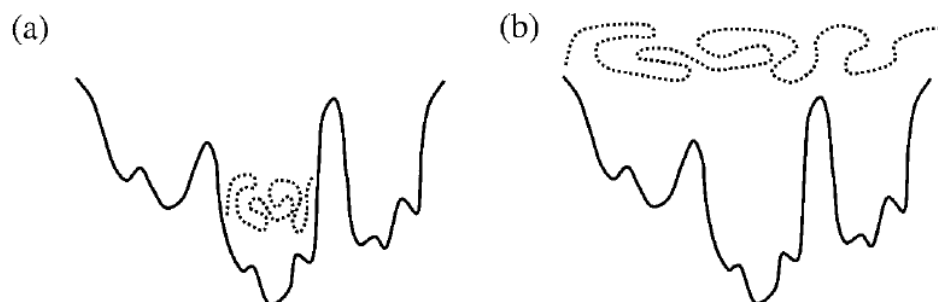


Figure 2.1. A schematic diagram of a) a low temperature b) a high temperature simulation [29]

2.6. Principal Coordinates Analysis Method

The Principal Coordinates Analysis (PCO) is a method to measure dissimilarities of data among the structures [37, 38]. The main purpose of the PCO is to reduce from dimension of the variables which defines the system to a low dimensional system to get rid of the complexity. After that, interested necessary information of system is obtained from low dimension. Since, it is hard to get and analyze information from large number of variables.

In this thesis, the conformational search of the protonated peptides has been done by the molecular dynamic simulations (MD). The approximately 4000 candidates of each protonated peptide type have been obtained. To find out the global minimum structure of the peptides, quantum chemical calculations will be applied to them. However, the numbers of candidate are enormously high to apply the quantum calculations due to the computational time and large data. So, with using PCO, clustering or making group of the 4000 conformers have been done to reduce number of candidate reasonable numbers which is enough to get the lowest stable conformer for the quantum calculations. The dissimilarities of the 4000 conformers have been

determined from conformer coordinates by the PCO and visualized in two-dimensional space. After that, dissimilar 36 conformers have been selected among them which have been used for the quantum calculations.

In this method, firstly the distance matrix between the conformers is calculated [37, 38]. The matrix of $n \times p$ is prepared. (where n (observable) are different conformers and p (variables) are pair distances of two atoms in the conformers)

(where $p = \frac{N(N-1)}{2}$, N is the number of atoms).

The distance matrix, d_{ij} is the measure of dissimilarity between the i^{th} and j^{th} configurations.

$$d_{ij} = \sum_{r=1}^p (X_{ir} - X_{jr})^2 \quad (2.10)$$

where; i and j are configuration indices, r is coordinate index, X are Cartesian coordinates. So, the distance between the conformers is determined.

After that centralized distance matrix is calculated.

- i) Define the A matrix, inter particle distances

$$A = -\frac{d_{ij}}{2} \quad (2.11)$$

- ii) Form the B matrix with Centralized from the A matrix using following formula

$$b_{ij} = a_{ij} - a_i - a_j + a_{..} \quad (2.12)$$

where a_i is the average of the i^{th} row A matrix, a_j is the average of the j^{th} column of A matrix, $a_{..}$ is the average of the whole matrix A. The b_{ij} is calculated to remove averages from the calculations and results.

- iii) The B matrix is diagonalized and the eigenvalues and eigenvectors are computed. The eigenvectors are scaled to make square of magnitude of each eigenvector equal to corresponding eigenvalue.

Moreover, the largest eigenvalue represents the maximum variance of the original set of variables and have the most information about the system. The eigenvector can be named as the 1st dimension, the eigenvector corresponding to the second largest is the 2nd dimension so on [37, 38]. Finally, in this study, the largest two eigenvectors have been taken and plot 2D graph, then selections of the conformers have been done from this graph.

2.7. Overview of the Thesis

In this thesis, the structures of different type, size and sequence of protonated b_n ions of the peptides have been analyzed by using computational methods.

The brief introduction of the amino acids, peptides, mass spectrometry, literature studies and the computational methods were given in Chapter 1 and Chapter 2.

In Chapter 3, the different type of the b_2^+ ions and larger b_4^+ and b_5^+ ions of peptides have been investigated and compared with the literature works for computational method validation.

In Chapter 4, the linear and macro-cyclic structures of b_5^+ ions consist of four nonpolar alanines with one X amino acid residue; XAAAA, AAXAA, AAAAX where X represents asparagine, aspartic acid, leucine, phenylalanine, tyrosine, and cysteine have been studied with the computational chemical methods.

In Chapter 5, the size effect of the histidine containing linear and macrocyclic structure of b_5^+ and b_7^+ ions have been studied and compared according to their energy differences.

In Chapter 6, the proton affinity of proline amino acid containing b_2^+ ions (PX, where P is Pro and X is Ala, Phe, Asp, Trp and His) which have different proton affinity and b_4^+ ions of AAAA have been calculated with the computational methods and compared with the experimental results obtained from mass spectrometer.

All mass spectrometry experiments were carried out in Biological Mass Spectrometry and Proteomics Facility Laboratory at the İzmir Institute of Technology under supervision of Prof.Dr. Talat Yalçın and Dr. A. Emin Atik.

CHAPTER 3

COMPUTATIONAL METHOD VALIDATION

3.1. The b_2^+ ions

In this part the b_2^+ ions of Glycine-Glycine (**GG**), Alanine-Alanine (**AA**), Alanine-Glycine (**AG**), Histidine-Alanine (**HA**) and Alanine-Histidine (**AH**) have been investigated and compared with the literature studies [19-22] for preliminary work to understand better the protonation of the peptides. The oxazolone and diketopiperazine structures (see Figure 3.1) of the b_2^+ ions have been considered since there is an energetic competition between them.

Five to eight (depends on the amino acid type) different protonation site of the b_2^+ fragments have been considered in order to investigate the protonation effect. After that the possible initial conformers of each of the protonated peptides are created by twisting around the rotatable bonds by using the Spartan'10 program [39]. Finally, Density Functional Theory (DFT) calculations were carried out to those conformers via Gaussian09 program [40] with the same level of theory in the literature to see whether initial conformers obtained from Spartan program will lead to find the most important structures for small protonated peptides. The frequency analyses have been performed after optimization calculations to characterize the critical point. All optimized structures presented in this work were true minima. The calculations of Molecular Mechanics and Molecular Dynamic simulations haven't been used due to the small size of b_2^+ ions.

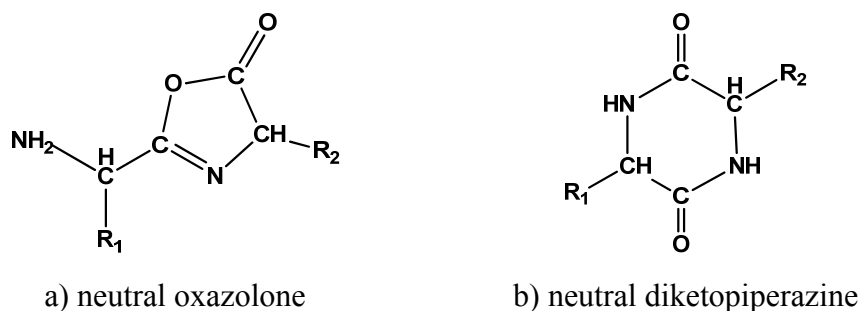


Figure 3.1. General neutral structure of b_2 ions of oxazolone and diketopiperazine

3.1.1. b_2^+ (Gly-Gly)

The six type of protonated b_2^+ of Gly-Gly (GG) structures have been investigated. The oxygen (diketo_op) and nitrogen (diketo_np) protonated diketopiperazine and nitrogen (oxa_np), oxygens (oxa_cop, oxa_op) and N-terminal nitrogen (oxa_nterm_p) of the oxazolone structures have been considered. The 85 conformers have been obtained by twisting around the rotatable bonds. Then the geometry optimizations of the conformers of b_2 (GG) have been carried out with B3LYP 6-31+G(d,p) level of theory. The lowest-energy conformers of each chemical structure of b_2 (GG) were given in Figure 3.2. It has been noticed that, after the optimization some of them has a hydrogen migration, bond or cycle breaking.

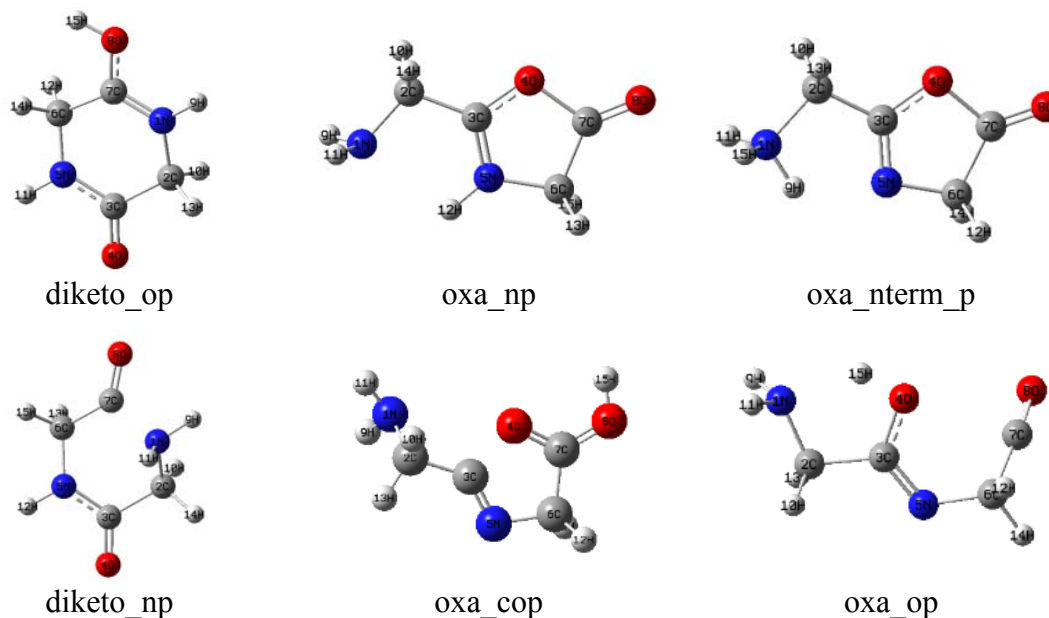


Figure 3.2. The lowest energy structures of b_2^+ ion of GG

Table 3.1. The ZPE corrected energies of b_2^+ ion of GG

Structure	E+ZPE (au) Ref [20]	E+ZPE (au)	Rel. (E+ZPE) (kJ/mol)
diketo_op	-416.238404	-416.25098	0.0
oxa_np	-416.235523	-416.24635	12.1
oxa_nterm_p	-416.226648	-416.23727	36.0
diketo_np	-	-416.22580	66.1
oxa_cop	-	-416.20425	122.7
oxa_op	-	-416.19468	147.8

The relative zero point energy (ZPE) corrected energies of the conformers are given in the ascending order (kJ/mol) in the following. This order also shows how the energies change with the protonation site.

$$E_{\text{diketo_op}} < E_{\text{oxa_np}} < E_{\text{oxa_nterm_p}} < E_{\text{diketo_np}} < E_{\text{oxa_cop}} < E_{\text{oxa_op}}$$

0.0	12.1	36.0	66.1	122.7	147.8
-----	------	------	------	-------	-------

As a result, diketopiperazine-oxygen protonated (diketo_op) was the most stable structure among them (Table 3.1). The oxazolone-N-protonated (oxa_np) is the most favorable structure among the oxazolone isomers. The least stable isomer was the oxazolone-O-protonated one (oxa_cop). According to computational calculations oxa_op structure in which the oxazolone ring opened was highly unfavorable. The calculations produced from this work have lower energy values than the similar calculations present in the literature [20].

Table 3.2. Energy difference diketo_op and oxa_np of GG with different level of theory

$(E_{\text{oxa}}-E_{\text{dik}})$	B3LYP	CAM- B3LYP	MP2
	6-31+G(d,p)	6-31+G(d,p)	6-31+G(d,p)
ΔE_{spe}	15.3	16.4	6.0
ΔE	15.3	16.2	8.1
$\Delta(E+ZPE)$	12.1	13.3	4.2

E_{spe} , single point energy on the b3lyp 6-31+G(d,p) geometry. The values were given in kJ/mol.

Furthermore, calculations with different level of theories were carried out (see Table 3.2). The structures of the conformers are almost the same in all optimization results. MP2 method has the lowest energy difference which is only 1 kcal/mol (4.2 kJ/mol). These theoretical results suggest that the diketopiperazine and oxazolone structures are competing each other. In contrast to computational findings, the oxazolone structure is more favorable than diketopiperazine according to experimental study [20].

3.1.2. b_2^+ (Ala-Ala)

The five type of protonated b_2^+ of Ala-Ala (AA) structures have been studied. Totally 56 conformers have been obtained with the Spartan'10 program and calculated via Gaussian09 with B3LYP/6-311+G(d,p) level of theory. The lowest-energy conformers of each chemical structure of b_2^+ ions of AA in Figure 3.3.

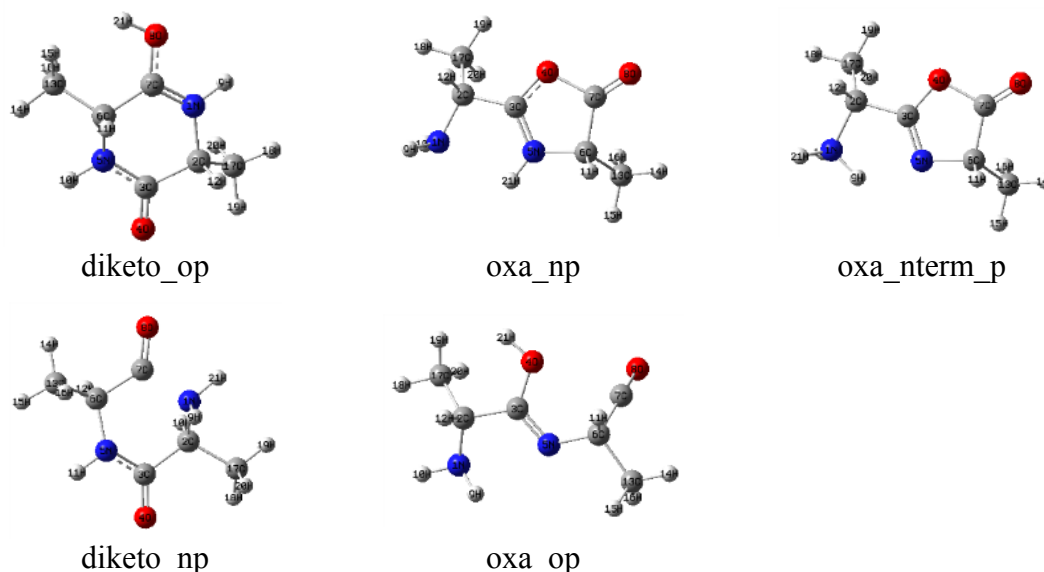


Figure 3.3. The lowest-energy structures of b_2^+ ion of AA

Table 3.3. The ZPE corrected energies of b_2^+ ions of AA

Structure	E+ZPE (au) Ref [21]	E+ZPE (au)	Rel. (E+ZPE) (kJ/mol)
diketo_op	-494.955391	-494.955390	0.0
oxa_np	-494.951624	-494.951590	10.0
oxa_nterm_p	-494.943518	-494.943484	31.3
diketo_np	-494.934565	-494.934565	54.7
oxa_op	-	-494.885358	183.9

The relative ZPE corrected energies of the conformers were given in Table 3.3 in ascending order (kJ/mol). This order also shows the protonation site effect.

$$E_{\text{diketo_op}} < E_{\text{oxa_np}} < E_{\text{oxa_nterm_p}} < E_{\text{diketo_np}} < E_{\text{oxa_op}}$$

$$0.0 \quad 10.0 \quad 31.3 \quad 54.7 \quad 183.9$$

The diketopiperazine-oxygen protonated is more stable than the oxazolone structures. The oxazolone-N-protonated is the most favorable structure among the oxazolone isomers. MP2 calculation reduces the energy difference between diketopiperazine and oxazolone to 1.2 kcal/mol. (Table 3.4).

Table 3.4. Energy difference diketo_op and oxa_np of AA with different level of theory

$(E_{\text{oxa}} - E_{\text{dik}})$	B3LYP	B3LYP	CAM- B3LYP	MP2
	6-311+G(d,p)	6-31+G(d,p)	6-31+G(d,p)	6-31+G(d,p)
ΔE_{spe}	3.2(13.4)	3.2 (13.4)	3.9 (16.3)	1.9 (8.0)
ΔE	3.2(13.3)	3.2 (13.4)	3.9 (16.3)	2.0 (8.5)
$\Delta(E+ZPE)$	2.4(10.0)	2.5 (10.4)	3.2 (13.4)	1.2 (5.1)

E_{spe} , single point energy on the b3lyp 6-31+G(d,p) geometry. No imaginary frequencies. The values are in kcal/mol. The italic values in parenthesis are in kJ/mol.

3.1.3. b_2^+ (Ala-Gly)

The different protonation site of the b_2^+ fragments of diketopiperazine and oxazolone structures of Ala-Gly (AG) have been performed with B3LYP/6-311++G(d,p) level of theory by using Gaussian09. The lowest energy conformers of each chemical structure of b_2^+ ion of AG) were given in Figure 3.4.

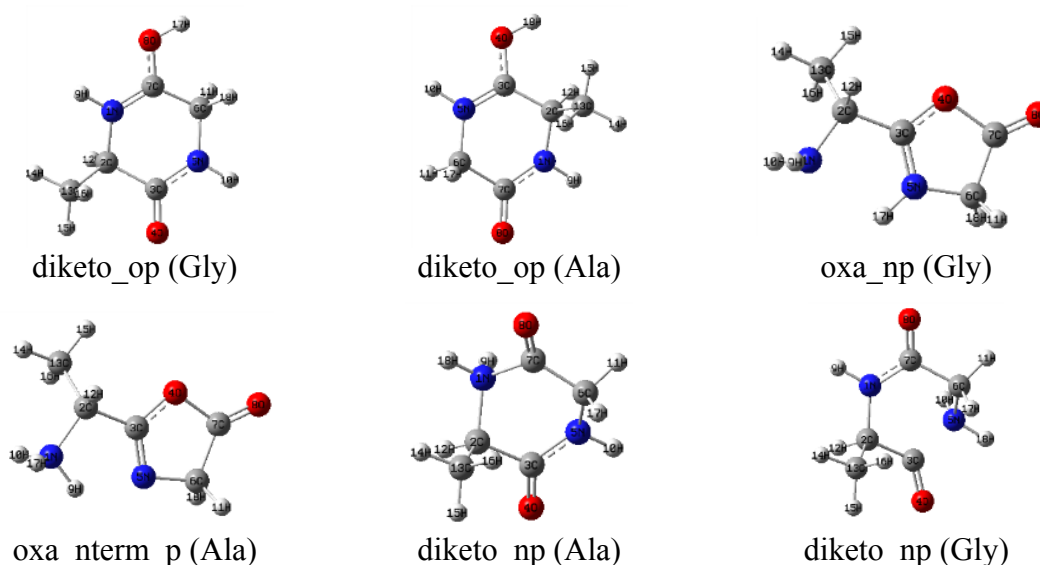


Figure 3.4. The lowest energy conformers of b_2^+ ion of AG

Table 3.5. Relative enthalpy and free energy changes (in kJ/mol) of the lowest energy conformers of b_2 ions of AG.

Structure	Rel. Δ H Ref [22]	Rel. Δ H	Rel. Δ G Ref [22]	Rel. Δ G
diketo_op (Gly)	0.0	0.0	0.0	0.0
diketo_op (Ala)	2.2	2.2	3.1	3.0
oxa_np (Gly)	16.8	16.8	16.7	16.7
oxa_nterm_p (Ala)	31.4	31.4	31.6	31.6
diketo_np (Ala)	56.1	60.6	56.9	62.3
diketo_np (Gly)	63.1	65.4	63.8	66.4

Computational results showed that diketopiperazine oxygen protonated Gly (diketo_op, Gly) and diketopiperazine-oxygen protonated Ala (diketo_op, Ala) was the most stable structures (Table 3.5). The diketopiperazine isomer energetically was more stable than the oxazolone structure by 16.8 kJ/mol. The oxazolone-N-protonated (oxa_np) was the most favorable structure in the oxazolone isomers. The nitrogen protonated diketopiperazine structures (diketo_np, Ala and diketo_np, Gly) are the less favorable ones.

3.1.4. b_2^+ (His-Ala)

The protonated oxygen, nitrogen and nitrogen on the histidine residue of diketopiperazine and oxazolone structures have been considered and calculated with B3LYP/6-311++G(d,p) level of theory. The lowest-energy conformers of each chemical structure of b_2 (His-Ala; HA) were given in Figure 3.5. The 171 conformers have been obtained with the Spartan Program and DFT calculations have been carried out with Gaussian09.

The diketopiperazine-histidine-N-protonated (diketo_his_np) is the most likely structure and the oxazolone-histidine-N-protonated (oxa_his_np) is the most favorable structure in the oxazolone isomers (Table 3.6). The results are almost same with the Ref[19] except diketo_op_ala and diketo_op_his conformers in this calculation. The energy order of these structures were changed in this work, the second most stable structure is the diketo_op_ala instead of oxa_his_np. The hydrogen generally attached or directed to histidine side chain nitrogen atom as result of optimization of conformers, although it was initially bonded to different positions for the most of the conformers.

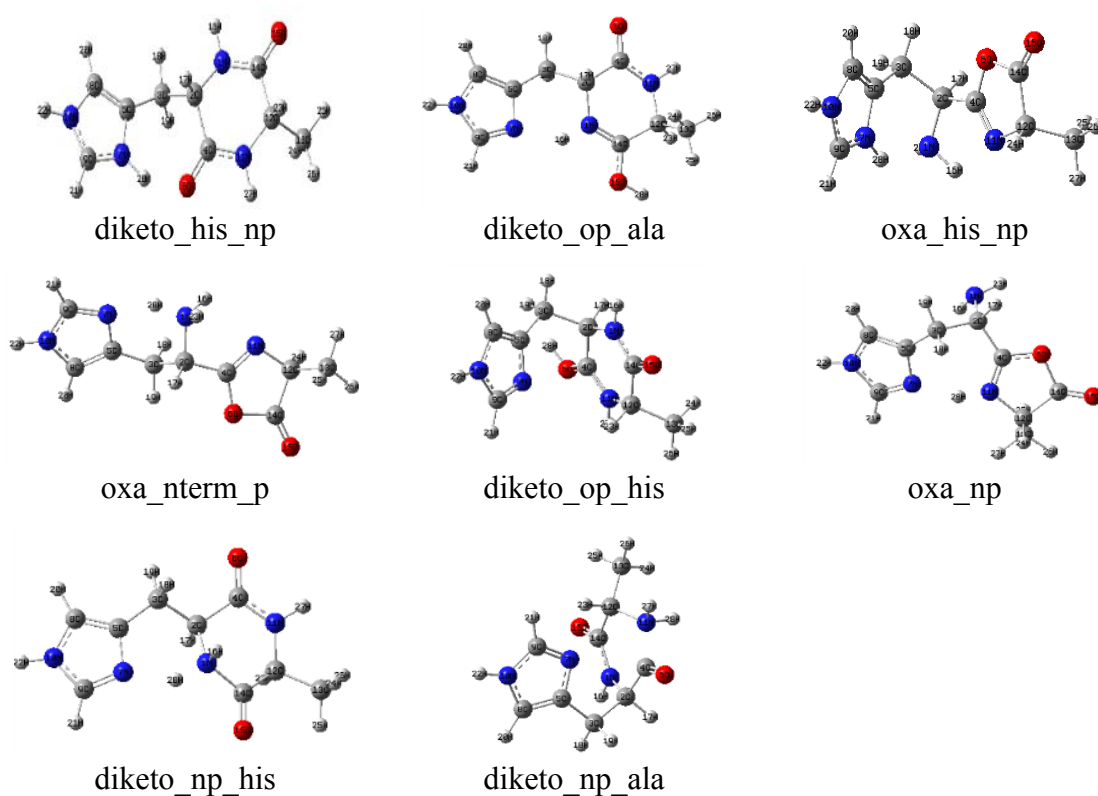


Figure 3.5. The lowest-energy conformers of b_2^+ ion of HA

Table 3.6. Relative enthalpy and free energy changes (in kJ/mol) of the lowest energy conformers of b_2 ions of HA

Structure	Rel. Δ H Ref[19]	Rel. Δ H Ref[19]	Rel. Δ G Ref[19]	Rel. Δ G Ref[19]
diketo_his_np	0.0	0.0	0.0	0.0
diketo_op_ala	100.1	66.1	98	66.2
oxa_his_np	86.2	82.8	85.4	81.7
oxa_nterm_p	87.6	87.6	87.7	86.4
diketo_op_his	124	92.2	119.5	88.8
oxa_np	94.8	93.5	93.7	93.2
diketo_np_his	-	104.5	-	105.3
diketo_np_ala	-	141.1	-	139.8

3.1.5. b_2^+ (Ala-His)

Eight type of protonated diketopiperazine and oxazolone isomers (HA case) have been carried out with B3LYP 6-311++G(d,p) level of theory. The lowest-energy conformers of each chemical structure of b_2 (Ala-His; AH) were given in Figure 3.6. The 171 conformers have been obtained with the Spartan Program and calculated with Gaussian09.

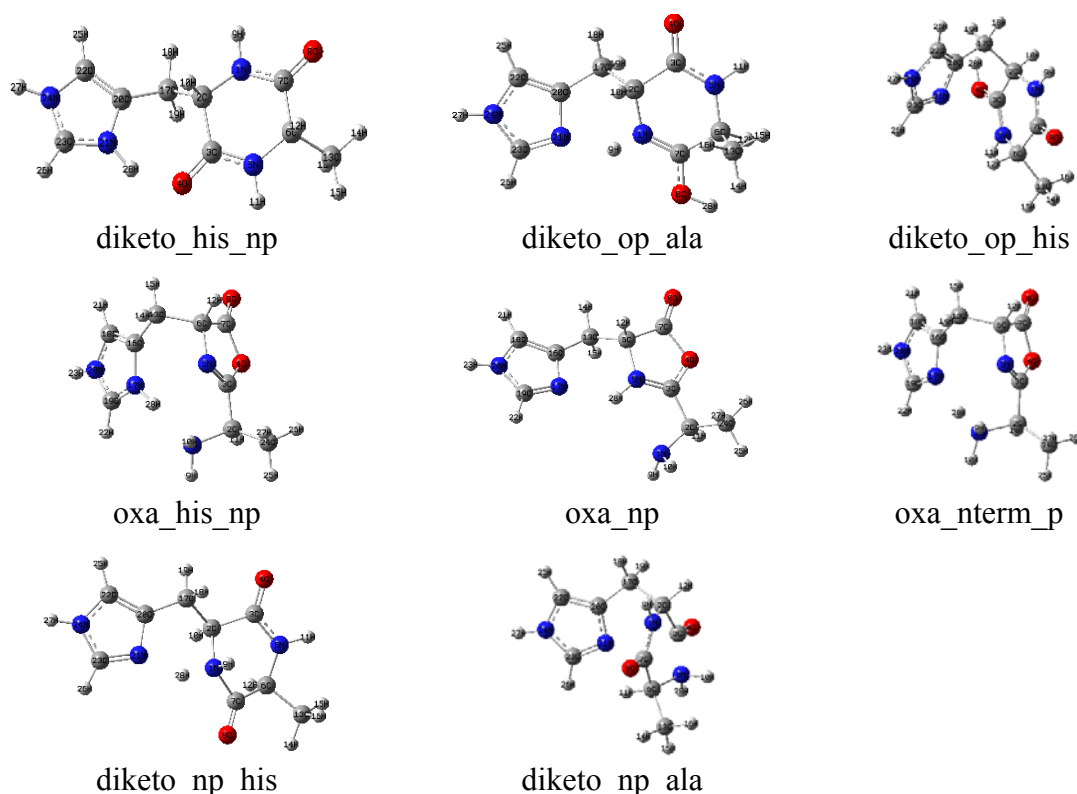


Figure 3.6. The lowest-energy conformers of b_2^+ ion of AH

Table 3.7. Relative enthalpy and free energy changes (in kJ/mol) of the lowest energy conformers of b_2 ions of AH

Structure	Rel.(E+ZPE)	Rel. ΔH	Rel. ΔG
diketo_his_np	0.0	0.0	0.0
diketo_op_ala	65.6	66.1	66.2
diketo_op_his	91.2	92.2	89.1
oxa_his_np	92.5	92.7	94.2
oxa_np	94.5	96.6	92.0
oxa_nterm_p	104.3	104.0	108.0
diketo_np_his	104.2	104.4	105.2
diketo_np_ala	140.1	141.1	139.8

The diketopiperazine-histidine-N-protonated (diketo_his_np) is the most likely structure (HA case) (see Table 3.7). The oxazolone-histidine-N-protonated (oxa_his_np) is the most favorable structure among the oxazolone isomers (HA case).

3.1.6. Conclusions of the b_2^+ ions

The b_2^+ fragment of **GG**, **AA**, **AG**, **HA** and **AH** structures have been investigated and compared with the literature studies [19-22]. The results are matched well with the literature works.

For the dipeptides in this study:

- The protonated diketopiperazine is always favorable than the protonated oxazolone structures. (The energy difference is 2.5-3.9 kcal/mol with DFT/B3LYP method (1.4-2.7 kcal/mol with MP2) for Glycine and Alanine dimers whereas 19.7-22.1 kcal/mol (15.4-16.0 kcal/mol with MP2) for HA and AH). The energies of these two conformers are very close to each other. They must be in competition except b_2^+ ions of HA and AH (Table 3.8).
- The protonated site is very important for the b fragment of the peptides
 - The diketopiperazine-O-protonated is most favorable structure among the diketopiperazine structures for the GG, AA and AG, but for the HA and AH the diketopiperazine-histidine protonated is the most likely one.
 - The oxazolone-N-protonated is the most favorable structure among the oxazolone isomers for the GG, AA and AG, but for the HA and AH the oxazolone-histidine protonated is the most stable one.
- The oxazolone structure is more accessible than the diketopiperazine structure based on experimental data though it is less favorable theoretically [20, 21].
- The calculation of the MP2 method results give the smaller energy difference between oxazolone and the diketopiperazine structure

Table 3.8. The relative energy, enthalpy and gibbs energy differences (in kcal/mol) between oxazolone and diketopiperazine structures of the GG, AA, AG, HA and AH

Peptide	Structure	$E_{\text{oxa}}-E_{\text{dik}}$ Rel.(E+ZPE) ^a	$E_{\text{oxa}}-E_{\text{dik}}$ Rel.(E+E _{Thermal}) ^b	$E_{\text{oxa}}-E_{\text{dik}}$ Rel. (E+H) ^c	$E_{\text{oxa}}-E_{\text{dik}}$ Rel.(E+G) ^d
GG	diketo_o_p oxa_np	2.9 (1.4)	3.0	3.0	3.0
AA	diketo_o_p oxa_np	2.5 (1.9)	2.7	2.7	2.2
AG	diketo_o_p oxa_np	3.9 (2.7)	4.0	4.0	4.0
HA	diketo_his_np oxa_his_np	19.7 (15.4)	19.8	19.8	19.5
AH	diketo_his_np oxa_his_np	22.1 (16.0)	22.2	22.2	22.5

For GG and AA, b3lyp/6-31+g(d,p) was used; For AG,HA and AH, b3lyp/6-311++g(d,p) was used. The values in parenthesis are MP2 6-31+g(d,p) single point energies on the given b3lyp geometry.

^a Relative sum of electronic and zero-point Energies (E+ZPE), ^b Relative sum of electronic and thermal Energies (E+E_{Thermal}), ^c Relative sum of electronic and thermal Enthalpies (E+H), ^d Relative sum of electronic and thermal Free Energies (E+ G)

Finally the procedure that we followed to find important conformers of the dipeptides is valid and gives better energy values than those of some in the literature.

3.2. The b_4^+ and b_5^+ ions

In this part, the b_4^+ and b_5^+ ions have been considered for the larger peptides. Another mechanism, head-to-tail cyclization reaction (macrocyclization) has been proposed [11, 12, 41, 42]. Firstly oxazolone structure is formed at the C-terminal (Figure 3.7). After that, N-terminal amino group is attacked to the carbonyl carbon of the oxazolone structure then the macrocycle structure is obtained in the gas phase. Afterwards, the macrocycle structure is reopened and converted to various oxazolone structures and generated nondirect sequence fragments. As a result, the CID mass spectra of peptide have become complicated. For that reason the databases of peptide search programs which are used with the MS/MS results will be insufficient to identify peptide/protein.

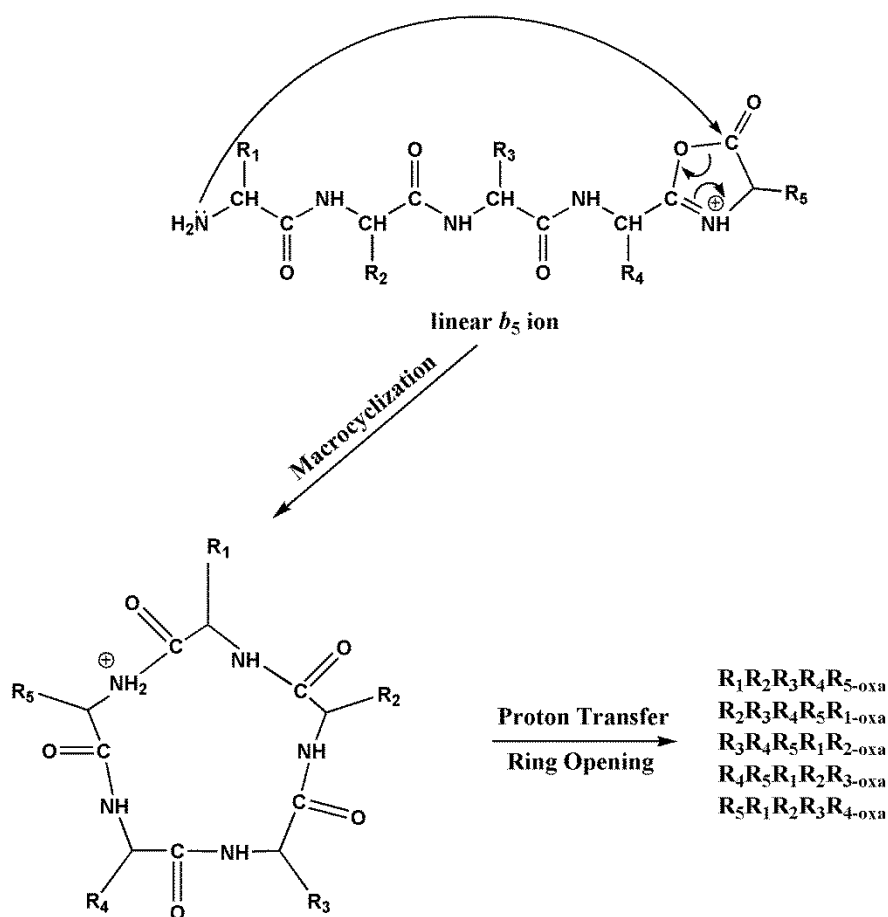


Figure 3.7. General macrocycle mechanism of the b_5^+ ions

The b_4^+ ions of **HAAA**, **AHAA**, **AAHA**, **AAAH** and the b_5^+ ions of **GGGGG**, **HAAAA**, **AAHAA**, **AAAAH** and **YAGFL** structures have been studied and compared with the previous works [11, 27, 28] for the computational method validation. The oxazolone and macrocycle structure of the b_4^+ and b_5^+ ions compete each other. The studies in the literature, the peptides conformers have been obtained by the use of molecular dynamics (MD) simulations. Then, quantum calculations were applied with Gaussian09 program [40] to get optimum structures of those conformers. In this work, the peptide conformers have been explored by Molecular Mechanics via Spartan'10 program [39] and molecular dynamics simulations with Amber'11 program [43].

3.2.1. The b_4^+ ions of HAAA, AHAA, AAHA and AAAH

The structures of b_4^+ ions of HAAA, AHAA, AAHA and HAAA composed of three alanines and one histidine have been investigated and compared with the work done by Bythell et al. [28]. Each peptide has protonated from three different sites such as oxazolone N-term protonated, oxazolone ring protonated and oxazolone His protonated isomers for linear ones. oxazolone His protonated and oxazolone Oxygen protonated isomers have been considered for the macro-cyclic structure.

Firstly, 1000-3500 initial conformers have been obtained with Molecular Mechanics techniques with Spartan Program. The conformers have been reduced to about 75 candidate structures by using Principal Coordinate Analysis (PCO) [37, 38]. Finally, the candidate structures have been used for the geometry optimization calculations were performed at the DFT/B3LYP/6-31+G(d,p) level of theory via Gaussian09 Program. These steps have been applied for each protonated isomers.

The results were in good agreement with the literature (see Table 3.9). The E-E* refers to energy difference between literature and this study. The b_4^+ ions of histidine N-protonated macrocycle isomer of HA₃ was most the stable one. The histidine N-protonated oxazolone linear HAAA structure was the second most stable isomer has 24.7 kJ/mol relative energy. The third stable isomer was The histidine N-protonated oxazolone linear AHAA (33.0 kJ/mol). Another macrocycle structure was oxygen protonated macrocycle (47.4 kJ/mol). This result showed that as well as geometry of peptides (linear or macrocycle), protonated sites of the structure significantly affect the

energy order. As a summary, the macrocycle structure of the b_4^+ ions of HA_3 was more favorable than the linear ones. The energy values obtained in this work for 14 conformers given in Table 3.9 were same with or even lower than (for some of them) the literature [28].

Table 3.9. The energies of b_4^+ ions of HA_3 isomers

Structures	$E^{*[28]}$ (au)	E (au)	$E-E^*$ (kJ/mol)	Rel.E. (kJ/mol)
AAAH b_4 Oxazolone His protonated	-1214.795860	-1214.795859	0.0	34.9
AAAH b_4 Oxazolone N-term protonated	-1214.781815	-1214.784571	-7.2	44.5
AAAH b_4 Oxazolone ring protonated	-1214.778417	-1214.778666	-0.7	56.6
AAHA b_4 Oxazolone His protonated	-1214.792304	-1214.792670	-1.0	43.2
AAHA b_4 Oxazolone N-term protonated	-1214.775835	-1214.780162	-11.4	66.0
AAHA b_4 Oxazolone ring protonated	-1214.781514	-1214.782552	-2.7	63.9
AHAA b_4 Oxazolone His protonated	-1214.785376	-1214.788784	-8.9	33.0
AHAA b_4 Oxazolone N-term protonated	-1214.779901	-1214.780113	-0.6	65.9
AHAA b_4 Oxazolone ring protonated	-1214.780682	-1214.780892	-0.6	59.6
HAAA b_4 Oxazolone His protonated	-1214.791942	-1214.791942	0.0	24.7
HAAA b_4 Oxazolone N-term protonated	-1214.788298	-1214.788298	0.0	54.3
HAAA b_4 Oxazolone ring protonated	-1214.783684	-1214.783684	0.0	69.8
Cyclic HA_3 His protonated	-1214.805248	-1214.80525	0.0	0.0
Cyclic HA_3 Oxygen protonated	-1214.787173	-1214.78719	0.0	47.4

3.2.2. The b_5^+ ions of GGGGG

The b_5^+ fragment of GGGGG have been investigated and compared with the previous work [27]. The b_5^+ ions of GGGGG have three important types of isomers; the oxazolone ring nitrogen protonated (Oxa_oxa_np), N-terminal amino protonated GGGGG_{oxa} (Oxa_nterm_p) and oxygen protonated Macrocyclic GGGGG_{cyclic} (Macro_op) isomers have been considered. At first, Molecular Mechanics have been used to explore peptide isomers. 1000-3500 initial geometries have been obtained in this step of the work. Then these conformers have been reduced to about 50 candidate structures for quantum chemical calculations by applying Principal Coordinate Analysis (PCO). Finally, the candidate structures have been used as initial geometry for the optimization with DFT/B3LYP/6-31+G(d,p) level of theory via Gaussian09 Program.

The energies of the ten lowest energy conformers of b_5^+ fragment of GGGGG isomers were shown in Table 3.10. It has been observed that the oxygen protonated macrocyclic GGGGG_{cyclic} structures have the lowest energy. The ten lowest relative energy values of Macro_op are between 0 and 28 kJ/mol (for all conformers; 0-208 kJ/mol), on the other hand the oxazolone ring nitrogen protonated and N-terminal amino protonated GGGGG_{oxa} conformers energies are between 44 and 82 kJ/mol (for all conformers; 44-267 kJ/mol). The Oxa_nterm_p and Oxa_oxa_np structures compete with each other energetically.

The lowest energy peptide structures and energies for the three isomers which have different protonation sites were given in Figure 3.8. According to these results, the energy values of the peptides are almost same with the literature work. The E-E* refers to energy difference between literature and this study. The oxygen protonated macrocyclic GGGGG_{cyclic} isomer has the minimum energy and supports the experimental data [27]. The N-terminal amino protonated GGGGG_{oxa} is more stable than the oxazolone ring nitrogen protonated GGGGG_{oxa}. The energy order of two isomers is different than work done by Erlekam et al. [27].

Table 3.10. The 10 lowest energy conformers of b_5^+ fragment of GGGGG isomers at the DFT/B3LYP/6-31+G(d,p) level of theory

	Conformers	Energy (au)	Rel. Energy (kJ/mol)
Macro_p	Macro_op_1	-1040.49866700	0.0
	Macro_op_2	-1040.49865472	0.0
	Macro_op_3	-1040.49731691	3.5
	Macro_op_4	-1040.49731672	3.5
	Macro_op_5	-1040.49731649	3.5
	Macro_op_6	-1040.49199631	17.5
	Macro_op_7	-1040.49199620	17.5
	Macro_op_8	-1040.48994965	22.9
	Macro_op_9	-1040.48805064	27.9
	Macro_op_10	-1040.48795245	28.1
Oxa_nterm_p	Nterm_p_1	-1040.48200112	43.8
	Nterm_p_2	-1040.47930629	50.8
	Nterm_p_3	-1040.47699775	56.9
	Nterm_p_4	-1040.47558227	60.6
	Nterm_p_5	-1040.47417990	64.3
	Nterm_p_6	-1040.47342158	66.3
	Nterm_p_7	-1040.47231878	69.2
	Nterm_p_8	-1040.47119511	72.1
	Nterm_p_9	-1040.46874547	78.6
	Nterm_p_10	-1040.46836839	79.5
Oxa_oxa_np	Oxa_np_1	-1040.48125977	45.7
	Oxa_np_2	-1040.47722202	56.3
	Oxa_np_3	-1040.47539954	61.1
	Oxa_np_4	-1040.47456558	63.3
	Oxa_np_5	-1040.47352310	66.0
	Oxa_np_6	-1040.47352297	66.0
	Oxa_np_7	-1040.47087815	73.0
	Oxa_np_8	-1040.47008809	75.0
	Oxa_np_9	-1040.46811922	80.2
	Oxa_np_10	-1040.46746964	81.9

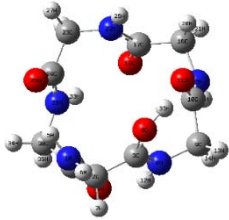

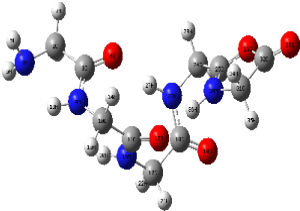
Peptide	Structure	$E^{*[27]}$ (au)	E (au)	$E-E^*$ (kJ/mol)
Macro_op		-1040.498670	-1040.498667	0.0
Oxa_nterm_p		-1040.478618	-1040.482001	-8.9
Oxa_oxa_np		-1040.481260	-1040.481260	0.0

Figure 3.8. The structures and energies of b_5^+ ions of GGGGG isomers

3.2.3. The b_5^+ ions of HAAAA, AAHAA, and AAAAH

The b_5^+ ions of HAAAA, AAHAA, AAAAH have been investigated and compared with the work done by Bythell et al. [28].

Each peptide has protonated from three different sites for the linear ones such as oxazolone His protonated, oxazolone N-term protonated and oxazolone ring protonated oxazolone His protonated and oxazolone oxygen protonated isomers have been considered for the macro-cyclic structure. Firstly, Molecular Mechanics have been used to explore peptide isomers. 50.000 initial geometries have been obtained in this step of the work. Among those, the 3500 lowest energy conformers have been selected for Principal Component Analysis (PCO). After that these conformers have been reduced to about 36 candidate structures for quantum chemical calculations. Finally, the candidate structures have been used as initial geometry for the optimization with DFT/B3LYP/6-31+G(d,p) level of theory via Gaussian09 Program.

Table 3.11. The energies of b_5^+ ions of HA_4 isomers

Structure	E* (au)	E (au)	E-E*(MM) (kcal/mol)	E-E*(MD) (kcal/mol)
HAAAA Oxazolone His protonated	-1462.145825	-1462.145825	2.8	0.0
HAAAA Oxazolone ring protonated	-1462.137049	-1462.137049	1.7	0.0
HAAAA Oxazolone N-term protonated	-1462.141926	-1462.141662	0.9	0.2
AAHAA Oxazolone His protonated	-1462.147467	-1462.147427	4.3	0.0
AAHAA Oxazolone ring protonated	-1462.140032	-1462.139526	0.6	0.3
AAHAA Oxazolone N-term protonated	-1462.133997	-1462.137641	-1.3	-2.3
AAAAH Oxazolone His protonated	-1462.148657	-1462.148655	-	0.0
AAAAH Oxazolone ring protonated	-1462.136593	-1462.136593	-	0.0
AAAAH Oxazolone N-term protonated	-1462.139313	-1462.133773	-	3.5
Cyclic HA_4 His protonated	-1462.167816	-1462.171600	-	-2.4
Cyclic HA_4 Oxygen protonated	-1462.160578	-1462.155992	-	2.9

*Energies were taken from Ref [28] ; E-E*refers to energy difference between literature and this study. (MM) and (MD) refers to molecular mechanics and molecular dynamics calculations

Molecular Mechanics calculations produced 50.000 conformers (for each of them) for b_5^+ ions of HA_4 isomers and than these were reduced to 36 conformers. So lots of conformers were lost. Hence, the errors were higher (Table 3.11). After that The MD simulations with Amber11 program [43] were used instead of Molecular Mechanics with Spartan'10 program [39] for the b_5^+ ions. In the MD calculations 4000 initial conformers have been obtained. A much better agreement was found with the literature. The macro-cyclic HA_4 His protonated was the most stable than the other isomers. The histidine N-protonated oxazolone linear AAAAH structure was the most stable among the linear ones.

3.2.4. The b_5^+ ions of YAGFL

The b_5^+ ions of YAGFL (Tyrosine, Alanine, Glycine, Phenylalanine, and Leucine) which consist of five different amino acids have been investigated. The linear oxazolone and the oxygen protonated between Phenyl and Leucine macrocycle structures of this protonated peptide have been considered for the calculations. The 4000 conformers have been obtained with MD simulations. The obtained conformers have been reduced to about 36 candidate structures via Principal Coordinate Analysis (PCO) Finally, the candidate structures have been calculated with the DFT/B3LYP/6-31+ G(d,p) level of theory via Gaussian09 Program and compared with the literature [11].

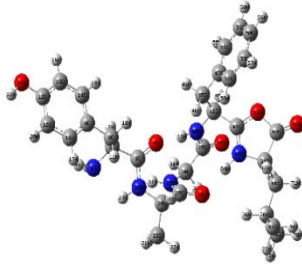
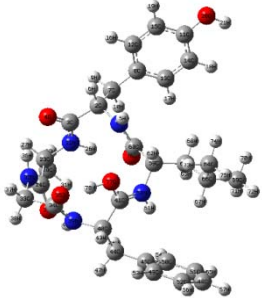
Peptide	Structure	$E^{*[11]}$ (au)	E (au)	E-E* (kJ/mol)
YAGFL Oxazolone Protonated		-1853.079184	-1853.078924 Rel. Energy (33.3 kJ/mol)	0.7
YAGFL Macrocycle Oxygen protonated (F-L)		-1853.092021	-1853.091598 Rel. Energy (0.0 kJ/mol)	1.1

Figure 3.9. The structures and energies of b_5^+ ions of YAGFL isomers

The oxygen protonated between Phenyl and Leucine macrocycle was 33.3 kJ/mol more stable than the linear protonated oxazolone structure. In Figure 3.9, the energy difference was 0.68 kJ/mol for linear, 1.11 kJ/mol for macro-cyclic higher energy than the literature [11]. The E-E* refers to energy difference between literature and this study.

3.2.5. Conclusions of the b_4^+ and b_5^+ ions

The method that was proposed in the content of this thesis involves three steps:

- 1) Conformer sampling by the use of Molecular Mechanics or molecular dynamics simulation
- 2) The reduction of these conformers via Principal Coordinates Analysis (PCO)
- 3) Initial geometries obtained in step 2 were used for the quantum mechanical calculations

This method is a valid method since it agrees well with the previous works [11, 27, 28].

It can be used for the structural analysis of b_4 - b_7 size peptides.

For the all peptide in this part of the work,

- The protonated macrocyclic structures have the lowest energies. The proton prefers to locate on the oxygen of the b^+ ions except histidine containing peptide where it prefers nitrogen of the histidine-ring.
- For the linear chains, HA_3 and HA_4 the nitrogen of the histidine-ring isomers are most stable one, on the other hand the nitrogen of oxazolone protonated is most likely structure for the GGGGG and YAGFL.

CHAPTER 4

AMINO ACID AND POSITION EFFECT ON THE STRUCTURES OF b_5 IONS

4.1. Introduction

In this chapter, the b_5^+ ions consist of nonpolar Alanine (Ala, A), Leucine (Leu, L), Phenylalanine (Phe, F), polar Tyrosine (Tyr, Y), Cysteine (Cys, C), Asparagine (Asn, N), and acidic Aspartic Acid (Asp, D) (Figure 4.1) have been considered in order to investigate amino acid effect on the macrocycle structure of peptides. The selected peptides also have different type of substituents groups; aliphatic (-CH₂-), aromatic (C rings), alcohol (-OH), thiol (-SH), amides (-CONH₂) and carboxyl (-COOH). Furthermore, three types of linear peptide sequences have been considered in the computational calculations for b_5^+ fragment to examine the position influence; XAAAA, AAXAA, AAAAX where X; Asn, Asp, Leu, Phe, Tyr, Cys and also macrocyclic structures of them.

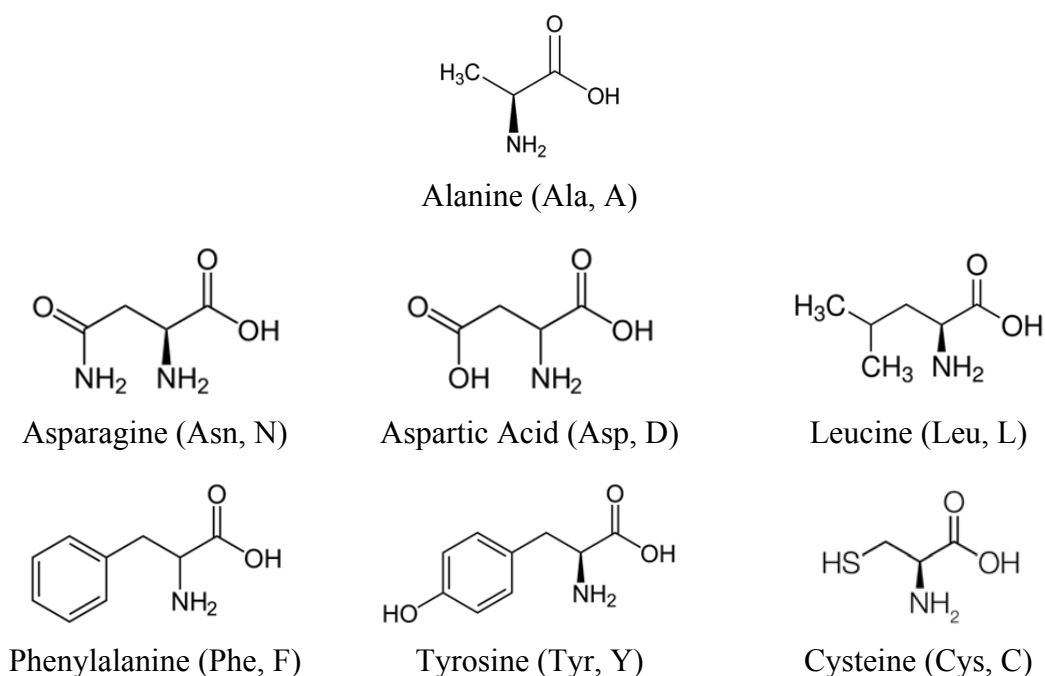


Figure 4.1. The structures of alanine, leucine, asparagine, aspartic acid, phenylalanine, tyrosine and cysteine

4.1.1. Computational Details

Firstly, each protonated isomer of the 4000 possible peptide conformers have been obtained by the molecular dynamics (MD) simulations with simulated annealing technique by AMBER'11 program [43] in conjunction with ff99sb force field to produce conformer samples for Principal Coordinate Analysis (PCO) [37, 38]. Afterwards, the obtained conformers have been reduced to about 36 candidate structures by using PCO. The aim of this method is to reduce dimension of variable that defines the system of study. The construction of dissimilarity matrix of different conformers has been calculated and then the distances of two atoms in the conformers were used as unit of measurement. So, the obtained structures were grouped and selected. Eventually, the candidate structures have been carried out quantum chemical calculations with the DFT/B3LYP/6-31+G(d,p) level of theory via Gaussian09 Program [40] to have optimum structures. Moreover, frequency calculations have been performed on the most stable structures with the same level of theory. These steps have been applied for each protonated isomers of the all residues.

The energy comparisons of the structures have been done with the relative zero point corrected energies (E+ZPE) in this study.

The N-terminal nitrogen and nitrogen in the oxazolone ring have been considered as the probable protonation sites of the b_5^+ ions of the peptides for the linear structures (Figure 4.2). On the other hand; For the macrocycle structures, proton is located on the oxygens and nitrogens in the cycle as shown in Figure 4.3. The side chain (R) of amino acids has been demonstrated by the single letter amino acid codes (where A=Ala, X=Asp, Asn, Leu, Phe, Tyr, Cys) in Figure 4.2 and Figure 4.3.

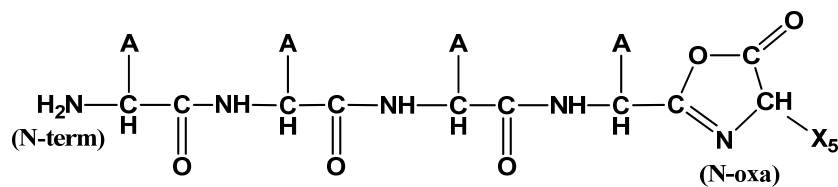
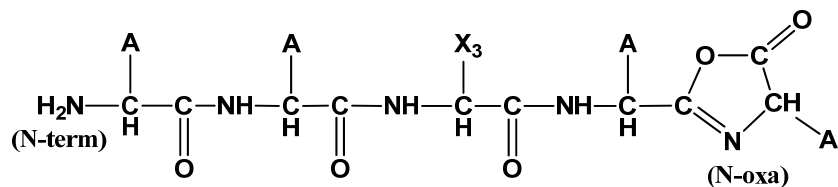
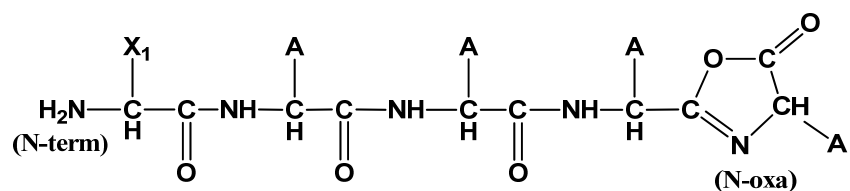


Figure 4.2. The general structures of linear oxazolone of neutral b_5 ions

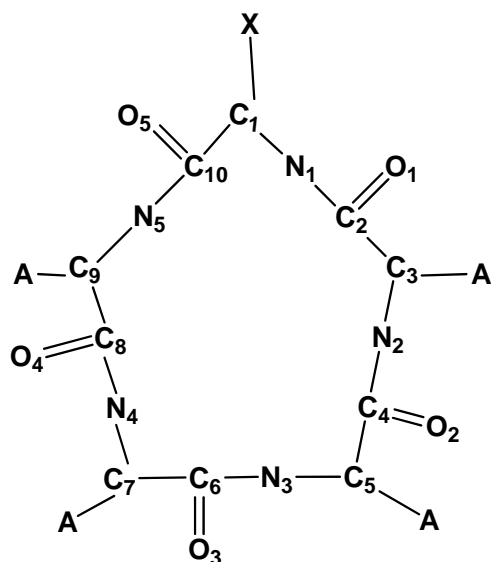


Figure 4.3. The general structure of macrocycle of neutral b_5 ion

The nomenclatures of the peptide conformers have been generated and shown in Table 4.1 in this section. In this description, the letter “X” can be Asp, Asn, Leu, Phe,

Tyr or Cys amino acids. The “O” and “N” letters have been used for the oxygen and nitrogen protonated isomers in the macrocycle structure. Furthermore, the side_np and side_op referred to the protonated nitrogen and oxygen of the side chain (R) group of the amino acids. In addition, the nomenclature of “**XA₄**” term has been referred to one X and four alanines residues; the position of X can be at the N-terminal, C-terminal and the center of the peptide. The protonated site of the ions has been showed in light blue color and the underlined text showed the most stable conformer in the following figures.

Table 4.1. Nomenclature of Protonated Conformers

Linear structures		Macrocycle structures	
<u>Name</u>	<u>Protonated site</u>	<u>Name</u>	<u>Protonated site</u>
X1_oxa	XAAAA; Oxazolone Nitrogen	O1	Oxygen 1
X3_oxa	AAXAA; Oxazolone Nitrogen	O2	Oxygen 2
X5_oxa	AAAAX; Oxazolone Nitrogen	O3	Oxygen 3
X1_nterm	XAAAA; N-terminal Nitrogen	O4	Oxygen 4
X3_nterm	AAXAA; N-terminal Nitrogen	O5	Oxygen 5
X5_nterm	AAAAX; N-terminal Nitrogen	N1	Nitrogen 1
X1_side_np	XAAAA; X' side Nitrogen	N2	Nitrogen 2
X3_side_np	AAXAA; X' side Nitrogen	N3	Nitrogen 3
X5_side_np	AAAAX; X' side Nitrogen	N4	Nitrogen 4
		N5	Nitrogen 5
		cyc_side_np	side Nitrogen
		cyc_side_op	side Oxygen

4.1.2. Mass Spectrometry Details

The C-terminal amidated synthetic model peptides (NAAAAAA-NH₂, AANAAAA-NH₂, AAAANAA-NH₂, DAAAAAA-NH₂, AADAAAA-NH₂, and AAAADAA-NH₂) were obtained from GL Biochem Ltd. (Shanghai, China). During the experiments, HPLC-grade methanol and formic acid were used. Approximately 1 mg of solid peptide samples were dissolved in a 1:1 (v/v) mixture of MeOH and deionized H₂O to give a concentration of 10⁻⁴ M.

All MS/MS experiments were carried out on a LTQ XL linear ion-trap mass spectrometer (Thermo Finnigan, San Jose, CA, USA) equipped with an ESI source. Before each experiment, the instrument was calibrated with the company’s calibration mixture. The spray voltage was +5.0 kV and the N₂ sheath gas flow rate was 10

(arbitrary units). The capillary temperature was maintained at 300 °C. Helium was used as the collision gas for CID and as a bath/buffer gas to improve trapping efficiency. A 100 μ M peptide solution was prepared in 50:50:1 (v/v/v) MeOH/H₂O/HCOOH and introduced into the ion source with an incorporated syringe pump at a flow rate of 5 μ L min⁻¹. The normalized collision energy was set at between 20 and 28% with activation (q) of 0.250, and an activation time of 30 ms was applied at each CID stage. The isolation width (*m/z*) for precursor ions was set at between 1.0 and 1.8 for both MS² and MS³ acquisitions and at least 300 scans were averaged. Data acquisition was carried out by using Xcalibur (ver. 2.0) software system.

4.2. The b₅⁺ ions of NAAAA, AANAA, AAAAN isomers

b₅⁺ ions of NAAAA, AANAA and AAAAN have been protonated from three different sites for linear conformers such as N-terminal nitrogen protonated (N1_termin, N3_termin, N5_termin), the nitrogen of oxazolone ring protonated (N1_oxa, N3_oxa, N5_oxa) and the nitrogen of asparagine protonated (N1_side_np, N3_side_np, N5_side_np) and also nitrogens (N1, N2, N3, N4, N5, cyc_side_np) and oxygens (O1, O2, O3, O4, O5, cyc_side_op) on the macrocycle. The computational results of the structures of the lowest energy conformers' electronic and ZPE corrected energies have been given in Table 4.2.

The lowest energy conformer of b₅⁺ ions of NA₄ residue has the O4 oxygen protonated macrocycle structure (Figure 4.4). It has been observed that, the proton could be located on any of the oxygens in the macrocycle since the energies of other oxygen protonated structures O1, O3, O5 and O2 were only differ as 0.7 to 3.5 kJ/mol. On the other hand; the least preferred protonated macrocycle structures were the nitrogen protonated isomers (Figure 4.6). The energies of N1, N2, N5, N4 and N3 were between 47.4-72.9 kJ/mol. And also the macrocycle conformer of the protonated nitrogens on the Asn (cyc_side_np; 56.1 kJ/mol) was not preferred at all.

In the linear ones of NA₄ (Figure 4.5), the energy order of the NAAAA residues were N1_oxa (23.3 kJ/mol), N1_termin (28.4 kJ/mol) and N1_side_np (101.7 kJ/mol). And the relative energies of the AANAA isomers were 14.4 kJ/mol, 21.2 kJ/mol, 112.3 kJ/mol for N3_oxa, N3_termin and N3_side_np respectively. Both of NAAAA and AANAA isomers had the same energy order, whereas the energy order of the AAAAN

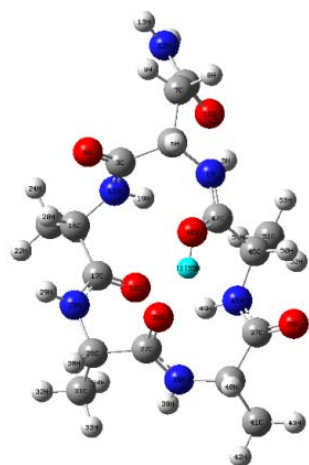
changed. The N5_nterm (14.6 kJ/mol) was the lowest one and the N5_oxa (28.1 kJ/mol) isomer was more stable than the N5_side_np (95.1 kJ/mol). The oxazolone and N-terminal protonated structures have been competed each other, but the protonated nitrogen on the Asn was not preferred at all.

Table 4.2. The electronic (E) and ZPE corrected energies of b₅⁺ ions of NA₄

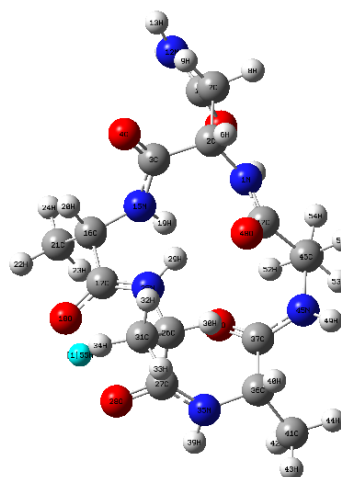
Protonated Site	E (au)	E+ZPE (au)	Rel E kJ/mol	Rel (E+ZPE) kJ/mol
O4	-1405.821641	-1405.362348	0.0	0.0
O1	-1405.821017	-1405.362073	1.6	0.7
O3	-1405.821417	-1405.361867	0.6	1.3
O5	-1405.819876	-1405.361170	4.6	3.1
O2	-1405.820308	-1405.361021	3.5	3.5
N3_oxa	-1405.814343	-1405.356872	19.2	14.4
N5_nterm	-1405.817401	-1405.356801	11.1	14.6
cyc_side_op	-1405.816357	-1405.356213	13.9	16.1
N3_nterm	-1405.813980	-1405.354280	20.1	21.2
N1_oxa	-1405.811099	-1405.353468	27.7	23.3
N5_oxa	-1405.808217	-1405.351658	35.2	28.1
N1_nterm	-1405.810379	-1405.351533	29.6	28.4
N1	-1405.803651	-1405.344286	47.2	47.4
N2	-1405.800891	-1405.341283	54.5	55.3
cyc_side_np	-1405.800723	-1405.340965	54.9	56.1
N5	-1405.798663	-1405.338945	60.3	61.4
N4	-1405.795470	-1405.335891	68.7	69.5
N3	-1405.793885	-1405.334571	72.9	72.9
N5_side_np	-1405.783753	-1405.326145	99.5	95.1
N1_side_np	-1405.780884	-1405.323628	107.0	101.7
N3_side_np	-1405.776415	-1405.319576	118.7	112.3

As a summary, the lowest energy of linear AANAA, AAAAN and NAAAA residues were AANAA_{oxa} (14.4 kJ/mol), AAAAN_{nterm}(14.6 kJ/mol) and NAAAA_{oxa} (23.3 kJ/mol). And the energy differences between macrocycle and linear ones were 14.4-23.3 kJ/mol.

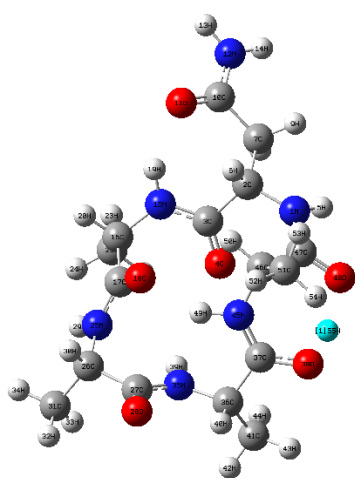
Finally, the oxygen protonated macrocycle of NA₄ was the most favorable one, and then the oxazolone and N-terminal protonated linear structures were preferred. The nitrogen protonated macrocycle and the nitrogen of asparagine protonated isomers were very unlikely conformers. Protonated nitrogens and oxygens on the linear backbone structures were energetically unlikely conformers (not shown here).



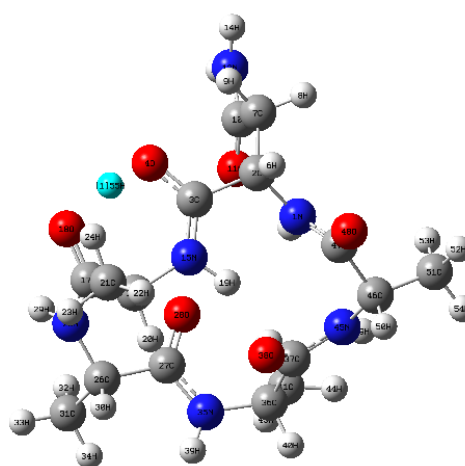
O1 (0.7 kJ/mol)



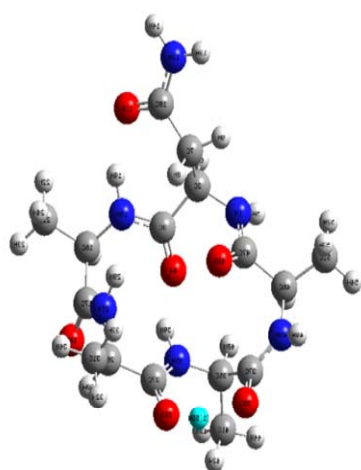
O4 (0.0 kJ/mol)



O2 (3.5 kJ/mol)

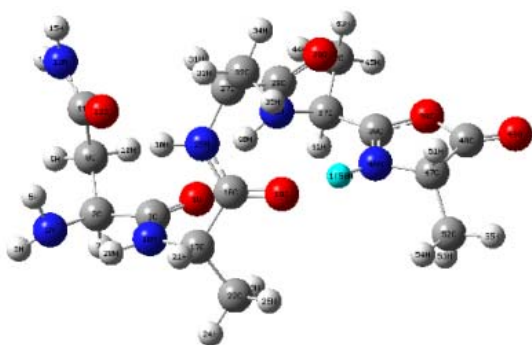


O5 (3.1 kJ/mol)

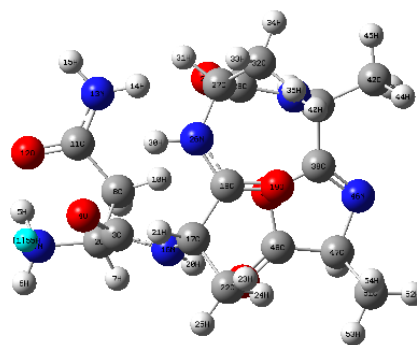


O3 (1.3 kJ/mol)

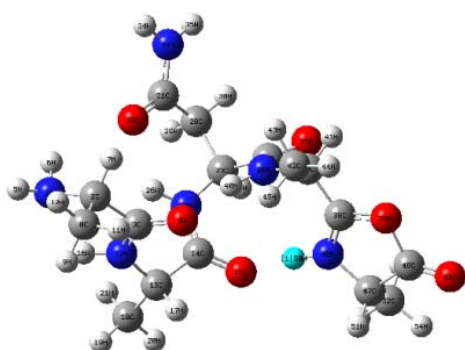
Figure 4.4. The macrocyclic structures of oxygen protonated conformers of NA₄



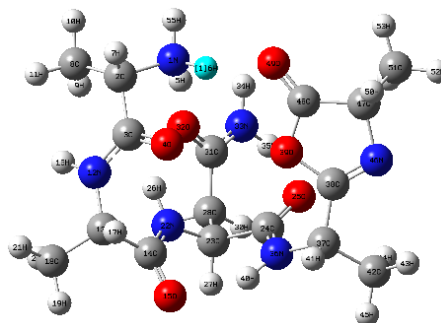
N1_oxa (23.3 kJ/mol)



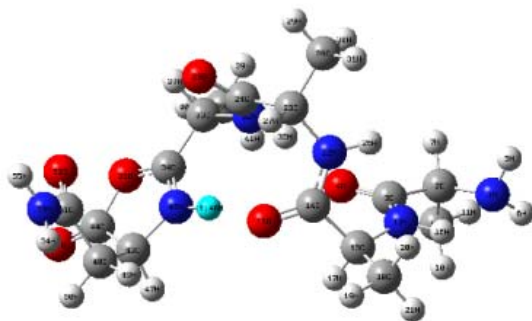
N1_nterm (28.4 kJ/mol)



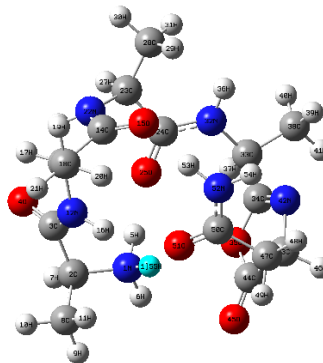
N3_oxa (14.4 kJ/mol)



N3_nterm (21.2 kJ/mol)

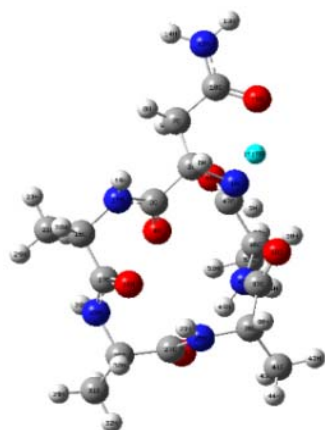


N5_oxa (28.1 kJ/mol)

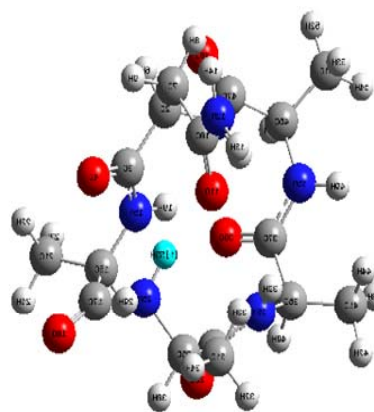


N5_nterm (14.6 kJ/mol)

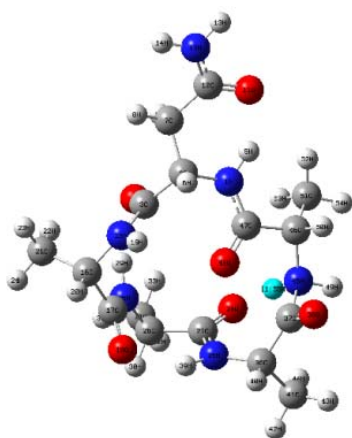
Figure 4.5. The linear structures of nitrogen protonated conformers of NA₄



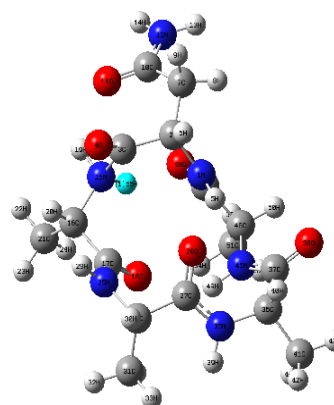
N1 (47.4 kJ/mol)



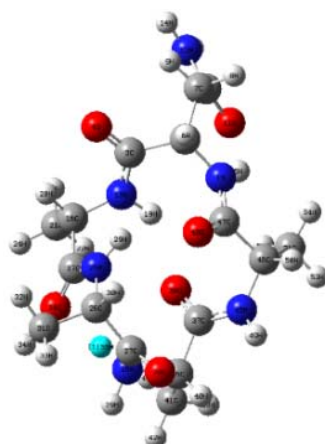
N4 (69.5 kJ/mol)



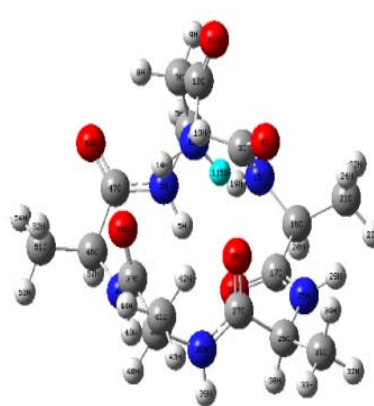
N2 (55.3 kJ/mol)



N5 (61.4 kJ/mol)



N3 (72.9 kJ/mol)



cyc_side_np (56.1 kJ/mol)

Figure 4.6. The macrocycle structures of nitrogen protonated conformers of NA₄

The CID mass spectra of the b_5 ions (m/z 399) obtained from NAAAAAA-NH₂, AANAAAA-NH₂, and AAAANAA-NH₂ are essentially same, as Figure 4.7 illustrates. The dominant fragment ion is ammonia loss from b_5 ion which is denoted as b_5^* (m/z 382) in the CID mass spectra, where the relative intensities of a_5 (m/z 371) and a_5^* (m/z 354) fragment ions are low. In addition, the elimination intensities of A (m/z 328), 2A (m/z 257), N (m/z 285), and D + A (m/z 214) have minor contributions to the mass spectra. It is clear to see that MS/MS spectrum consist of both direct and non-direct sequence ions during low-energy CID. Hence, we can conclude that one asparagine and four alanine containing model peptides fully cyclize to macrocyclic structure.

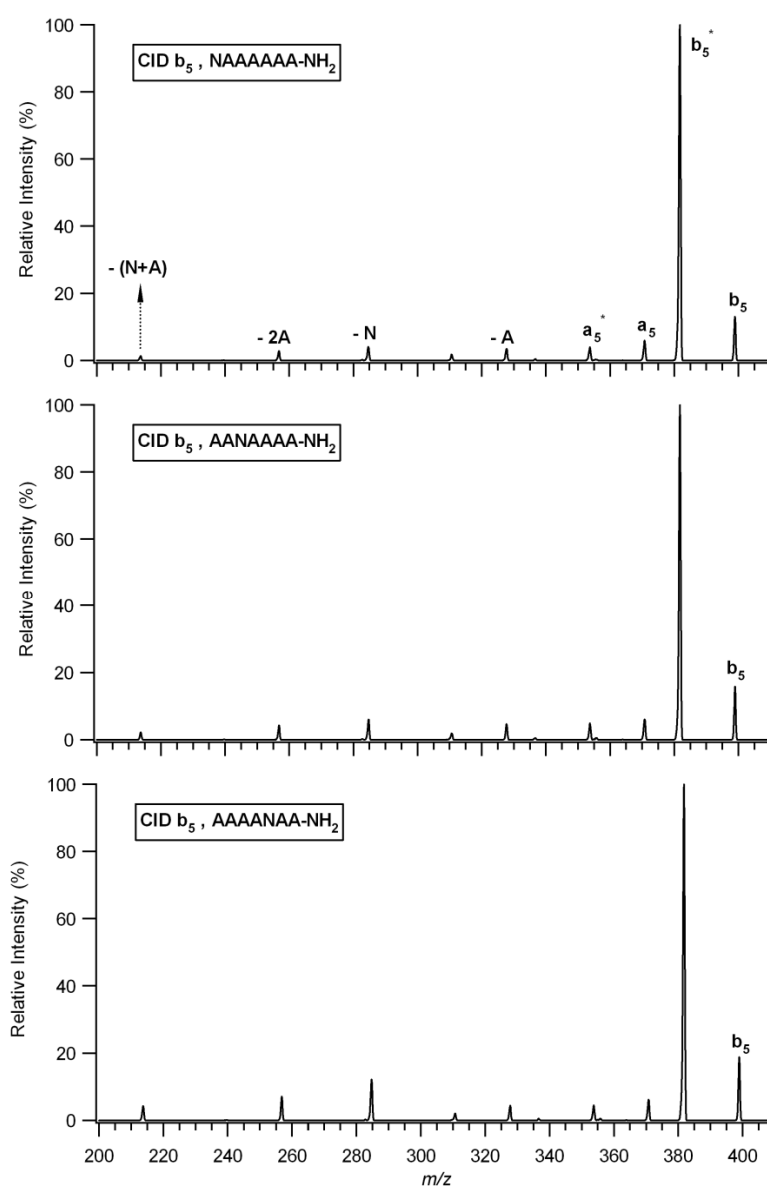


Figure 4.7. Comparison of the CID mass spectra of b_5 ions of NAAAAAA-NH₂, AANAAAA-NH₂, and AAAANAA-NH₂

4.3. The b_5^+ ions of DAAAA, AADAA, AAAAD isomers

The linear b_5^+ ions of DAAAA, AADAA and AAAAD have protonated from two different sites such as N-terminal nitrogen protonated, the nitrogen of oxazolone ring and also nitrogens and oxygens were protonated in the macrocycle structures. The electronic and ZPE corrected energies of the lowest energy conformers have been given in Table 4.3.

Table 4.3. The electronic (E) and ZPE corrected energies of b_5^+ ions of DA₄

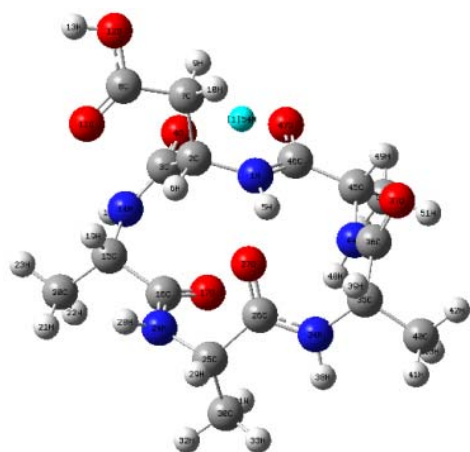
Protonated Site	E (au)	E+ZPE (au)	Rel E kJ/mol	Rel (E+ZPE) kJ/mol
O2	-1425.686309	-1425.238461	0.0	0.0
O5	-1425.683139	-1425.235823	8.3	6.9
O3	-1425.682512	-1425.235342	10.0	8.2
O1	-1425.680544	-1425.233918	15.1	11.9
D5_nterm	-1425.678682	-1425.230942	20.0	19.7
O4	-1425.672057	-1425.227454	37.4	28.9
D3_nterm	-1425.672279	-1425.226175	36.8	32.3
D1_oxa	-1425.670727	-1425.226119	40.9	32.4
D5_oxa	-1425.668355	-1425.223405	47.1	39.5
D1_nterm	-1425.669721	-1425.222280	43.6	42.5
D3_oxa	-1425.665937	-1425.220949	53.5	46.0
N1	-1425.661250	-1425.214646	65.8	62.5
N4	-1425.659511	-1425.212912	70.4	67.1
N3	-1425.659900	-1425.212458	69.3	68.3
N2	-1425.650876	-1425.203880	93.0	90.8
N5	-1425.643141	-1425.196362	113.3	110.5

The most stable conformer of b_5^+ ions of DA₄ residue was the O2 oxygen protonated macrocycle isomer (Figure 4.8). The relative energies of O5, O3, O1 and O4 were between 6.9 and 28.9 kJ/mol. Then again; the least stable protonated macrocycle structures were the nitrogen protonated structures (Figure 4.10). The relative energies of N1, N4, N3, N2 and N5 were in the range of 62.5-110.5 kJ/mol.

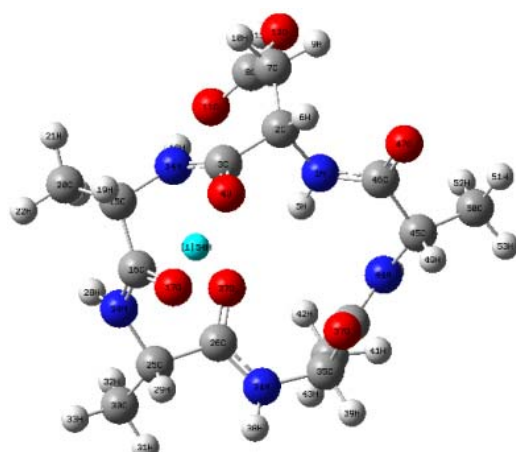
In the linear isomers of DA₄ (Figure 4.9), the relative energies of linear b_5^+ ions of DAAAA were 32.4 kJ/mol, 42.5 kJ/mol for D1_oxa and D1_nterm respectively. However, in the AADAA the N-terminal protonated structure D3_nterm (32.3 kJ/mol) was more favorable than the oxazolone protonated isomer D3_oxa (46.0 kJ/mol). In addition to that, D5_nterm (19.7 kJ/mol) has lower energy than the D5_oxa (39.5

kJ/mol) in AAAAD. Briefly, the lowest energy conformers of linear AAAAD, AADAA and DAAAA residues were AAAAD_{nterm} (19.7 kJ/mol), AADAA_{nterm} (32.3 kJ/mol), and DAAAA_{oxa} (32.4 kJ/mol).

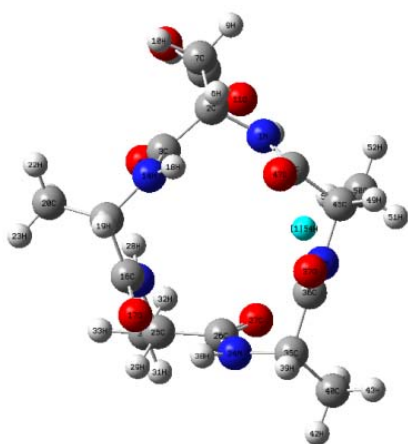
In conclusion, the oxygen protonated macrocycle of DA₄ was the most favorable isomer. Furthermore, the oxazolone and N-terminal protonated linear structures have lower energy values than the nitrogen protonated macrocycle.



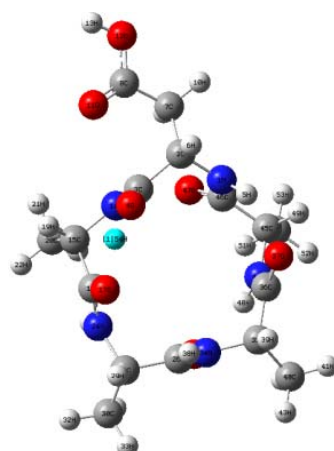
O1 (11.9 kJ/mol)



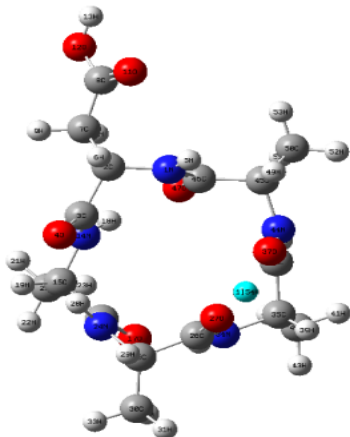
O4 (28.9 kJ/mol)



O2 (0.0 kJ/mol)

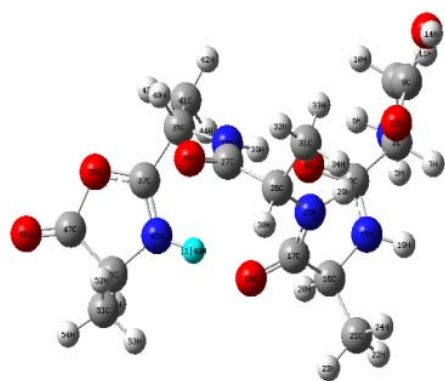


O5 (6.9 kJ/mol)

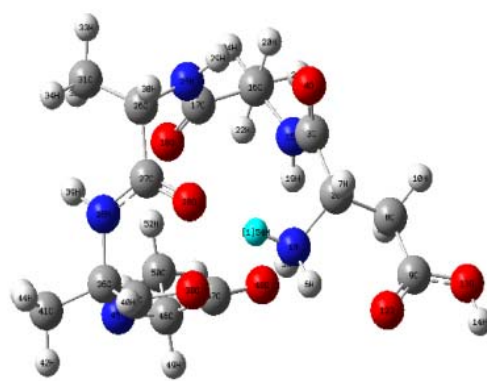


O3 (8.2 kJ/mol)

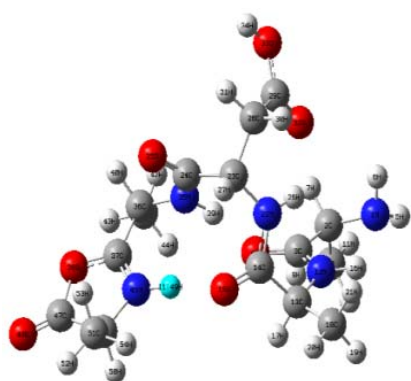
Figure 4.8. The macrocyclic structures of oxygen protonated conformers of DA₄



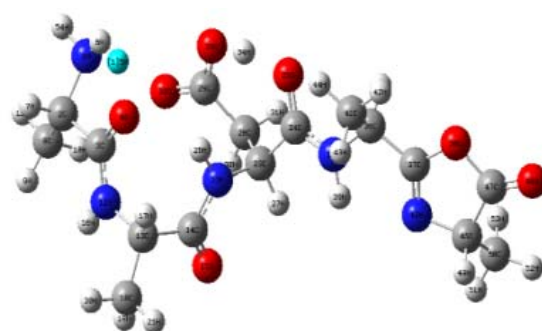
D1_oxa (32.4 kJ/mol)



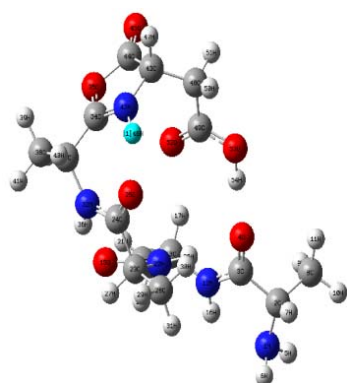
D1_nterm (42.5 kJ/mol)



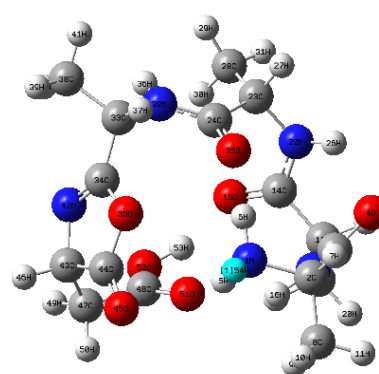
D3_oxa (46.0 kJ/mol)



D3_nterm (32.3 kJ/mol)

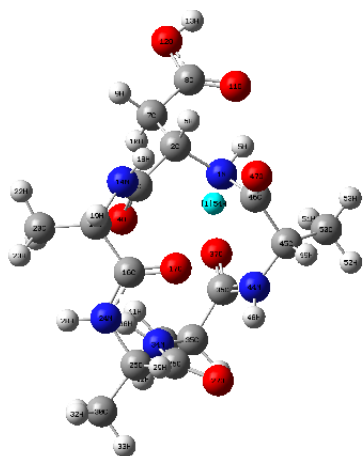


D5_oxa (39.5 kJ/mol)

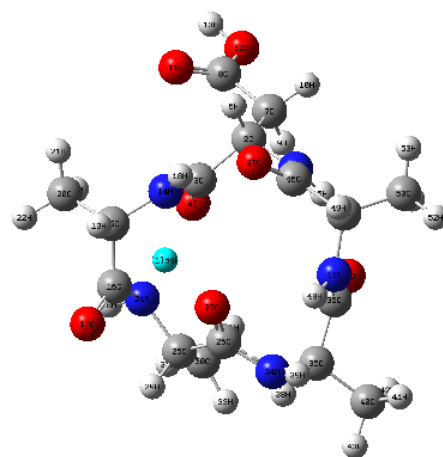


D5_nterm (19.7 kJ/mol)

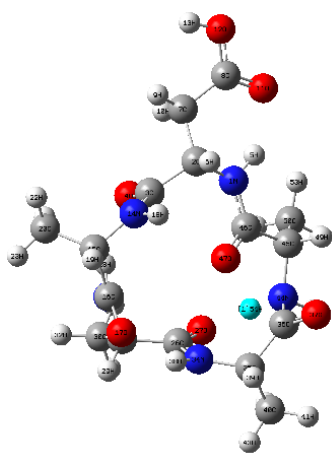
Figure 4.9. The linear structures of nitrogen protonated conformers of DA₄



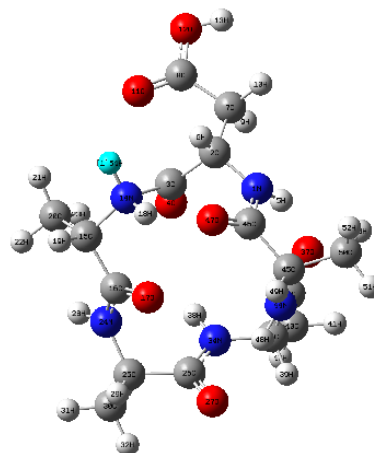
N1 (62.5 kJ/mol)



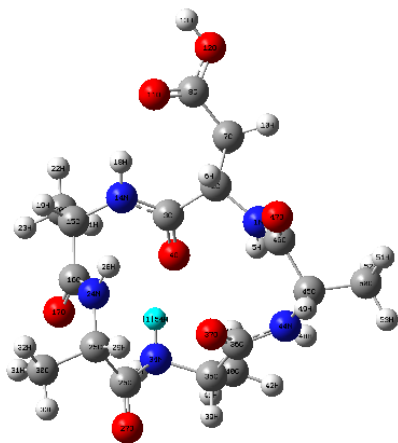
N4 (67.1 kJ/mol)



N2 (90.8 kJ/mol)



N5 (110.5 kJ/mol)



N3 (68.3 kJ/mol)

Figure 4.10. The macrocycle structures of nitrogen protonated conformers of DA₄

The CID mass spectra of the b_5 ions at m/z 400 obtained from DAAAAAA-NH₂, AADAAAA-NH₂, and AAAADAA-NH₂ are identical, as shown in Figure 4.11. The b_5° ($b_5 - \text{H}_2\text{O}$) fragment ion (m/z 382) is the most abundant peak. Moreover, the elimination intensities of CO (a_5 , m/z 372), CO + NH₃ (a_5^* , m/z 355), and CO + H₂O (a_5° , m/z 354) are also significant. The product ion mass spectra of b_5 ions also contain loss of A (m/z 329), A + H₂O (m/z 311), 2A (m/z 258), D (m/z 285), and D + A (m/z 214). In a similar explanation with asparagine containing peptides it is apparent that the b_5 ion obtained from one aspartic acid and four alanine containing model can also undergo cyclization reaction.

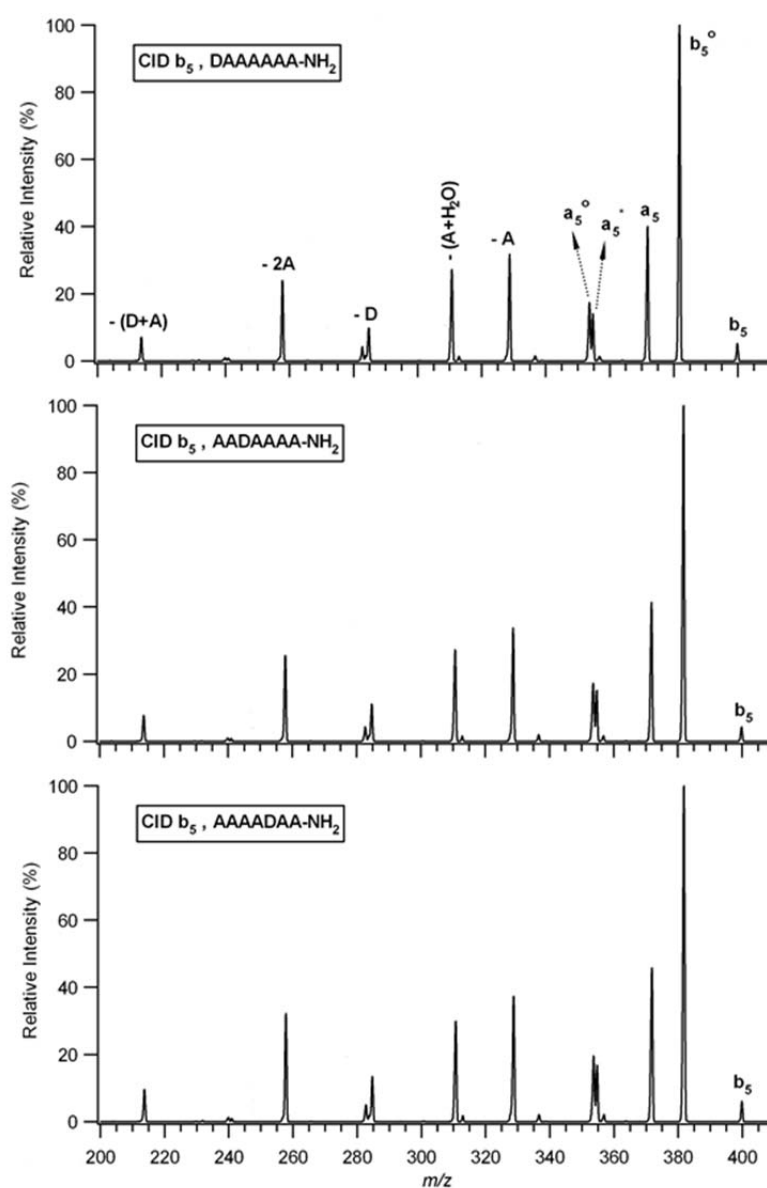


Figure 4.11. Comparison of the CID mass spectra of b_5 ions of DAAAAAA-NH₂, AADAAAA-NH₂ and AAAADAA-NH₂

4.4. The b_5^+ ions of LAAAA, AALAA, AAAAL isomers

The linear b_5^+ ions of LAAAA, AALAA and AAAAL have protonated from N-terminal nitrogen protonated and the nitrogen of oxazolone ring. In addition, the nitrogens and oxygens have protonated in the macrocycle structures. The electronic and ZPE corrected energies of the lowest energy conformers have been given in Table 4.4.

Table 4.4. The electronic (E) and ZPE corrected energies of b_5^+ ions of LA₄

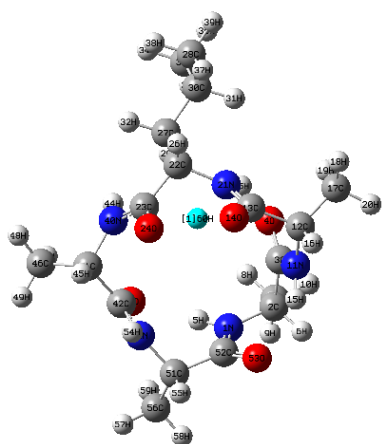
Protonated Site	E (au)	E+ZPE (au)	Rel E kj/mol	Rel (E+ZPE) kj/mol
O1	-1355.055948	-1354.539113	0.0	0.0
O5	-1355.055440	-1354.538703	1.3	1.1
O2	-1355.055284	-1354.538514	1.7	1.6
O3	-1355.054775	-1354.537877	3.1	3.2
L5_oxa	-1355.045230	-1354.530949	28.1	21.4
O4	-1355.046141	-1354.529528	25.7	25.2
L1_oxa	-1355.043189	-1354.529018	33.5	26.5
L5_nterm	-1355.040791	-1354.524558	39.8	38.2
L1_nterm	-1355.038694	-1354.522254	45.3	44.3
L3_oxa	-1355.034329	-1354.520822	56.8	48.0
L3_nterm	-1355.036587	-1354.519723	50.8	50.9
N5	-1355.032506	-1354.516279	61.5	60.0
N2	-1355.031381	-1354.515062	64.5	63.1
N4	-1355.030726	-1354.514556	66.2	64.5
N3	-1355.031008	-1354.514476	65.5	64.7
N1	-1355.030287	-1354.513879	67.4	66.3

The O1 oxygen protonated macrocycle structure is found as the most likely conformer among the b_5^+ isomers of LA₄ residues (Figure 4.12). The relative energies of O5, O2 and O3 were between 1.1 and 3.2 kJ/mol. However, the O4 protonated isomer was unfavorable by the energy of 25.2 kJ/mol. The least stable protonated macrocycle structures were the nitrogen protonated structures (Figure 4.14). The relative energies of N5, N2, N4, N3 and N1 were very close to each other and they were in the range of 60.0-66.3 kJ/mol.

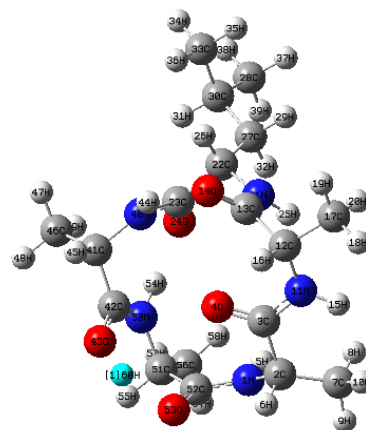
Among the linear isomers of LA₄ (Figure 4.13), L1_oxa (26.5 kJ/mol) structure was more favorable than the L1_nterm (44.3 kJ/mol) in LAAAA residue. Likewise, the oxazolone protonated were more stable than N-terminal protonated isomers in the AALAA and AAAAL residues. The L3_oxa (48.0 kJ/mol) and the L3_nterm (50.9

kJ/mol) isomers have similar energies. However, L5_oxa (21.4 kJ/mol) has lower energy than the L5_ nterm (38.2 kJ/mol). In summary, the lowest energy conformers of linear AAAAL, LAAAA and AALAA residues were AAAAL_{oxa} (21.4 kJ/mol), LAAAA_{oxa} (26.5 kJ/mol), and AALAA_{oxa} (48.0 kJ/mol).

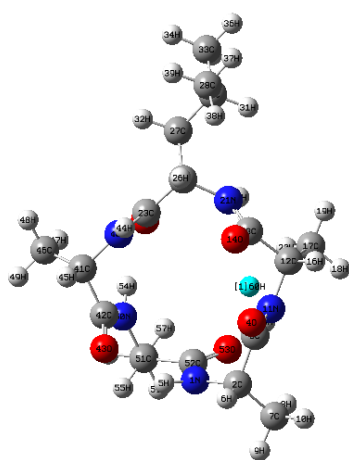
Consequently, the oxygen protonated macrocycle of LA₄ was the most favorable isomer. Moreover, the oxazolone and N-terminal protonated linear structures have lower energy values than the nitrogen protonated macrocycle.



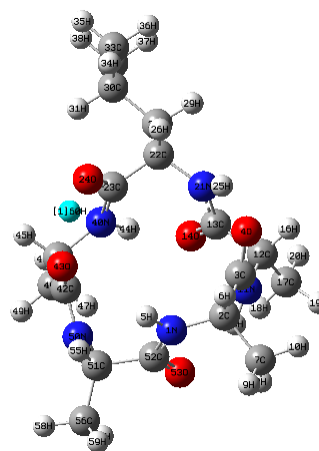
O1 (0.0 kJ/mol)



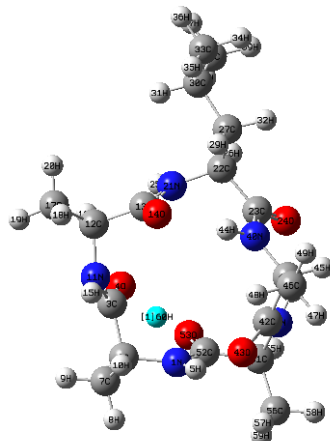
O4 (25.2 kJ/mol)



O2 (1.6 kJ/mol)

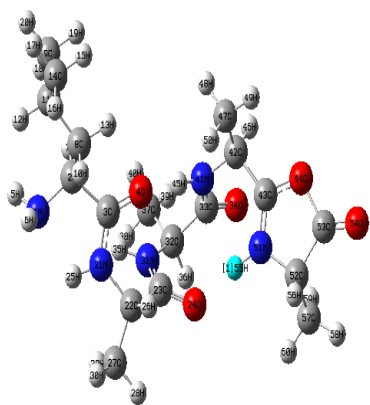


O5 (1.1 kJ/mol)

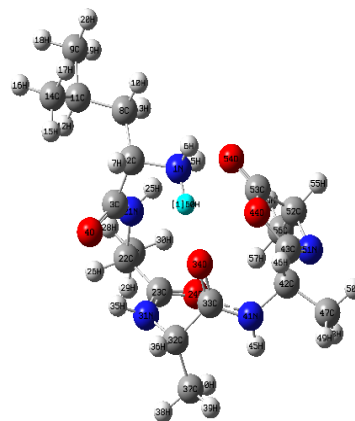


O3 (3.2 kJ/mol)

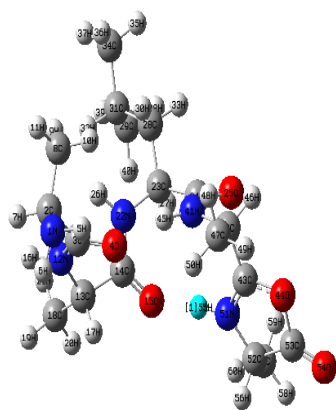
Figure 4.12. The macrocyclic structures of oxygen protonated conformers of LA₄



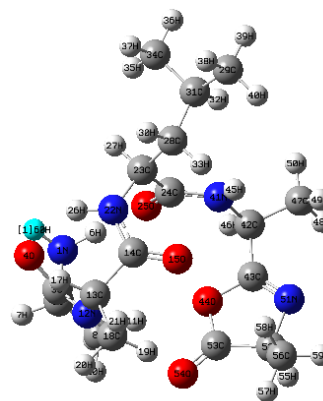
L1_oxa (26.5 kJ/mol)



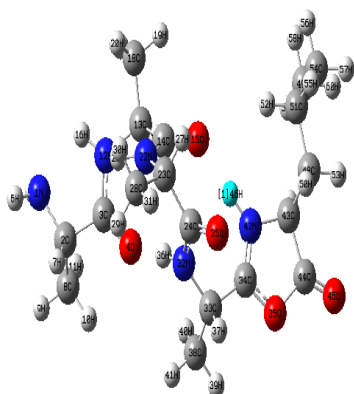
L1_nterm (44.3 kJ/mol)



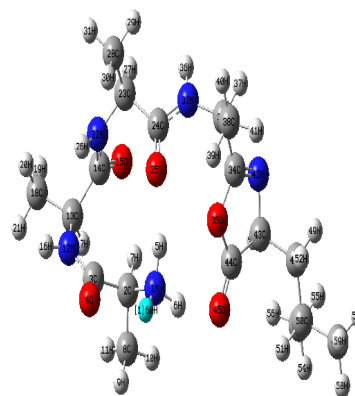
L3_oxa (48.0 kJ/mol)



L3_nterm (50.9 kJ/mol)

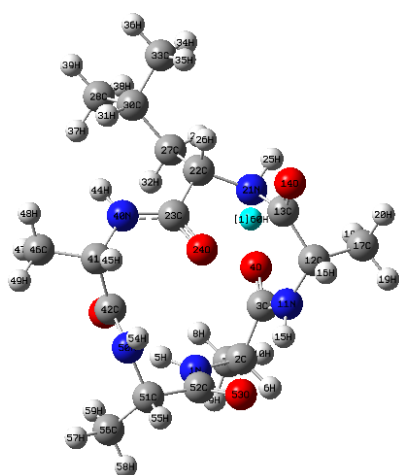


L5_oxa (21.4 kJ/mol)

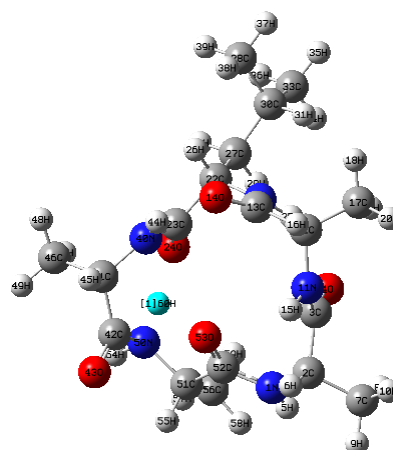


L5_nterm (38.2 kJ/mol)

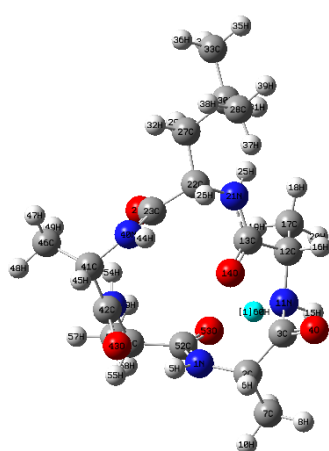
Figure 4.13. The linear structures of nitrogen protonated conformers of LA₄



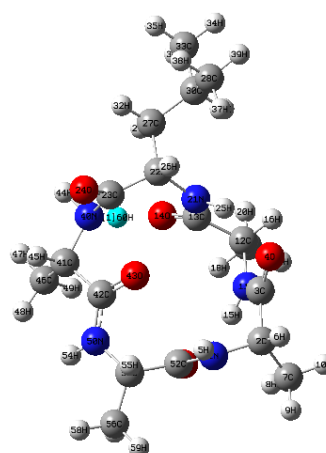
N1 (66.3 kJ/mol)



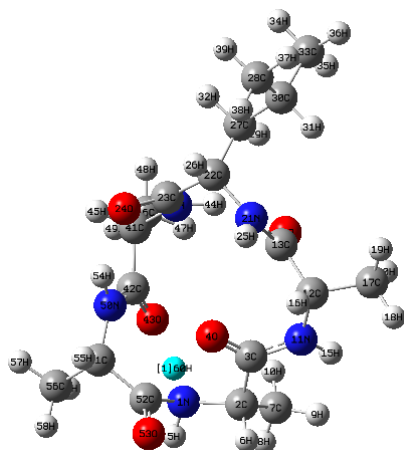
N4 (64.5 kJ/mol)



N2 (63.1 kJ/mol)



N5 (60.0 kJ/mol)



N3 (64.7 kJ/mol)

Figure 4.14. The macrocycle structures of nitrogen protonated conformers of LA₄

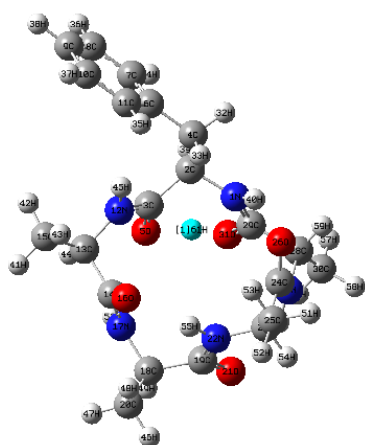
4.5. The b_5^+ ions of FAAAA, AAFAA, AAAAF isomers

The linear b_5^+ ions of FAAAA, AAFAA and AAAAF have protonated from N-terminal nitrogen protonated and the nitrogen of oxazolone ring. In addition, the oxygens have protonated in the macrocycle structures. However, the macrocycle structures which were the nitrogen protonated isomers haven't been considered on account of their higher energies. The electronic and ZPE corrected energies of the lowest energy conformers have been given in Table 4.5.

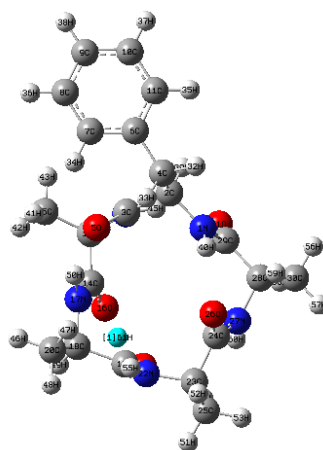
Table 4.5. The electronic (E) and ZPE corrected energies of b_5^+ ions of FA₄

Protonated Site	E (au)	E+ZPE (au)	Rel E kj/mol	Rel (E+ZPE) kj/mol
O1	-1468.171160	-1467.658486	0.8	0.0
O4	-1468.171478	-1467.658450	0.0	0.1
O5	-1468.168665	-1467.655260	7.4	8.5
O2	-1468.168021	-1467.654459	9.1	10.6
O3	-1468.161993	-1467.649544	24.9	23.5
F3_oxa	-1468.157085	-1467.646423	37.8	31.7
F1_oxa	-1468.157017	-1467.646178	38.0	32.3
F5_oxa	-1468.155873	-1467.645367	41.0	34.4
F1_nterm	-1468.152800	-1467.641062	49.0	45.7
F3_nterm	-1468.149742	-1467.636945	57.1	56.6
F5_nterm	-1468.148956	-1467.635964	59.1	59.1

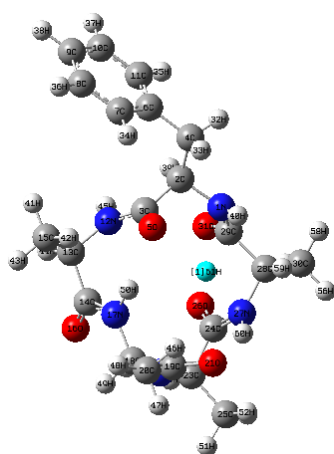
The O1 and O4 protonated structures were isoenergetic isomers (Figure 4.15). The energies of O5, O2 and O3 are far 8.5, 10.6 and 23.5 kJ/mol from those conformers. The oxazolone protonated F3_oxa, F1_oxa and F5_oxa were more stable than N-terminal protonated isomers F1_nterm, F3_nterm and F5_nterm in the all linear FA₄ residues (Figure 4.16). The relative energies of oxazolone protonated structures were around 32.8 kJ/mol, they are almost isoenergetic. Besides, the energies of N-terminal protonated isomers were in a range of 45.7-59.1 kJ/mol. It has been observed that the proton prefer to be on the oxazolone ring and the position effect was not predicted for the phenylalanine. In summary, the oxygen protonated macrocycle of FA₄ was the most favorable isomer and the oxazolone protonated linear structures have lower energy values than the nitrogen protonated isomers.



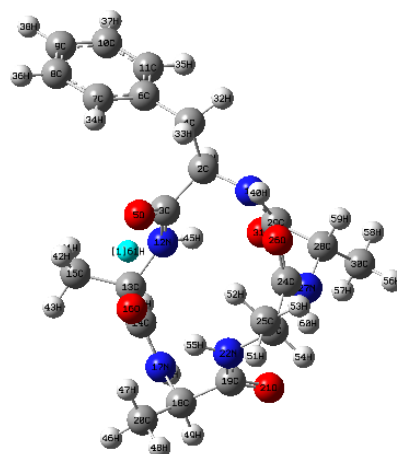
O1 (0.0 kJ/mol)



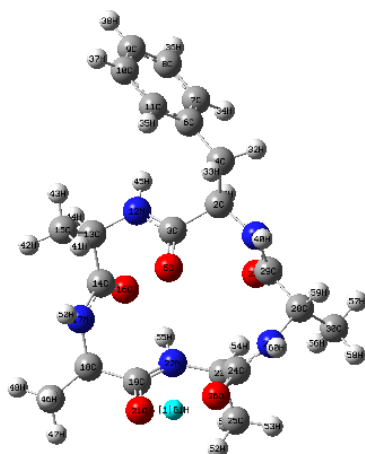
O4 (0.1 kJ/mol)



O2 (10.6 kJ/mol)

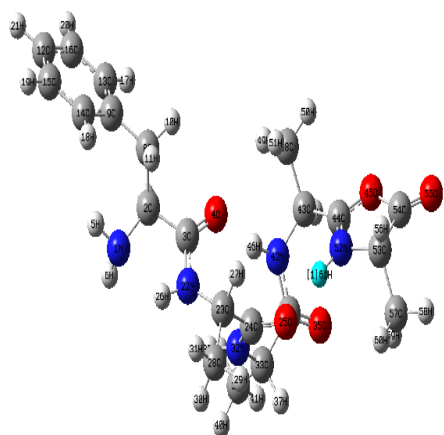


O5 (8.5 kJ/mol)

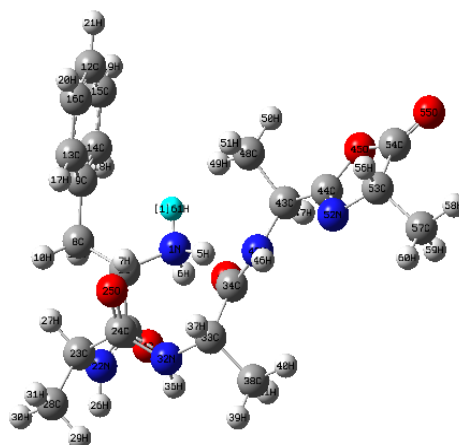


O3 (23.5 kJ/mol)

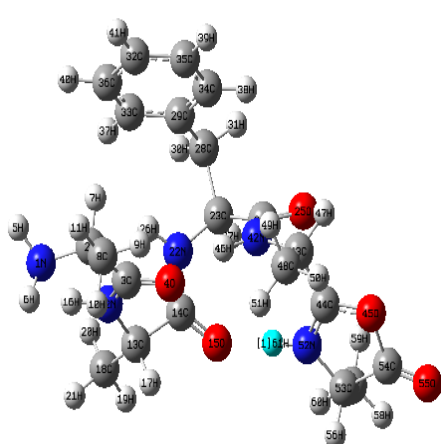
Figure 4.15. The macro-cyclic structures of oxygen protonated conformers of FA₄



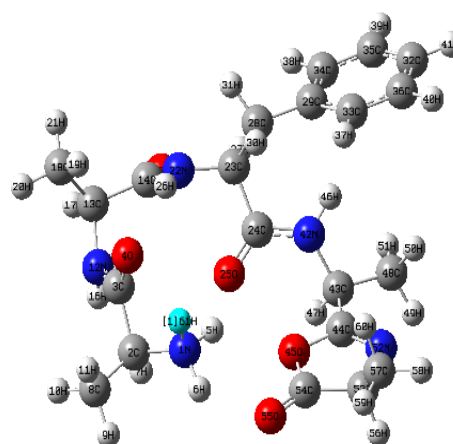
F1_oxa (32.3 kj/mol)



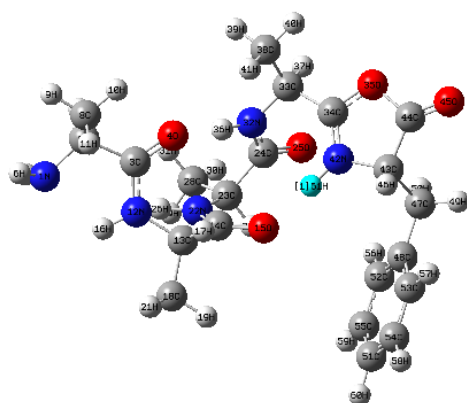
F1_nterm (45.7 kj/mol)



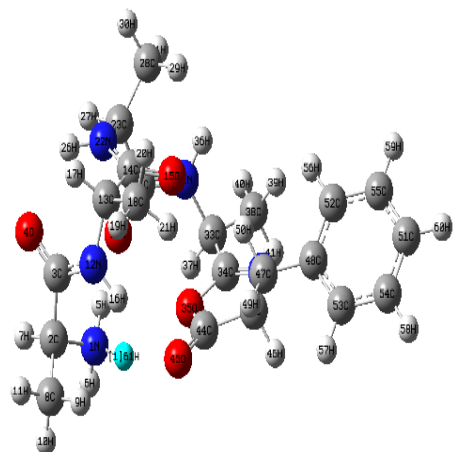
F3_oxa (31.7 kj/mol)



F3_nterm (56.6 kj/mol)



F5_oxa (34.4 kj/mol)



F5_nterm (59.1 kj/mol)

Figure 4.16. The linear structures of nitrogen protonated conformers of FA₄

4.6. The b_5^+ ions of YAAAA, AAYAA, AAAAY isomers

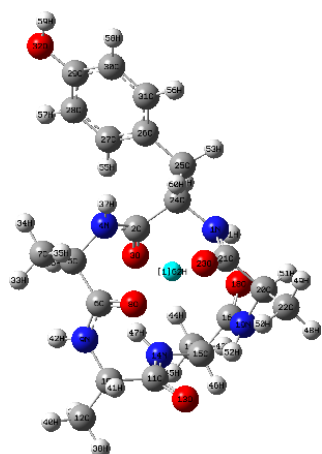
The linear b_5^+ ions of YAAAA, AAYAA and AAAAY have protonated from N-terminal nitrogen protonated and the nitrogen of oxazolone ring, and also oxygens have protonated in the macrocycle structures. The electronic and ZPE corrected energies of the lowest energy conformers have been given in Table 4.6.

Table 4.6. The electronic (E) and ZPE corrected energies of b_5^+ ions of YA₄

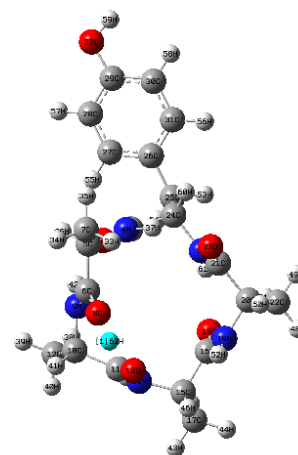
Protonated Site	E (au)	E+ZPE (au)	Rel E kj/mol	Rel (E+ZPE) kj/mol
O4	-1543.400510	-1542.883660	0.0	0.0
O3	-1543.399742	-1542.883016	2.0	1.7
O2	-1543.398310	-1542.881184	5.8	6.5
O5	-1543.395222	-1542.877985	13.9	14.9
O1	-1543.390942	-1542.876696	25.1	18.3
Y5_oxa	-1543.383035	-1542.868523	45.9	39.7
Y3_oxa	-1543.383540	-1542.868492	44.6	39.8
Y1_oxa	-1543.382773	-1542.867866	46.6	41.5
Y1_nterm	-1543.379245	-1542.863199	55.8	53.7
Y5_nterm	-1543.375448	-1542.858888	65.8	65.0
Y3_nterm	-1543.374593	-1542.857822	68.0	67.8

The lowest energy conformer is found as the O4 oxygen protonated macrocycle isomer (Figure 4.17) among the b_5^+ ions of YA₄ residues. The relative energies of O3, O2, O5 and O1 were between 1.7 and 18.3 kJ/mol. The oxazolone protonated Y5_oxa, Y3_oxa and Y1_oxa were more stable than N-terminal protonated isomers Y1_nterm, Y5_nterm and Y3_nterm in the all linear YA₄ residues (Figure 4.18). The relative energies of oxazolone protonated structures were very similar around 40.3 kJ/mol. So, there is no position effect for those linear isomers. Also, the energies of N-terminal protonated isomers were in a range of 53.7-67.8 kJ/mol.

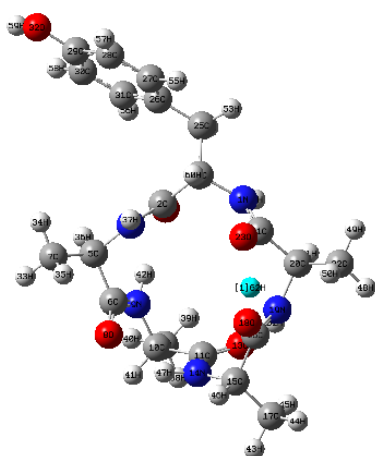
As a result, the oxygen protonated macrocycle of YA₄ was the most favorable isomer. And the oxazolone protonated linear structures have lower energy values than the nitrogen protonated isomers. Similar to phenylalanine case, tyrosine can be joined to the N-terminal, C-terminal side or at the mid-part of the peptide.



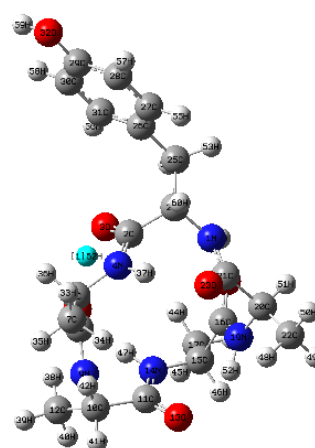
O1 (18.3 kj/mol)



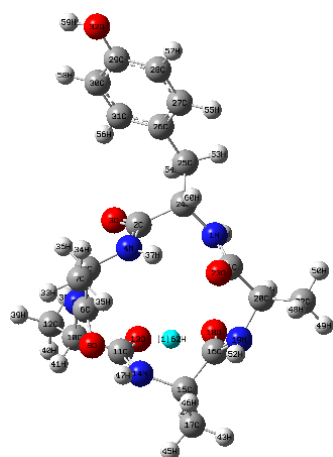
O4 (0.0 kj/mol)



O2 (6.5 kj/mol)

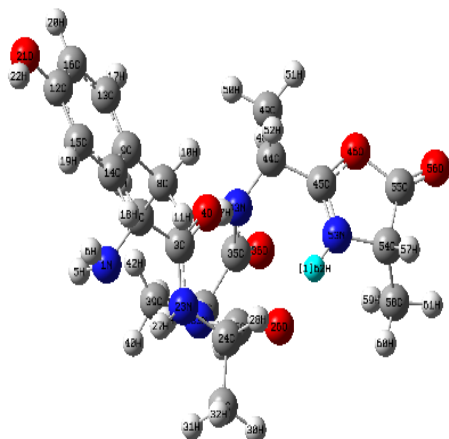


O5 (14.9 kj/mol)

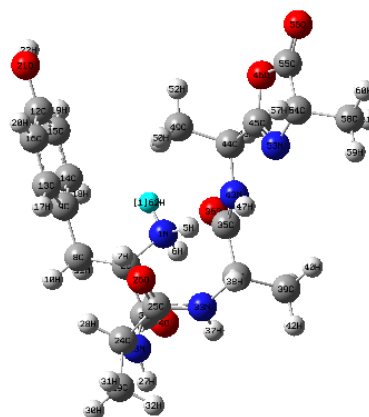


O3 (1.7 kj/mol)

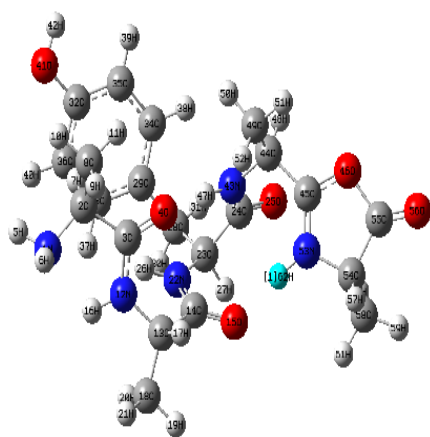
Figure 4.17. The macrocyclic structures of oxygen protonated conformers of YA₄



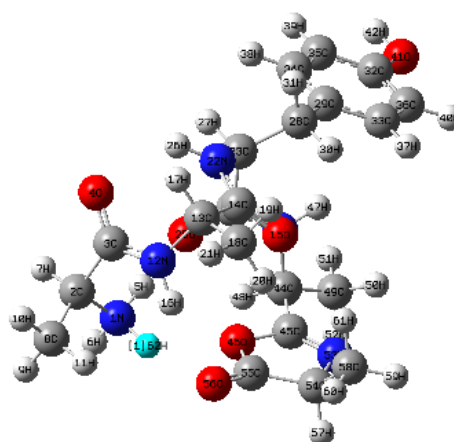
Y1_oxa (41.5 kJ/mol)



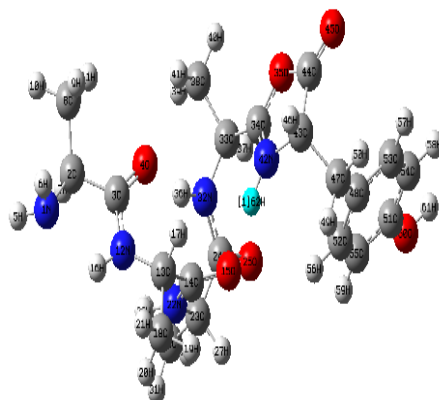
Y1_nterm (53.7 kJ/mol)



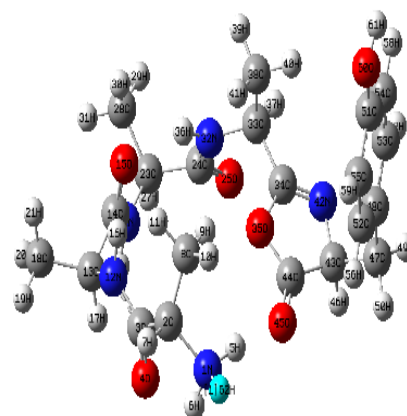
Y3_oxa (39.8 kJ/mol)



Y3_nterm (67.8 kJ/mol)



Y5_oxa (39.7 kJ/mol)



Y5_nterm (65.0 kJ/mol)

Figure 4.18. The linear structures of nitrogen protonated conformers of YA₄

4.7. The b_5^+ ions of CAAAA, AACAA, AAAAC isomers

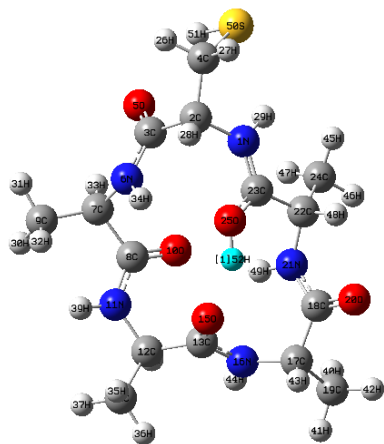
The linear b_5^+ ions of CAAAA, AACAA and AAAAC have protonated from two different sites; N-terminal nitrogen protonated and the nitrogen of oxazolone ring. Moreover, oxygens and sulfur on the cysteine side (C_cys_sp) were protonated in the macrocycle skeleton. The electronic and ZPE corrected energies of the lowest energy conformers have been given in Table 4.7.

Table 4.7. The electronic (E) and ZPE corrected energies of b_5^+ ions of CA₄

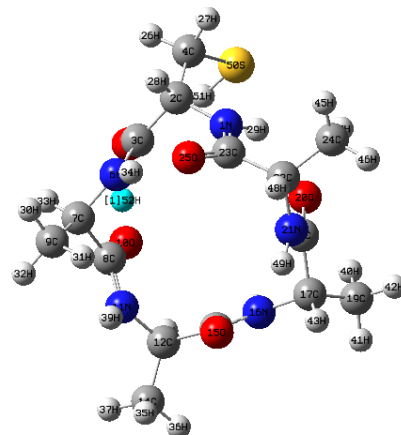
Protonated Site	E (au)	E+ZPE (au)	Rel E kJ/mol	Rel (E+ZPE) kJ/mol
O5	-1635.288063	-1634.856877	0.0	0.0
O2	-1635.287782	-1634.855845	0.7	2.7
O4	-1635.284706	-1634.853954	8.8	7.7
O1	-1635.283098	-1634.851659	13.0	13.7
O3	-1635.281555	-1634.850592	17.1	16.5
C3_oxa	-1635.276091	-1634.846933	31.4	26.1
C1_oxa	-1635.273731	-1634.844595	37.6	32.2
C5_oxa	-1635.272089	-1634.843010	41.9	36.4
C1_nterm	-1635.268244	-1634.836895	52.0	52.5
C5_nterm	-1635.267828	-1634.836764	53.1	52.8
C3_nterm	-1635.267078	-1634.835964	55.1	54.9
C_cys_sp	-1635.229020	-1634.799456	155.0	150.8

The O5 oxygen protonated macrocycle structure is obtained as the most stable structure (Figure 4.19) among the b_5^+ ions of CA₄ residues. The relative energies of O2, O4, O1 and O3 were between 2.7 and 16.5 kJ/mol. The protonated sulfur on the cysteine side (C_cys_sp) isomer was the least favorable among them. The oxazolone protonated C3_oxa (26.1 kJ/mol), C1_oxa (32.2 kJ/mol) and C5_oxa (36.4 kJ/mol), were more stable than N-terminal protonated isomers. C1_nterm, C5_nterm and C3_nterm have close energies (Figure 4.20).

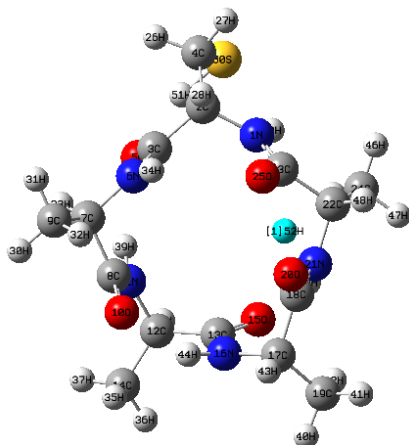
Consequently, the oxygen protonated macrocycle of CA₄ was the most favorable isomer. And the oxazolone protonated linear structures have lower energy values than the nitrogen protonated isomers.



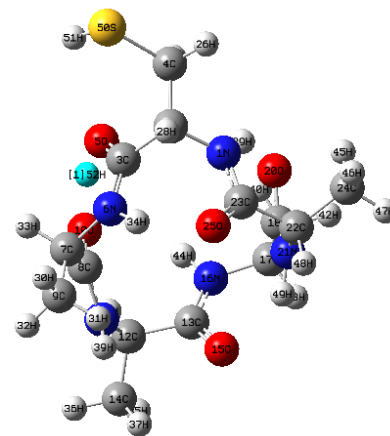
O1 (13.7 kj/mol)



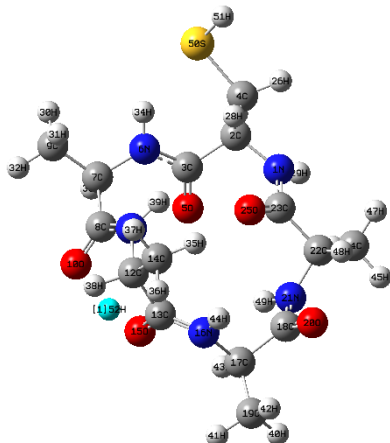
O4 (7.7 kj/mol)



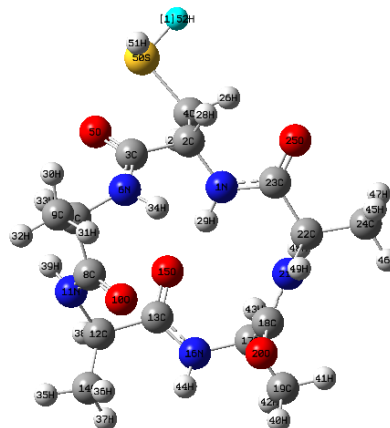
O2 (2.7 kj/mol)



O5 (0.0 kj/mol)

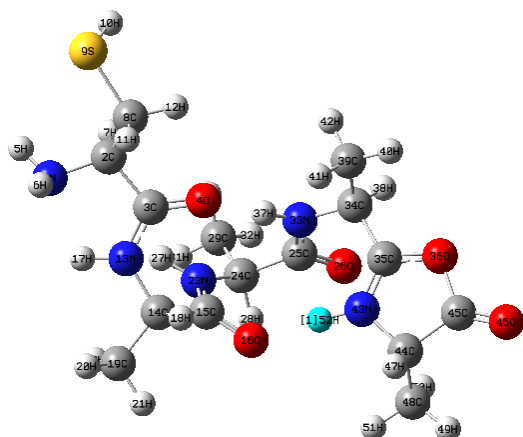


O3 (16.5 kj/mol)

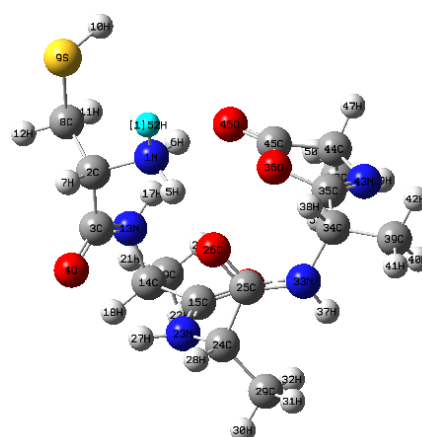


C_cys_sp (150.8 kj/mol)

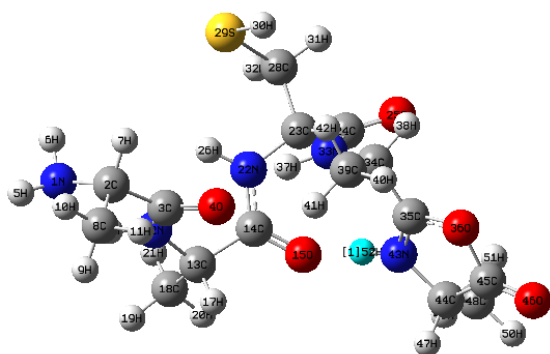
Figure 4.19. The macrocyclic structures of oxygen protonated conformers of CA₄



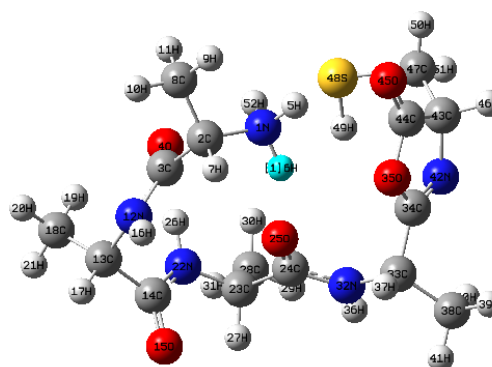
C1_oxa (32.2 kJ/mol)



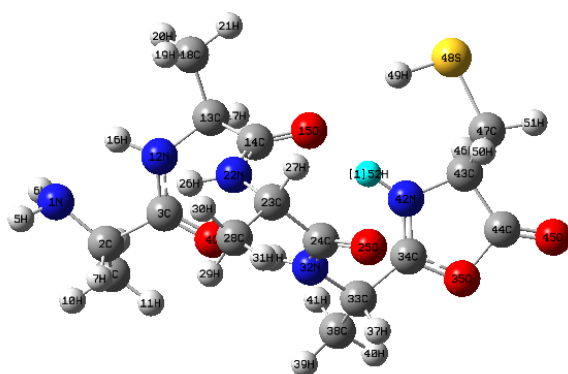
C1_termin (52.5 kJ/mol)



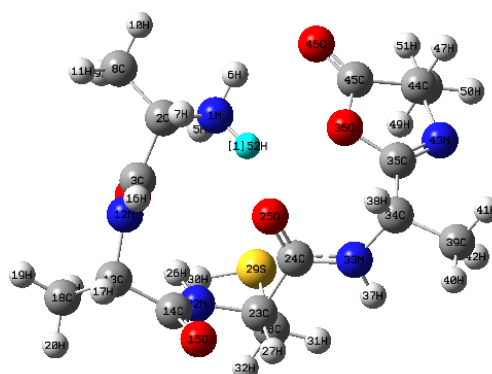
C3_oxa (26.1 kJ/mol)



C3_termin (52.8 kJ/mol)



C5_oxa (36.4 kJ/mol)



C5_termin (54.9 kJ/mol)

Figure 4.20. The linear structures of nitrogen protonated conformers of CA4

4.8. The Conformational Analyses of the b_5 ions

In this part of the thesis, the relative ZPE corrected energies ($E+ZPE$) of the most stable b_5^+ ions of the five protonated oxygen macrocycle (O1, O2, O3, O4, O5) and three protonated linear isomers (X1, X3, X5) have been summarized for the Asn, Asp, Leu, Phe, Try and Cys residues.

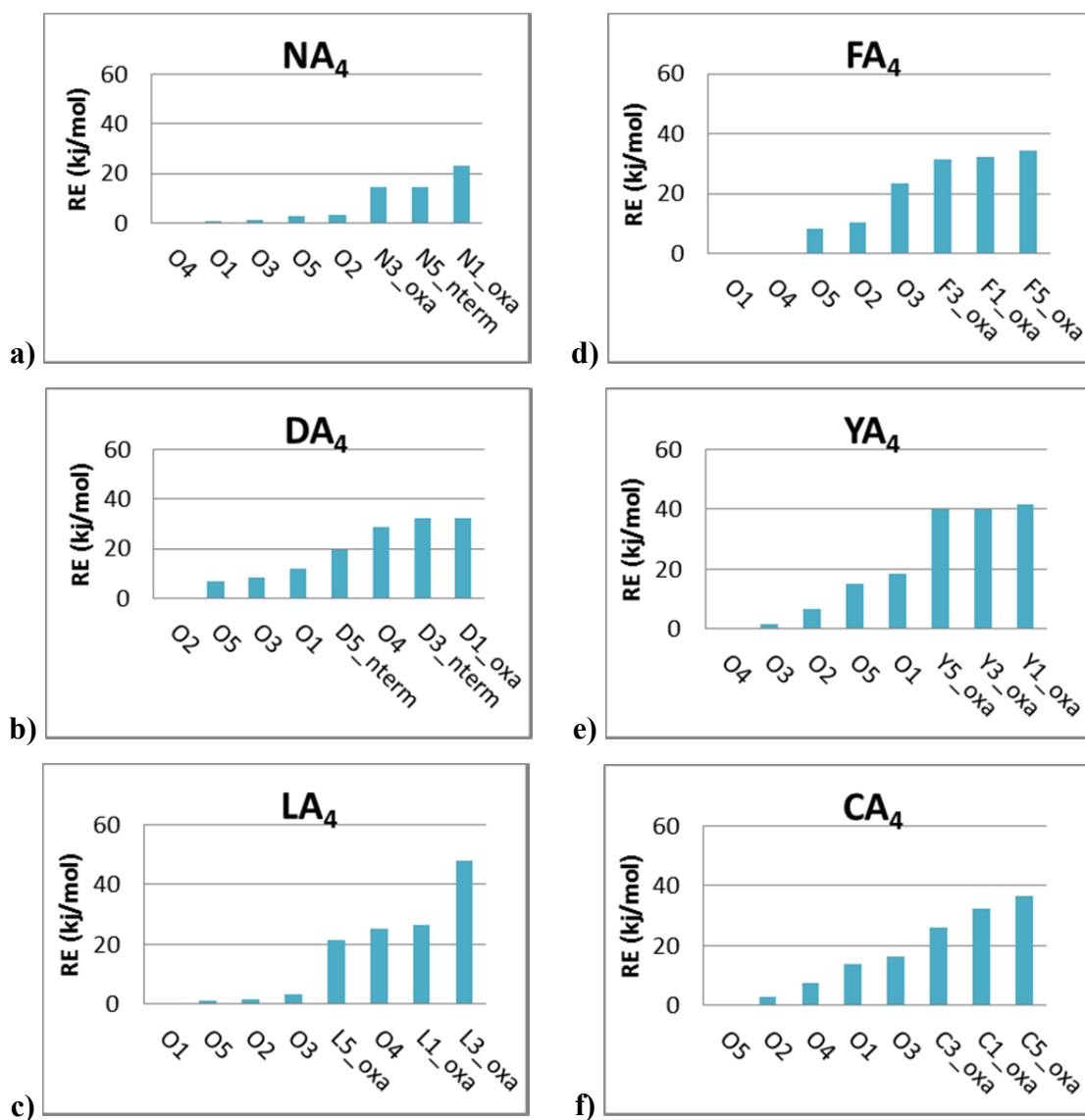


Figure 4.21. Relative Energy ($E+ZPE$) of protonated oxygen macrocycle and linear of b_5^+ ions

In all b_5^+ ions subject to this thesis, oxygen protonated macrocycle structures were the most likely isomers (see Figure 4.21). In NA₄ and LA₄ residues, the proton can be found on any oxygen in the macrocycle except O4 oxygen protonated of LA₄ cycle.

On the other hand; for the rest of b_5^+ ions, the stability of isomers were effected by the position of protonated oxygen. Some of the oxygen protonated isomers have higher energies than the linear structures such as the O4 of the DA₄ and LA₄. Moreover, the nitrogen protonated in the macrocycle isomers were unlikely found isomers. The relative energies of nitrogen protonated in the cycle were in the range of 47.4-72.9 kJ/mol for NA₄ (Table 4.2), 60.0-66.3 kJ/mol for LA₄ (Table 4.4). Also the DA₄ residue has least unfavorable nitrogen protonated structures. Since the energies of the structures were between 62.5 and 110.5 kJ/mol (Table 4.3).

In the linear structures, the oxazolone protonated structures have the lower energies than the N-terminal nitrogen protonated isomers in all positions except NA₄ and DA₄ residues (see Figure 4.21). The N5_terminus was more stable than the N5_oxa in NA₄, D5_terminus and D3_terminus were more favorable than the oxazolone ones in DA₄ residue. The energy difference between macrocycle and linear ones were almost the same for the all position of the residues for FA₄ and YA₄. These differences have about 8 kJ/mol higher energy values in YA₄ than the FA₄ residue. This result could be arisen from the -OH group of the tyrosine. Because the side group (R) of the tyrosine has -OH group, whereas phenylalanine has not. Furthermore, the NA₄ has the smallest energy differences between macrocycle and linear isomers less than 20 kJ/mol. In addition, that difference becomes around 20 kJ/mol for D, L and C containing ions. On the other hand, Y case has highest difference, around 40 kJ/mol energy differences.

4.9. The Geometry and Charge Analyses of the most favorable b_5 ions

In this section, the bond lengths, angles and Natural Bond Orbital (NBO) charge analysis of the most stable isomers of the b_5^+ ions structures have been investigated. In Figure 4.22, the “A” has been denoted Ala and “X” has been represented Asn, Asp, Leu, Phe, Try or Cys.

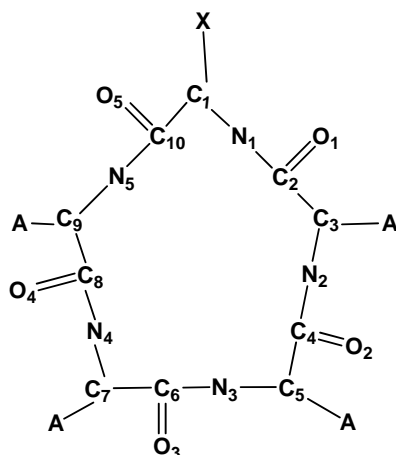


Figure 4.22. The general structure of macrocycle of neutral b_5 ions

Table 4.8. The bond lengths (in Å) of protonated b_5^+ ions

	Asn(N)	Asp(D)	Leu(L)	Phe(F)	Tyr(Y)	Cys (C)
C1-N1	1.4622	1.4721	1.4854	1.4858	1.4680	1.4657
N1-C2	1.3486	1.3280	1.3173	1.3220	1.3582	1.3614
C2-O1	1.2417	1.2574	1.2934	1.2873	1.2352	1.2400
C2-C3	1.5497	1.5401	1.5295	1.5308	1.5486	1.5410
C3-N2	1.4670	1.4852	1.4720	1.4667	1.4719	1.4749
N2-C4	1.3565	1.3175	1.3592	1.3602	1.3534	1.3567
C4-O2	1.2297	1.2934	1.2408	1.2398	1.2336	1.2367
C4-C5	1.5543	1.5288	1.5436	1.5428	1.5451	1.5497
C5-N3	1.4641	1.4725	1.4694	1.4695	1.4768	1.4730
N3-C6	1.3438	1.3605	1.3555	1.3553	1.3328	1.3540
C6-O3	1.2482	1.2395	1.2378	1.2379	1.2542	1.2335
C6-C7	1.5369	1.5447	1.5472	1.5468	1.5401	1.5461
C7-N4	1.4815	1.4710	1.4803	1.4793	1.4841	1.4782
N4-C8	1.3128	1.3559	1.3535	1.3538	1.3210	1.3318
C8-O4	1.2925	1.2373	1.2345	1.2338	1.2889	1.2554
C8-C9	1.5305	1.5453	1.5477	1.5491	1.5310	1.5410
C9-N5	1.4515	1.4802	1.4766	1.4765	1.4660	1.4846
N5-C10	1.3674	1.3553	1.3343	1.3288	1.3594	1.3207
C10-O5	1.2237	1.2335	1.2537	1.2583	1.2406	1.2896
C10-C1	1.5451	1.5508	1.5411	1.5417	1.5413	1.5287

In Table 4.8, bond lengths of the atoms in the macrocycle have been explored. For the macrocycle including Asparagine (Asn), the C-N bond distances are about 1.465 Å, except the C7-N4 and C9-N5 bonds. As the C7-N4 bond length was increased to 1.481 Å, the C9-N5 length was decreased to 1.451 Å. The N-C (nitrogen-carbonyl carbon; peptide bond) bond lengths are ~1.350 Å. But N4-C8 bond length was decreased to 1.313 Å and the N5-C10 bond was increased to 1.367 Å. So, it has been detected that C-N bond lengths were larger than the N-C bond. The C-O (carbonyl carbon-oxygen) bond lengths were between 1.224-1.292 Å. The largest one was the C8-O4. The C-C bonds were about 1.530-1.550 Å. The smallest C-C bond lengths were observed for the C8-C9 and C6-C7 bonds. It has been observed that, the bonds deviated more from their average values in the field of the proton.

When the all macrocycle structures including with different amino acids N, D, L, F, Y, C, have been analyzed, the results similar to Asn have been observed. The bond lengths have been mostly changed at the protonated part of the ions. The C-N and C-O bond distances have been deviated from their average bond lengths in a range of 0.009-0.016 Å and 0.038-0.045 Å respectively. On the other hand; N-C and C-C bond lengths have been deviated from the average distances 0.022-0.033 Å and 0.010-0.013 Å respectively at the protonation part of the macrocycle. The most affected bond is the C-O bonds, since oxygen of the carbonyl has been bonded to the hydrogen (protonated site) and the hydrogen like to be close to the other oxygen, so this bond has weakened. It has been noticed that, in the protonated region, there were a small cycle present in the structure of all macrocycles. The average bond distance in all macrocycles of the C-O, N-C, C-N, C-C were about 1.251 Å, 1.345 Å, 1.474 Å, 1.542 Å respectively. The change of the amino acid residue (X) in the macrocycle hasn't much affected the bond distances on the macrocycle skeleton. As shown in Figure 4.23, that means there is no amino acid effect on the bond lengths of macrocycle isomer.

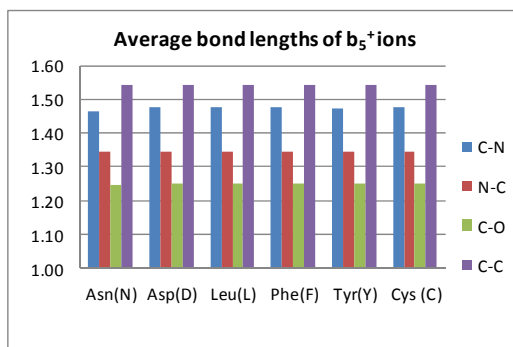


Figure 4.23. The average bond lengths (Å) of the macrocycle isomers

Table 4.9. The NBO charges of the b_5^+ ions

	Asn(N)	Asp(D)	Leu(L)	Phe(F)	Tyr(Y)	Cys(C)
C1	-0.159	-0.142	-0.147	-0.141	-0.145	-0.152
N1	-0.673	-0.622	-0.599	-0.603	-0.656	-0.667
C2	0.701	0.694	0.725	0.731	0.684	0.698
O1	-0.698	-0.693	-0.656	-0.657	-0.660	-0.663
C3	-0.156	-0.154	-0.146	-0.144	-0.156	-0.155
N2	-0.651	-0.600	-0.662	-0.660	-0.643	-0.659
C4	0.685	0.726	0.701	0.699	0.676	0.688
O2	-0.654	-0.656	-0.672	-0.669	-0.659	-0.665
C5	-0.161	-0.145	-0.156	-0.155	-0.153	-0.157
N3	-0.614	-0.661	-0.662	-0.653	-0.603	-0.643
C6	0.718	0.700	0.684	0.683	0.696	0.675
O3	-0.659	-0.669	-0.660	-0.661	-0.678	-0.656
C7	-0.161	-0.155	-0.156	-0.156	-0.154	-0.150
N4	-0.584	-0.664	-0.645	-0.645	-0.604	-0.601
C8	0.729	0.683	0.680	0.681	0.728	0.696
O4	-0.660	-0.658	-0.661	-0.659	-0.655	-0.680
C9	-0.150	-0.156	-0.153	-0.151	-0.144	-0.155
N5	-0.688	-0.646	-0.606	-0.596	-0.656	-0.602
C10	0.686	0.677	0.699	0.697	0.704	0.729
O5	-0.614	-0.650	-0.679	-0.686	-0.672	-0.665

The charge analyses of the lowest energy macrocycles of b_5^+ have been carried out with NBO calculations given in Table 4.9. For the Asn, the carbon atoms; C1, C3, C5, C7, C9, have negative charges which are in a range of -0.150 au and -0.161 au, whereas carbon atoms which are bonded to oxygen atoms (C2, C4, C6, C8, C10) have positive charges between +0.685 au and +0.729 au. Moreover, the nitrogen atoms N1, N2, N3, N4, N5, have negative charges, change from -0.584 to -0.688u. The oxygen atoms O1, O2, O3, O4, O5, also have negative values between -0.614 au and -0.698 au. The most positive charge of atoms were carbon atoms bonded to oxygen atoms. The least negative charges of atoms were carbon atoms. The charge of oxygen atoms were slightly more negative values than the nitrogen atoms.

For all type of macrocycle structures, the positive and negative charges of atoms were same but the magnitudes of the charges were changed according to the different protonation site and containing different amino acid. The carbonyl carbon atom has the highest positive charges, where the protonated oxygen bonded. The charge for this carbon C8 (for Asn, Tyr) , C2 (for Leu, Phe), C4 (for Asp), C10 (for Cys) atom was around +0.73u which deviates from corresponding average value by 0.03 au. In contrast

to carbon atoms, the nitrogen atoms near to protonation site have the lowest negative charge in magnitude (0.60 au, about 0.05 au deviation from the corresponding average) (N4; Asn, N2; Asp, N1; Leu). In Phe, Tyr, Leu substituted macrocycles, beside this nitrogen atom, there was second nitrogen atom which has about the same charge (N1,N5; Phe, N4,N3; Tyr, N5,N4; Cys).

The charge of oxygens of Asn was the most affected among the others. The difference of the charge between O1 and O5 was 0.084u on the other hand; the others were between 0.023 and 0.043u. The Asn has influenced on the charge of oxygen more than the other type of amino acids. When the comparison of the same protonated oxygen (O1) of the Leu and Phe has been done, the trends of the atomic charges of were almost similar. For the O4 protonated of the Asn and Tyr, the charges of the atoms were not same in magnitude. For instance, the carbon atoms of the Asn were lower negative charges than the Tyr in the range of -0.06 and -0.014 u.

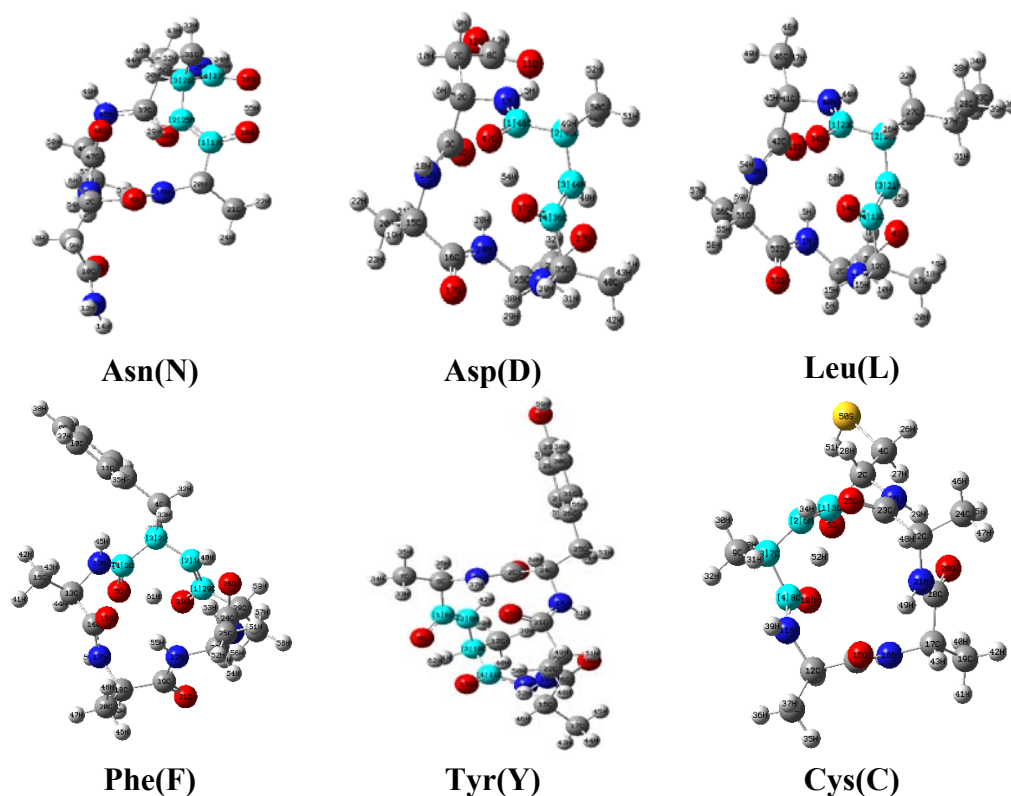


Figure 4.24. The most stable structures of the b_5^+ ions
The light blue color shows that the small proton cycle region in the macrocycle structures.

The small protonation cycle has been observed in the macrocycle structure for all amino acid types where the hydrogen bonded to the oxygen atom (see Figure 4.24). In Figure 4.25, the new labels were given to the atoms in this proton cycle for an easy discussion. The protonated oxygen was labeled as O2 for the all macrocycles.

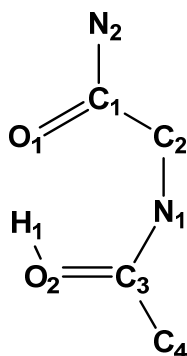


Figure 4.25. The general structure of the proton cycle

Table 4.10. The bond lengths (in Å) and angles of the proton cycles of b_5^+ ions

	Asn(N)	Asp(D)	Leu(L)	Phe(F)	Tyr(Y)	Cys(C)
O1-C1	1.248	1.257	1.254	1.258	1.254	1.255
C1-C2	1.537	1.540	1.541	1.542	1.540	1.541
C2-N1	1.481	1.485	1.485	1.486	1.484	1.485
N1-C3	1.313	1.318	1.317	1.322	1.321	1.321
C3-O2	1.292	1.293	1.293	1.287	1.289	1.290
O2-H1	1.036	1.040	1.040	1.057	1.047	1.051
H1-O1	1.502	1.502	1.498	1.439	1.471	1.456
O1-C1-C2	118.4	117.6	117.4	117.1	117.5	117.5
C1-C2-N1	109.1	107.2	106.7	107.3	107.3	107.5
C2-N1-C3	129.2	126.4	126.6	127.4	126.9	127.0
N1-C3-O2	123.9	123.0	123.2	123.1	123.3	123.3
C3-O2-H1	112.3	110.7	110.7	109.7	110.5	110.6
O2-H1-O1	159.0	157.1	156.5	158.9	158.1	158.6
H1-O1-C2	107.8	109.1	109.5	111.3	110.2	110.6

The bond lengths of the proton cycle have been listed in Table 4.10. For the Asn, the O2-H1 bond length is the shortest one which was 1.036 Å, whereas the C1-C2 (carbon-carbon) is the largest distance of 1.537 Å. The C3-O2 (1.292 Å) bond length is larger than the O1-C1 (1.248 Å). Furthermore, N1-C3 (1.313 Å) bond is shorter than the C2-N1 (1.481 Å) distance. The O1 atom was closed to the H1 atom which bonded to O2 atom with a distance of 1.501 Å.

The same trend has been seen in the all the macrocycle structures. For all macrocycles, the average bond distance of the O2-H1, O1-C1, C3,O2, N1-C3, H1-O1, C2-N1, C1-C2 were about 1.045 Å, 1.255 Å, 1.291 Å, 1.319 Å, 1.478 Å, 1.484 Å, 1.540 Å respectively. And also there were no significant change in bond angles of the small protonation cycle structures when the amino acid species is changed. (see Table 4.10).

In this cycle, by the effect of proton the bonds are weakened or strengthened alternatively with respect to the same type of bonds in the entire macrocycle. The C3-O2 bonds (the protonated one) were longer by +0.046 Å from other C-O bonds in the macrocycle. In the same way, the C1-O1 bond which was also in the proton cycle and located on the other side of proton were lengthened by +0.016 Å. Furthermore, C2-N1 bond lengths were +0.012 Å stretched with respect to the other C-N bonds. On the other hand, N1-C3 bond lengths and were decreased by -0.028 Å with respect to the same type N-C bonds in the macrocycles. In addition, C1-C2 bond lengths slightly shortened as -0.005 from the other C-C bonds.

Table 4.11. The NBO charges of the proton cycles of b_5^+ ions

	Asn(N)	Asp(D)	Leu(L)	Phe(F)	Tyr(Y)	Cys(C)
O1	-0.659	-0.693	-0.679	-0.686	-0.678	-0.680
C1	0.718	0.694	0.699	0.697	0.696	0.696
C2	-0.161	-0.154	-0.147	-0.141	-0.154	-0.155
N1	-0.584	-0.600	-0.599	-0.603	-0.604	-0.602
C3	0.729	0.726	0.725	0.731	0.728	0.729
O2	-0.660	-0.656	-0.656	-0.657	-0.655	-0.665
H1	0.548	0.548	0.549	0.547	0.548	0.549
Total	-0.069	-0.135	-0.108	-0.112	-0.119	-0.128

The NBO charge analysis of the small protonation cycle has been investigated and given in Table 4.11. Similar to the bond distances, the charges of atoms which construct the small proton ring deviates from the same type of atom in the macrocycle. For the Asn, the highest negative charges were in the oxygen atoms O1 and O2 with a charge of -0.66 au. The second highest negative charge was in the N1 (-0.584u). The largest positive charges were in C3 (+0.73 au) and C1 (+0.72 u), whereas the C2 (-0.16 au) has the negative charge. The charge of proton, H1 was the +0.55 au.

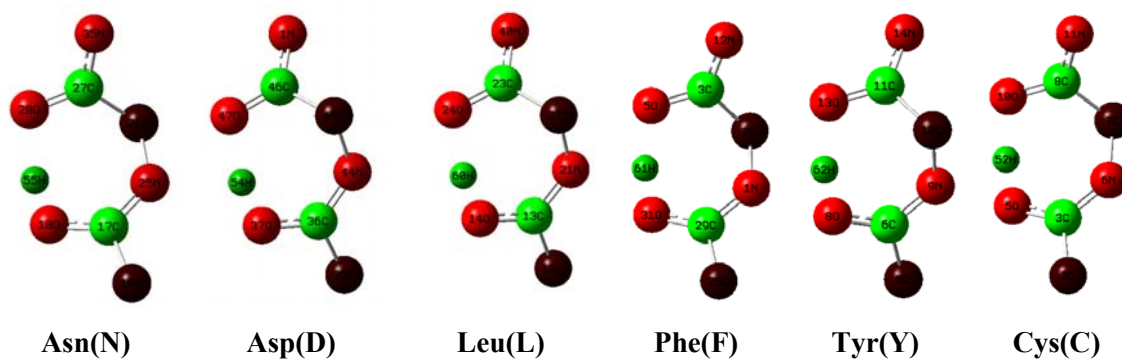


Figure 4.26. The NBO charged with color of the proton cycles of b5+ ions

For the all macrocycle structures we have observed the same trend;, almost the same charge distribution as shown in Figure 4.26. (The red atomic color indicates the negative charges; the green atomic color indicates the positive charges). The oxygen atoms have the highest negative charges. The carbon atoms C1 ($\sim+0.70u$) and C3 ($\sim+0.73u$) have the largest positive charge. In addition to that, the proton, charges were approximately $+0.55u$. The charge of C3 has higher positive charge than C1 between $0.011u$ and $0.034u$. Furthermore, the charge of the O1 was larger than the O2 except Asn. The total NBO charge on the protonation cycle was about $-0.12u$ except Asn where this charge was around $-0.07u$.

CHAPTER 5

The b_5 and b_7 of HISTIDINE CONTAINING PEPTIDES

In this chapter, the size effect of the histidine containing peptide on the production of macrocycle structure has been studied. Bythell et al demonstrated that the position of the basic His residue is important for the macro-cyclization of b_5 ions. They reported their experimental results as, if the histidine residue is close to the N-terminal position, no clear evidence for cyclization whereas, if the histidine residue is near to the C-terminal position cyclization is observed [28]. On the other hand, in an unpublished experimental work, the position of the histidine residue was not significant for the macro-cyclization for larger b_7^+ ions of histidine containing peptides. To see the size effect on the cyclization, the structures of the b_5^+ ions of HAAAA, AAHAA, AAAAH and the b_7^+ ions of HAAAAA, AAAHAAA and AAAAAAH have been studied and compared each other according to their energy differences between linear and macrocycle isomers in this part of the thesis.

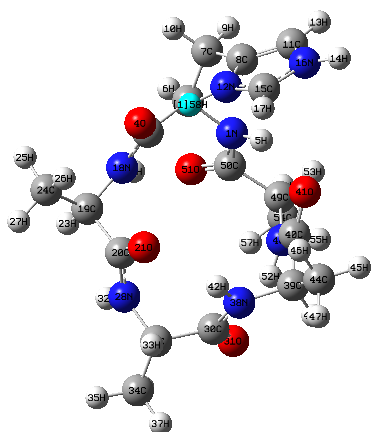
5.1. The b_5^+ ions of HAAAA, AAHAA, AAAAH isomers

The b_5^+ ions of HAAAA, AAHAA, AAAAH have been studied and some results were given and compared with the computational work done by Bythell et al. [28] to validate our method in the chapter 3. Each peptide has protonated from three different sites for the linear oxazolone structures; such as side chain nitrogen of histidine (H1_his_np, H3_his_np, H5_his_np), nitrogen of the oxazolone (H1_oxa, H3_oxa, H5_oxa) and nitrogen of the N-terminal (H1_nterm, H3_nterm, H5_nterm). On the other hand, side chain nitrogen of histidine (cyc_his_np) and oxygens of the residues (O1, O2, O3, O4, O5) have been protonated in the macro-cyclic structure. The electronic and ZPE corrected energies of the lowest energy conformers have been given in Table 5.1.

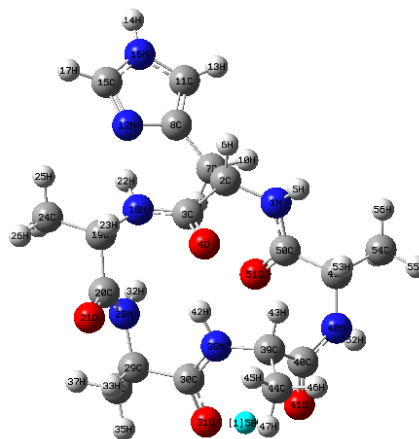
Table 5.1. The electronic (E) and ZPE corrected energies of b_5^+ ions of HA₄

Protonated Site	E (au)	E+ZPE (au)	Rel E kJ/mol	Rel (E+ZPE) kJ/mol
cyc_his	-1462.171600	-1461.685727	0.0	0.0
O5	-1462.155992	-1461.671454	41.0	37.5
O1	-1462.152064	-1461.667645	51.3	47.5
O3	-1462.150758	-1461.666179	54.7	51.3
H5_his_np	-1462.148655	-1461.665546	60.2	53.0
O4	-1462.149732	-1461.665391	57.4	53.4
H3_his_np	-1462.147427	-1461.665368	63.5	53.5
O2	-1462.149133	-1461.664697	59.0	55.2
H1_his_np	-1462.145825	-1461.663496	67.7	58.4
H3_oxa	-1462.139526	-1461.657765	84.2	73.4
H1_nterm	-1462.141662	-1461.657159	78.6	75.0
H1_oxa	-1462.137049	-1461.654664	90.7	81.6
H5_oxa	-1462.136593	-1461.654642	91.9	81.6
H3_nterm	-1462.137641	-1461.653475	89.2	84.7
H5_nterm	-1462.133773	-1461.651184	99.3	90.7

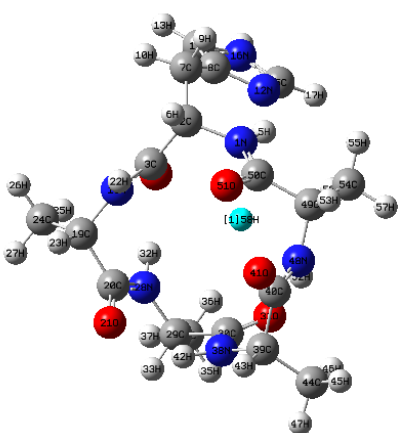
The side chain nitrogen of the histidine protonated macrocycle structure has the lowest energy conformer in b_5^+ ions of HA₄ residue (Figure 5.1). The O5 oxygen protonated structure with 37.5 kJ/mol relative energy was the most stable isomer among the oxygen protonated isomers. The relative energies of the other oxygen protonated structures were between 47.5 kJ/mol and 55.2 kJ/mol. On the other hand, the protonated side chain nitrogen on the histidine isomers has the lowest energy among the linear oxazolone structures (Figure 5.2). The relative energies of the structures of H5_his_np (53.0 kJ/mol) and H3_his_np (53.5 kJ/mol) were almost the same and they were approximately 5 kJ/mol more stable than the H1_his_np (58.4 kJ/mol) isomer. Moreover, the protonated nitrogen of the oxazolone structures H3_oxa and H5_oxa have lower energies than the protonated nitrogen of the N-terminal isomers H3_nterm and H5_nterm respectively. In contrast, H1_nterm has lower energy than the H1_oxa isomer.



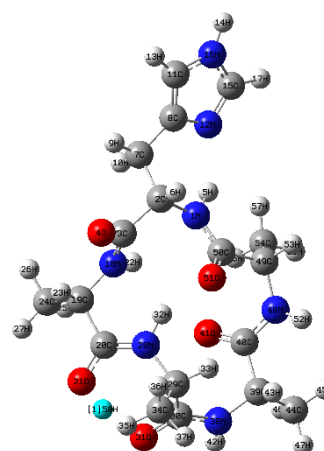
cyc his np (0 kj/mol)



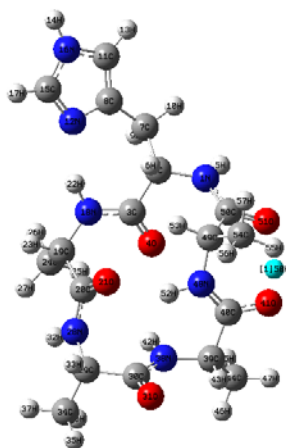
O3 (51.3 kj/mol)



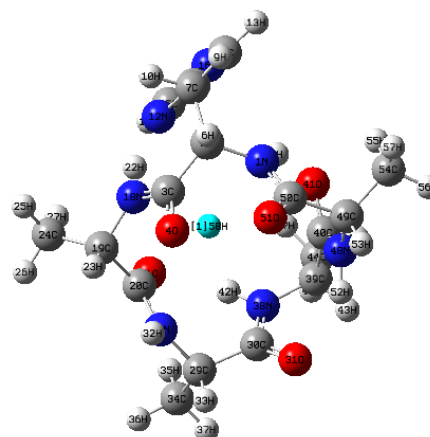
O1 (47.5 kj/mol)



O4 (53.4 kj/mol)

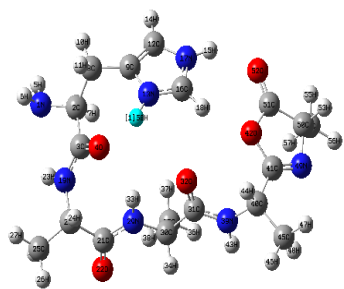


O2 (55.2 kj/mol)

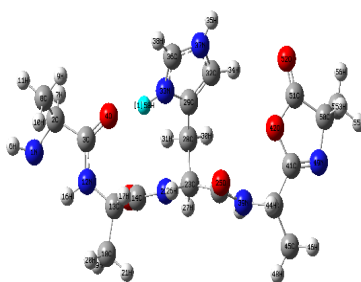


O5 (37.5 kj/mol)

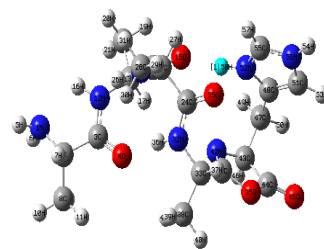
Figure 5.1. The macrocyclic structures of oxygen protonated conformers of HA₄



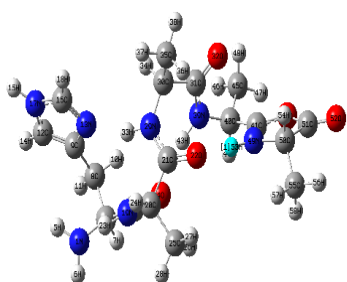
H1_his_np (58.4 kJ/mol)



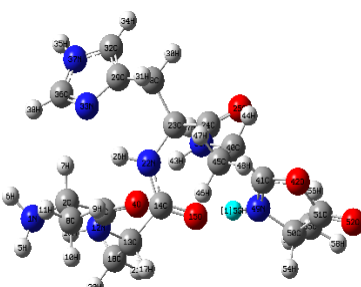
H3_his_np (53.5 kJ/mol)



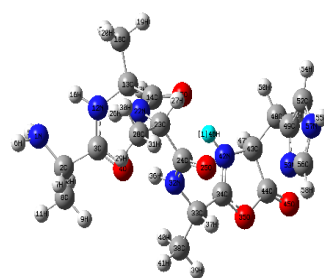
H5_his_np (53.0 kJ/mol)



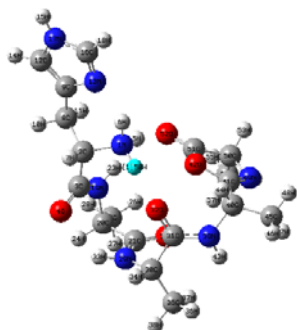
H1_oxa (81.6 kJ/mol)



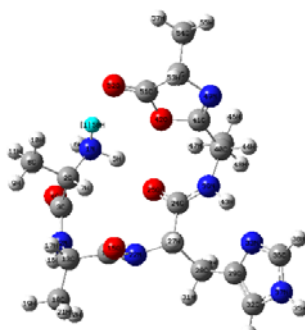
H3_oxa (73.4 kJ/mol)



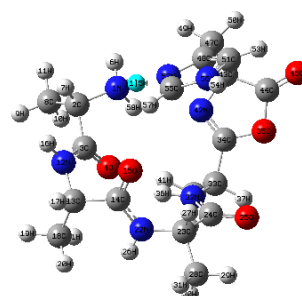
H5_oxa (81.6 kJ/mol)



H1_nterm (75.0 kJ/mol)



H3_nterm (84.7 kJ/mol)



H5_nterm (90.7 kJ/mol)

Figure 5.2. The linear structures of nitrogen protonated conformers of HA₄

5.2. The b_7^+ ions of HAAAAAA, AAAHAAA, AAAAAAH isomers

In this section, the structures of b_7^+ ions of HAAAAAA, AAAHAAA and AAAAAAH have been analyzed. Each peptide has been protonated from three different sites for the linear oxazolone ones such as; side chain nitrogen of histidine (H1_his_np, H4_his_np, H7_his_np), nitrogen of the oxazolone (H1_oxa, H4_oxa, H7_oxa), N-terminal nitrogen (H1_nterm, H4_nterm, H7_nterm). Alternatively, side chain nitrogen of histidine (cyc_his_np) and oxygens of the residues (O1, O2, O3, O4, O5, O6, O7,) have been protonated in the macro-cyclic structure. The optimization of b_7 ions have been carried out at B3LYP/6-31G(d) level of theory and then the energies are corrected by single point energy calculations at the B3LYP/6-31+G(d,p) level of theory. The electronic and ZPE corrected energies of the lowest energy conformers are given in Table 5.2.

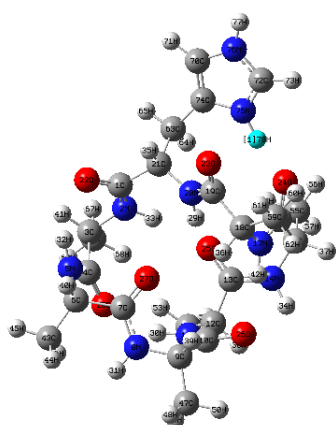
Table 5.2. The electronic (E) and ZPE corrected energies of b_5^+ ions of HA₆

Protonated Site	E (au)	E+ZPE (au)	Rel E kj/mol	Rel (E+ZPE) kj/mol
cyc_his_np	-1956.878850	-1956.223610	0.0	0.0
O1	-1956.866439	-1956.213531	32.6	26.5
O3	-1956.860826	-1956.207863	47.3	41.3
O7	-1956.860859	-1956.207802	47.2	41.5
O2	-1956.858116	-1956.206158	54.4	45.8
H7_his_np	-1956.857947	-1956.205574	54.9	47.4
O5	-1956.858674	-1956.205095	53.0	48.6
O4	-1956.854020	-1956.201470	65.2	58.1
H4_his_np	-1956.851208	-1956.200839	72.6	59.8
O6	-1956.853223	-1956.198982	67.3	64.7
H1_his_np	-1956.850242	-1956.197386	75.1	68.9
H7_oxa	-1956.846584	-1956.195787	84.7	73.0
H1_nterm	-1956.847615	-1956.194816	82.0	75.6
H1_oxa	-1956.845174	-1956.193983	88.4	77.8
H7_nterm	-1956.847448	-1956.193401	82.4	79.3
H4_nterm	-1956.842673	-1956.190434	95.0	87.1
H4_oxa	-1956.839144	-1956.187772	104.2	94.1

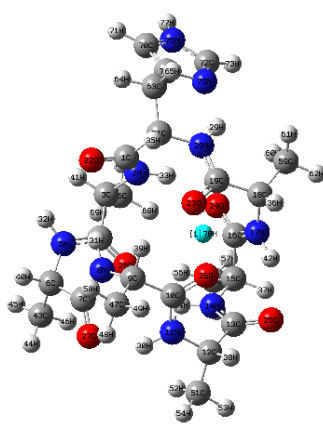
The lowest energy conformer of b_7^+ ions of HA₆ residue has the side chain nitrogen of the Histidine protonated macrocycle structure (Figure 5.3). In the oxygen protonated structures, O1 has the lowest relative energy (26.5 kj/mol) among them. Furthermore, the least stable oxygen protonated isomer was O6 with 64.7 kj/mol

relative energy and the relative energies of the other protonated oxygen isomers were higher than the 40 kJ/mol.

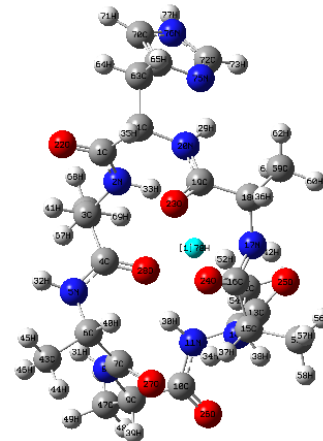
In the linear oxazolone structures, the side chain nitrogen of histidine protonated isomers have the lowest relative energies in all HA₆ residues (Figure 5.4). The relative energies of H7_his, H4_his and H1_his were 47.4 kJ/mol, 59.8 kJ/mol and 68.9 kJ/mol respectively. In addition, the protonated nitrogen of the N-terminal isomers were lower relative energies than the protonated nitrogen of the oxazolone structures except where histidine at the C-terminal (H7).



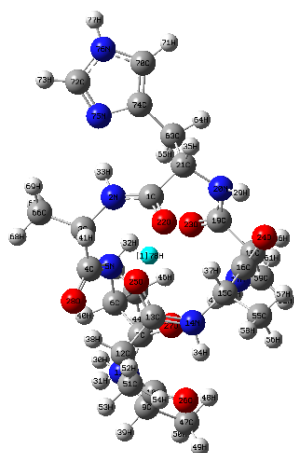
cyc his np (0 kJ/mol)



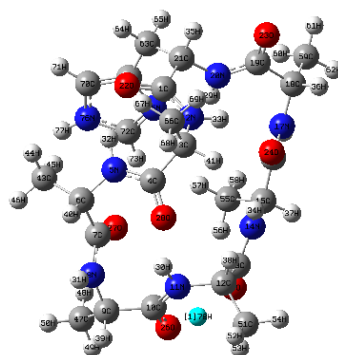
O1 (26.5 kJ/mol)



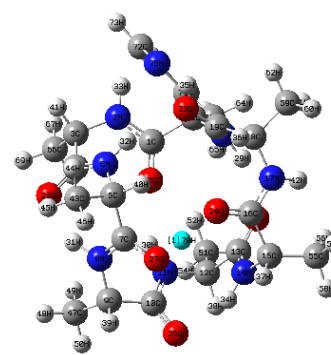
O2 (45.8 kJ/mol)



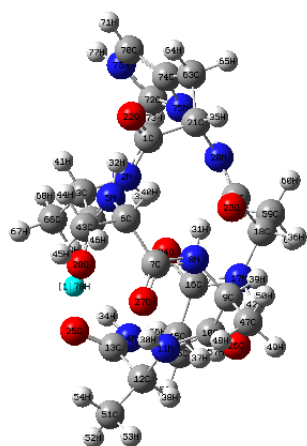
O3 (41.3 kJ/mol)



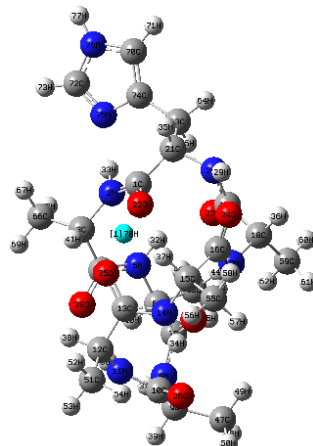
O4 (58.1 kJ/mol)



O5 (48.6 kJ/mol)

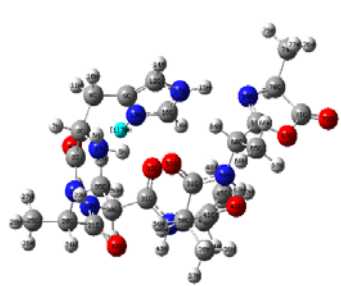


O6 (64.7 kJ/mol)

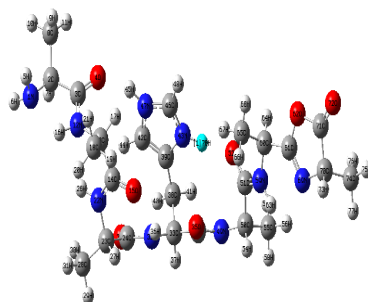


O7 (41.5 kJ/mol)

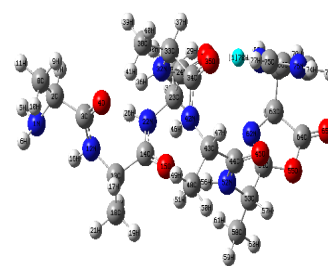
Figure 5.3. The macro-cyclic structures of oxygen protonated conformers of HA₆



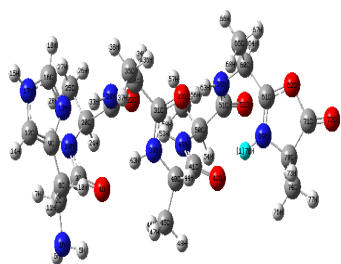
H1_his_np (68.9 kJ/mol)



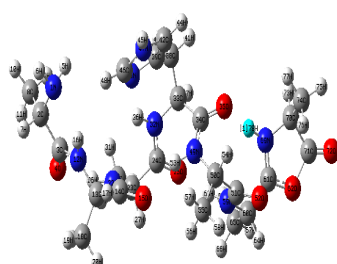
H4_his_np (59.8 kJ/mol)



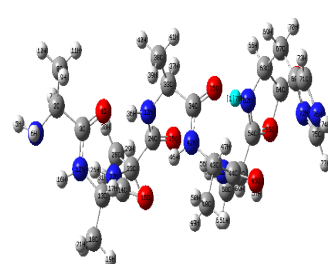
H7_his_np (47.4 kJ/mol)



H1_oxa (77.8 kJ/mol)



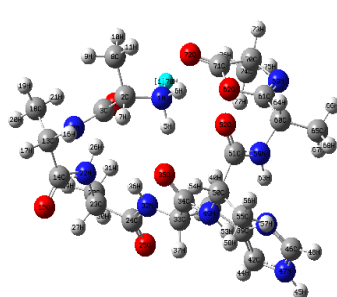
H4_oxa (94.1 kJ/mol)



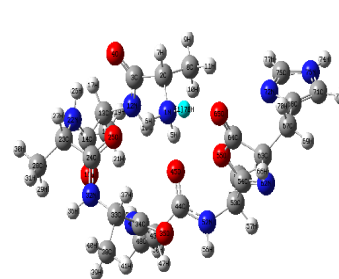
H7_oxa (73.0 kJ/mol)



H1_nterm (75.6 kJ/mol)



H4_nterm (87.1 kJ/mol)



H7_nterm (79.3 kJ/mol)

Figure 5.4. The linear structures of nitrogen protonated conformers of HA₆

5.3. Analysis of the b_5^+ and b_7^+ ions of histidine containing peptides

The relative ZPE corrected energies of the linear b_5 and b_7 isomers of histidine where nitrogen on the histidine was protonated at the N-terminal, center and C-terminal of the peptides were given in Figure 5.5. The results showed that, the histidine position was not significant for the b_5 isomers energetically since the stabilities of the isomers of HA_4 ions are very close to each other; the relative energies are in the range of 53-58 kJ/mol. Furthermore, in the b_7 , the energies of the isomers decreased as the histidine was close to the C-terminal side. The relative energy order was 48 kJ/mol, 60 kJ/mol and 69 kJ/mol for the H7_his_np (His-C-term), H4_his_np (His-center) and H1_his_np (His-N-term). However, the energies of those linear isomers were not dramatically altered since the largest energy difference is about 21 kJ/mol (5 kcal/mol). So, it can be said that, there was no significant position effect of the histidine on the b_7 ions. These results do not explain exactly the experimental observations for the position effect of histidine in HA_4 and HA_6 . The position of histidine is important for cyclization of b_5 ions whereas it is not for b_7 ions experimentally [44]. According to our results both size of b ions produce macrocycle which is preferable by 12-13 kcal/mol than linear structures. It should be noted that, these relative energy values might change, if more conformers were taken from PCO analyses due to many rotatable bonds. (Remember that 36 conformers of b_7 were used in quantum calculations as in the b_5 ions due to computational cost).

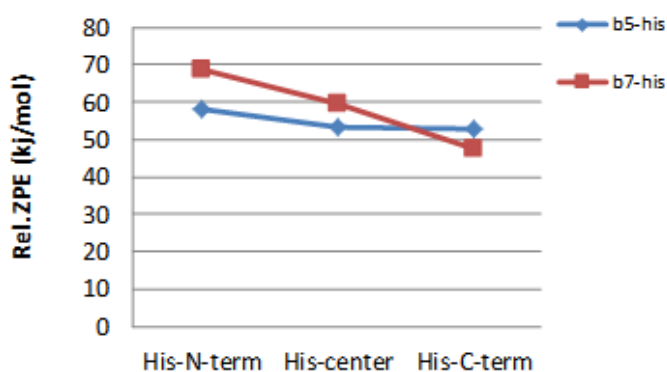


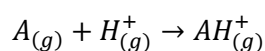
Figure 5.5. The relative ZPE corrected energies of the linear protonated b_5^+ and b_7^+ histidine isomers

CHAPTER 6

EFFECT OF PROTON AFFINITY ON THE FRAGMENTATION REACTIONS OF N-TERMINAL PROLINE CONTAINING HEXAPEPTIDES

6.1. Introduction

The observability of fragment ions as well as their relative abundances in the tandem mass spectra of protonated peptides entirely depends on the proton affinity of the fragment species in the gas-phase. Proton affinity of compound A is defined as the negative the enthalpy change in the gas phase based on the following reaction.



In a very simple point of view, basic amino acid residues have higher proton affinity than the aliphatic and acidic residues. Proton affinity issue needs to be well known in order to understand the gas-phase fragmentation mechanism of protonated peptides. The proton affinity study was well reviewed by Harrison [45]. In addition, the proton affinity of the amino acids and peptides has been investigated by numerous studies in detail by several groups [46-52]. Moreover, Maksic et al. [53] and Paizs et al. [54] determined the proton affinity of the 20 amino acids with computational methods and compared with experimental results. The Table 6.1 represents the experimental results of proton affinity of twenty natural amino acid residues.

Proline is the only cyclic amino acid found in the primary structure of proteins. Its unique structure greatly influences the fragmentation reaction of peptides which is currently known as a “proline effect” [55-61]. In particular, the fragmentation is proceeds via cleavage N-terminal to proline in the presence of a mobile proton. This aspect can be explained by steric hindrance of the side chain of proline residue.

To our knowledge, there has been no computational study on the proton affinity of oxazolone and diketopiperazine isomers of the N-terminal proline containing dipeptides. In this chapter, the proton affinity of proline containing b_2^+ ions (PX, where

P=Pro and X=Ala, Phe, Asp, Trp and His) which have different proton affinity and linear oxazolone structure of AAAA sequence ions have been calculated with the computational methods and compared with the experimental results obtained from mass spectrometer.

Table 6.1 Proton affinity of the natural amino acids

Amino acids	Harrison	Hunter/Lias
Gly	210.5	211.9
Cys	214.0	215.9
Ala	214.2	215.5
Ser	215.2	218.6
Asp	216.4	217.2
Val	216.5	217.6
Leu	217.4	218.6
Ile	218.6	219.3
Thr	219.5	220.5
Phe	219.9	220.6
Asn	220.6	222.0
Tyr	220.9	221.3
Met	221.1	223.6
Gln	222.0	224.1
Pro	222.1	220.0
Glu	223.4	218.2
Trp	223.9	226.8
His	231.5	236.1
Lys	235.6	238.0
Arg	244.8	251.2

* All proton affinity values (in kcal/mol) were taken from Ref [54]

6.1.1. Computational Details

The protonated and neutral oxazolone and diketopiperazine structures of the b_2 ions of the proline containing dipeptides (PX) have been studied in this work (Figure 6.2). Commonly, the probable protonation sites of the b_2^+ ions of the nitrogen of proline, nitrogen of the oxazolone ring and the nitrogen of the side chain (R) structure for the oxazolone, oxygens and nitrogens for the diketopiperazine structures have been considered. The possible protonation sites of structures have been showed by arrow (Figure 6.1). The protonation of oxygens of oxazolone structures have been disregarded because of their low energies [16, 20, 62].

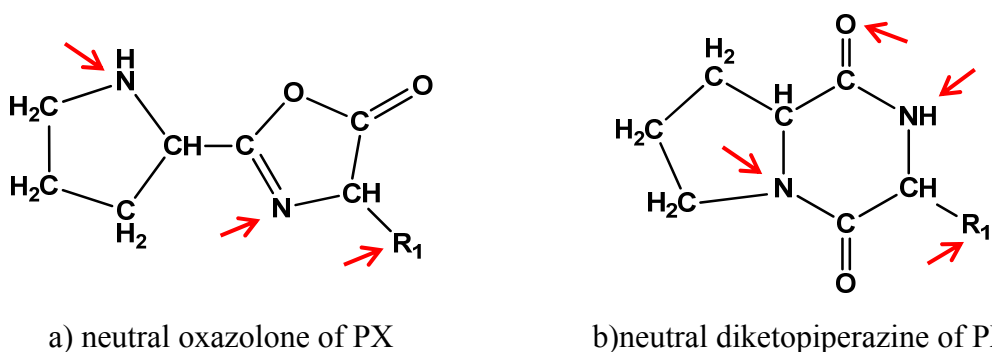


Figure 6.1. The neutral oxazolone and diketopiperazine structures of the b_2 ions of PX (R₁ is represented as side chain of X's amino acid)

Initially, low-energy conformers of the neutral and protonated structures have been generated by the molecular mechanics with Merck Molecular Force Field (MMFF) by using Spartan'10 program [39]. In addition to that, different initial structures have been obtained from twisting the rotatable bonds manually. Later, all the obtained structures have been performed with quantum chemical calculations by using the DFT/B3LYP/6-31+G(d,p) level of theory via Gaussian09 program to have optimum structures. Furthermore, frequency calculations have been carried out on the structures with the same level of theory. These steps have been applied for each protonated isomers.

The energies and zero point corrected energies (ZPE) of b ions of AAAA and PX structures were given in Table 6.2.

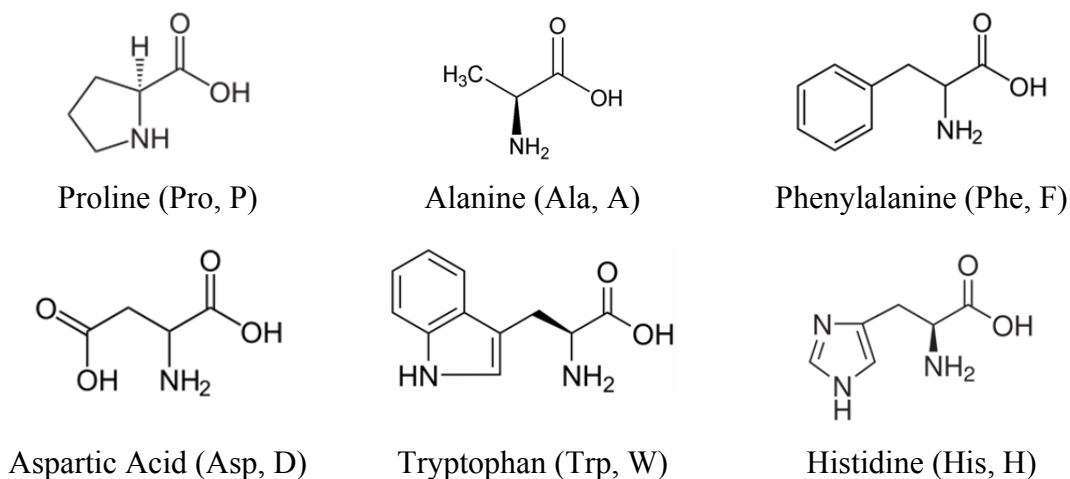


Figure 6.2. The structures of proline, alanine, phenylalanine, aspartic acid, tryptophan and histidine

6.1.2. Mass Spectrometry Details

The C-terminal amidated model peptides having a sequence of PAAAAAA-NH₂, PFAAAA-NH₂, PDAAAA-NH₂, PWAAAA-NH₂, and PHAAAA-NH₂ were purchased from GL Biochem Ltd. (Shanghai, China). Approximately 1 mg of each of the solid peptide samples was dissolved to a concentration of 10⁻⁴ M in 1:1 (v/v) mixture of HPLC-grade MeOH and deionized H₂O.

All tandem mass spectrometry experiments were carried out were conducted on a LTQ XL linear ion-trap mass spectrometer (Thermo Finnigan, San Jose, CA, USA) equipped with an electrospray ionization (ESI) source. A 100 pmol μL⁻¹ peptide solutions prepared in 50:50:1 (vol/vol/vol) MeOH/H₂O/HCOOH were introduced via infusion at a flow rate of 5 μL min⁻¹ with an incorporated syringe pump. The scan range was set to m/z 150 to 1000 in the positive-ion mode for all MS_n stages, and at least 400 scans were averaged in profile mode. The spray voltage was maintained at +5.0 kV and the N₂ sheath gas flow rate was 10 (arbitrary units). The heated capillary temperature was set to 300 °C. The normalized collision energy was varied from 20% to 30% for the fragmentation of precursor ion. The activation time was set to 30 ms at each CID stage using activation (q) of 0.250 and the isolation width (m/z) for precursor ions was set at between 1.0 and 1.8 for each CID acquisitions and at least 400 scans were averaged. Data acquisition was carried out with Xcalibur (ver. 2.0) software system..

6.2. The b_4^+ ions of AAAA

The protonated nitrogen of the oxazolone (AAAA_oxa_np) was found as the most favorable structure. The proton (hydrogen) located between the nitrogen of the oxazolone and the oxygen. The oxygen protonated macro-cyclic structure (cyc_AAAA_op) of AAAA residue has 4.1 kcal/mol higher energy than the linear oxazolone structure. The energy difference between protonated macro-cyclic and linear structures has lower than the energy difference in the b_3^+ ions of the AAA which has 12.5 kcal/mol (Table 6.2). Moreover, the neutral macro-cyclic isomer cyc_AAAA has 5.7 kcal/mol lower energy than the neutral oxazolone structure (AAAA_oxa).

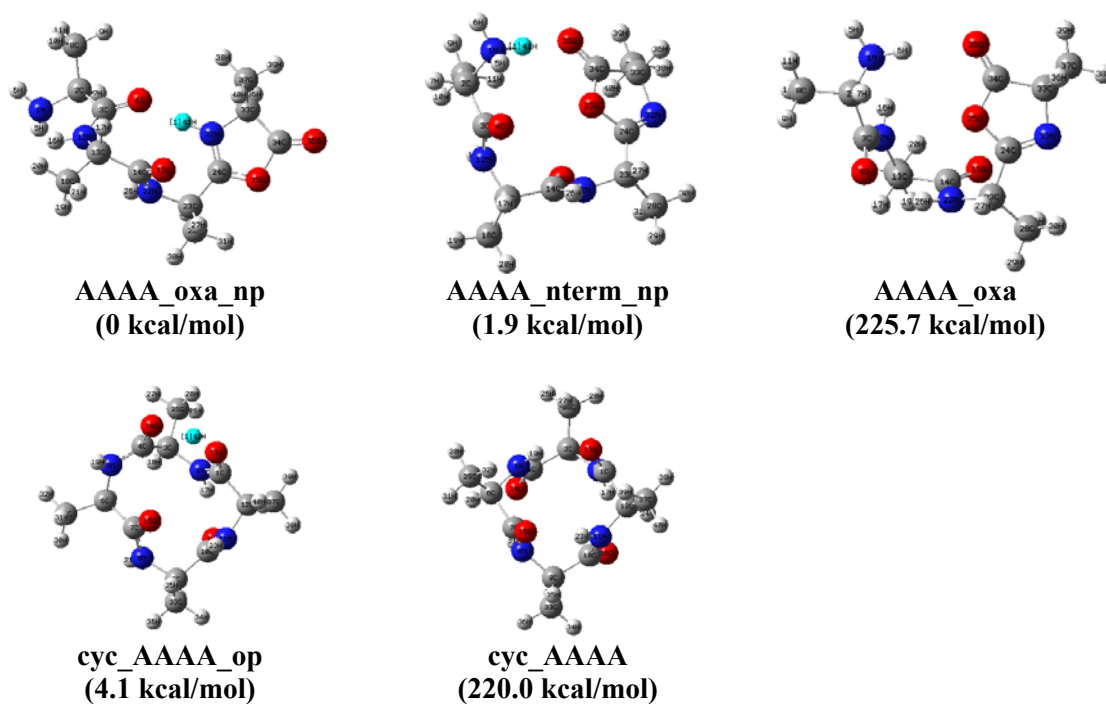


Figure 6.3. The favorable conformers of b_4 ion of AAAA

6.3. The b_2^+ ions of PA

The most favorable conformer of PA was obtained as the oxygen protonated diketopiperazine (PA_dik_op2) (Figure 6.4). In this structure, the hydrogen was directed to the methyl group of the alanine residue. A configuration (PA_dik_op1) in which hydrogen directed to the proline cycle (not close to nitrogen side of Pro) has 3.8 kcal/mol higher energy than PA_dik_op2. Moreover, protonated nitrogens in the diketopiperazine structures (PA_dik_pro_np, PA_dik_np) were not as favorable as (about 17 kcal/mol) above structures.

In the oxazolone structures, protonated nitrogen of the proline isomer (PA_oxa_pro_np) was 1.6 kcal/mol more stable than the nitrogen of the oxazolone isomer (PA_oxa_np). Furthermore, the neutral diketopiperazine structure has 23.1 kcal/mol lower energy than the neutral oxazolone isomer whereas this difference was became 8.7 kcal/mol for the protonated isomers. The most accessible neutral and protonated diketopiperazine and oxazolone structures of PA were almost the same

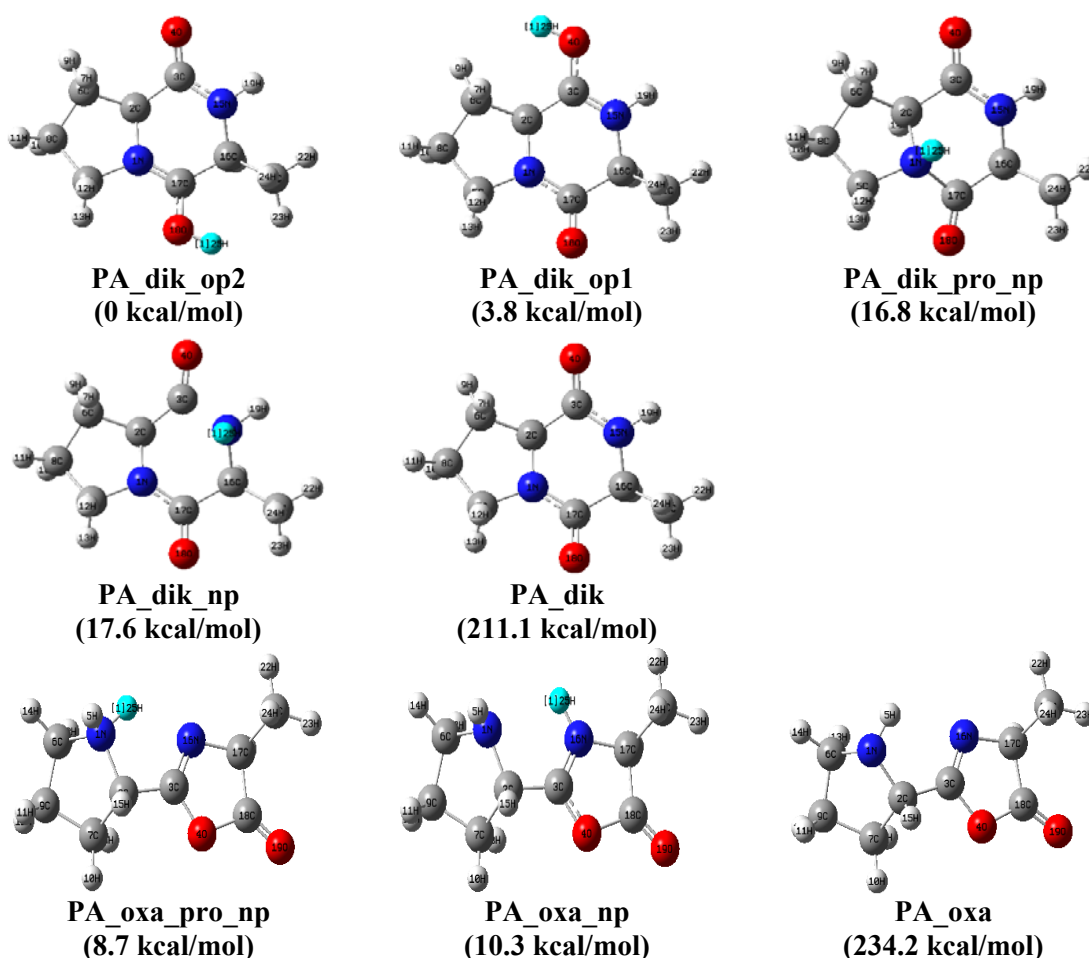


Figure 6.4. The favorable conformers of b_2 ion of PA

6.4. The b_2^+ ions of PF

The oxygen protonated diketopiperazine (PF_dik_op2) of PF, which the hydrogen was faced to the phenyl group, was the favorable isomer (Figure 6.5). It was 6.1 kcal/mol more stable than hydrogen directed to the side chain group of the proline isomer (PF_dik_op1). Furthermore, protonated nitrogen of the proline isomer (PA_oxa_pro_np) was 0.1 kcal/mol slightly more stable than the nitrogen of the oxazolone isomer (PA_oxa_np) in the oxazolone structures. They are isoenergetic conformers and competing with each other energetically.

Additionally, the neutral diketopiperazine structure was 24.6 kcal/mol more stable than the neutral oxazolone isomer. However, this energy difference was 13.4 kcal/mol for the most stable protonated ones.

When the most stable neutral diketopiperazine were protonated from its oxygen, the phenyl group was faced to the protonated oxygen. While the most stable neutral oxazolone were protonated from nitrogen of proline ring, it was directed to nitrogen of the oxazolone.

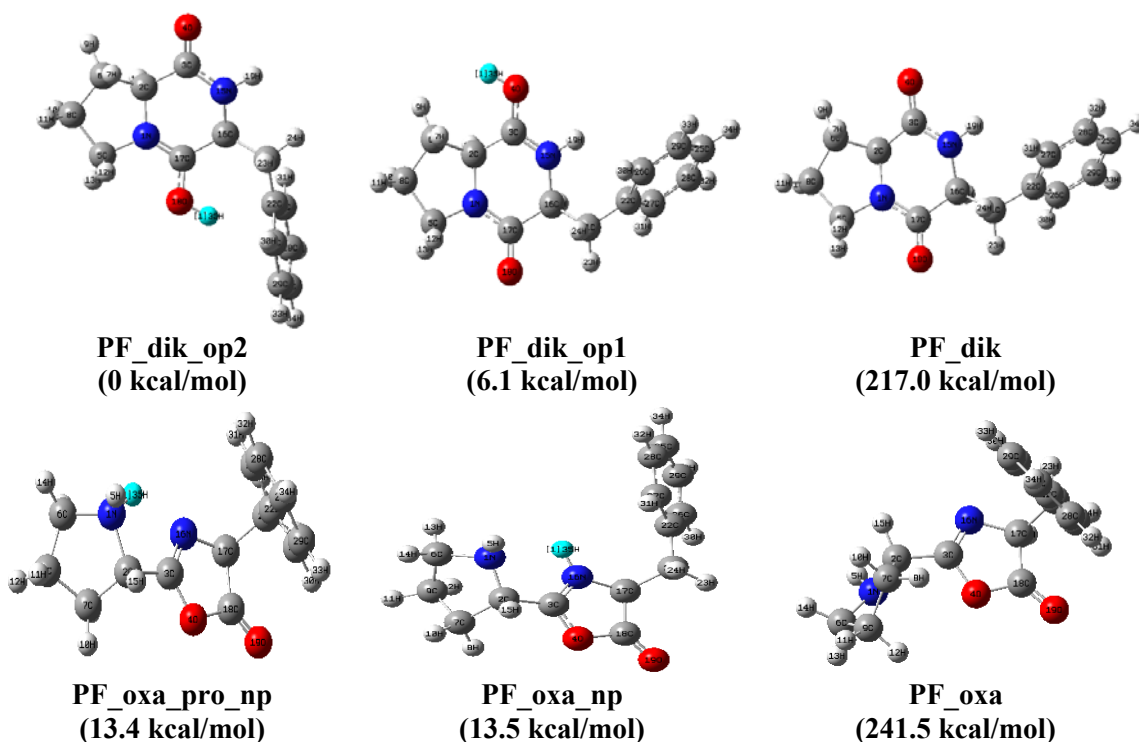


Figure 6.5. The favorable conformers of b_2 ion of PF

6.5. The b_2^+ ions of PD

In this part, the structures of b_2^+ ions of PD were analyzed (Figure 6.6). The oxygen protonated diketopiperazine (PD_dik_op2) isomer in which the hydrogen near the oxygen atom of the side chain group of the Asp was found as the most favorable one. It was 7.2 kcal/mol and 14.4 kcal/mol more stable than hydrogen faced to the side chain group of the Pro isomer (PD_dik_op1) and (PD_dik_asp_op). Moreover, nitrogen protonated proline isomer (PD_oxa_pro_np) has 3 kcal/mol lower energy than the nitrogen protonated the oxazolone structure (PD_oxa_np).

The neutral diketopiperazine structure was 24.7 kcal/mol more stable than the neutral oxazolone isomer. But, this energy difference was 14.2 kcal/mol for the most stable protonated ones. When the neutral diketopiperazine was protonated from its oxygen, oxygen in the side chain of Asp was rotated about 180° and faced to the protonated oxygen. On the other hand, when the neutral oxazolone was protonated from nitrogen of Pro, the oxazolone were twisted and oxygen of the side chain of Asp was closed to protonation site of the oxazolone.

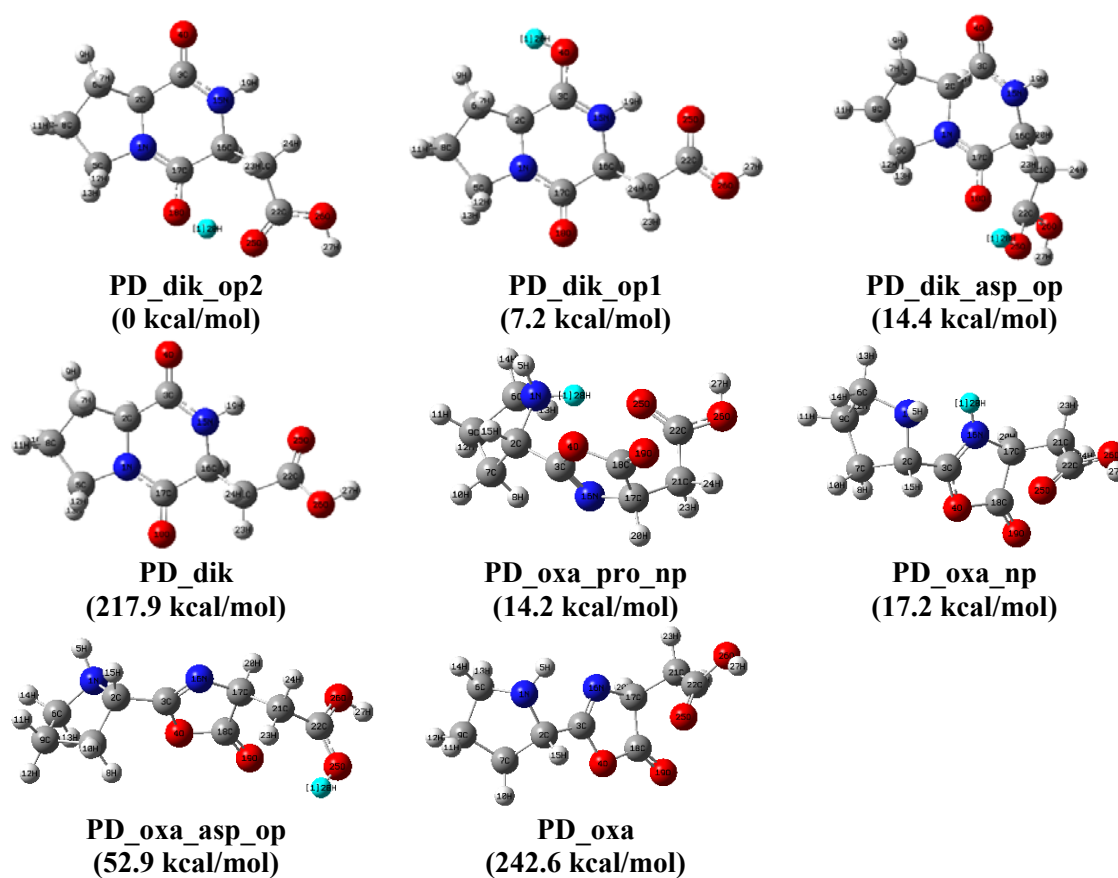


Figure 6.6. The favorable conformers of b_2 ion of PD

6.6. The b_2^+ ions of PW

Similarly, the oxygen protonated diketopiperazine (PW_dik_op2) structure, which the hydrogen was faced to the side chain group of the tryptophan, was the most stable in the b_2^+ ions of PW (Figure 6.7). This isomer was 7.9 kcal/mol and 19.7 kcal/mol more stable than hydrogen near the side chain group of the Pro isomer (PW_dik_op1) and protonated nitrogen of the tryptophan structure (PW_dik_trp_np). In addition, the energy order of the protonated oxazolone structures were 12.6 kcal/mol, 14.9 kcal/mol and 43.1 kcal/mol for the protonated nitrogen of the proline isomer (PW_oxa_pro_np), the nitrogen of the oxazolone structure (PW_oxa_np) and protonated nitrogen of the tryptophan isomer (PW_oxa_trp_np) respectively. Also, the neutral diketopiperazine structure was 24.0 kcal/mol more stable than the neutral oxazolone isomer. This energy difference was 12.6 kcal/mol for the most stable protonated ones. When the neutral diketopiperazine was protonated from its oxygen, the side chain of Trp was rotated to the protonated oxygen. However, the neutral oxazolone (PW_oxa) was almost the same structure as the protonated one.

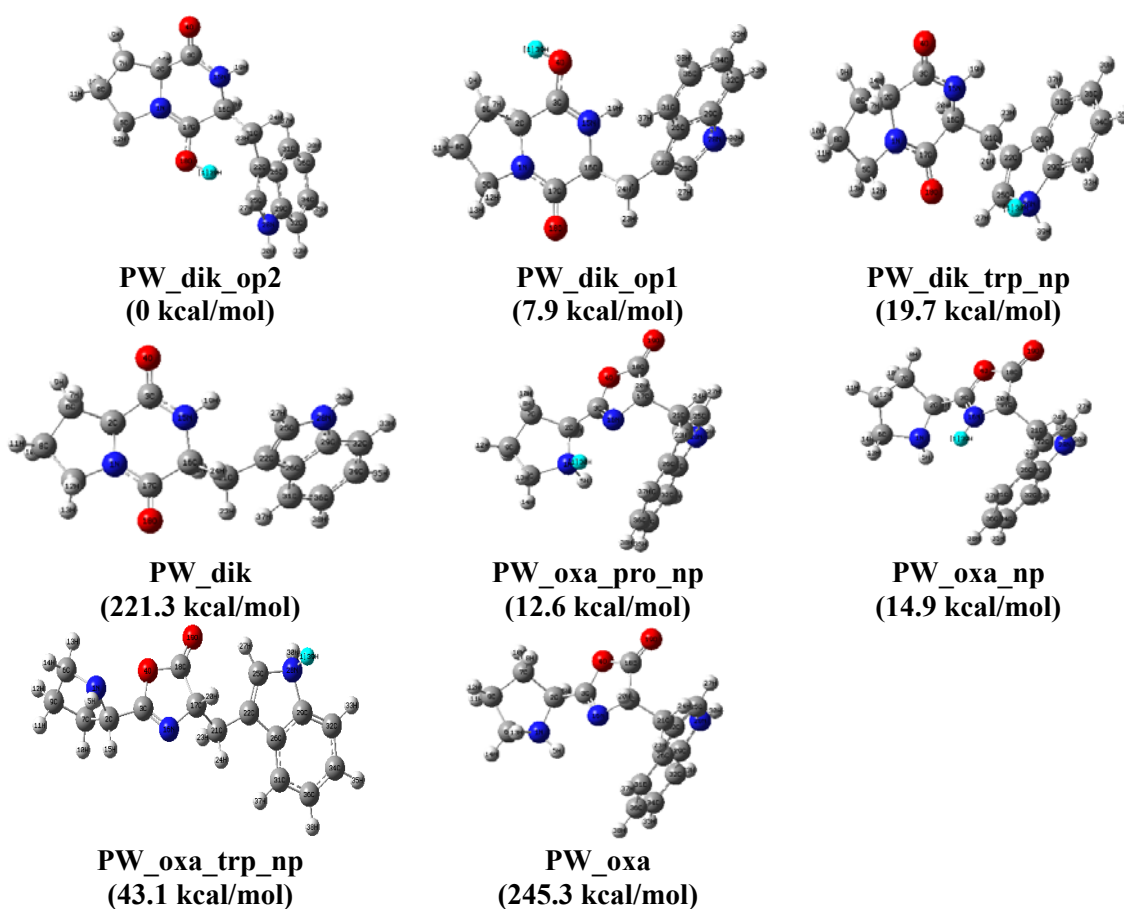


Figure 6.7. The favorable conformers of b_2 ion of PW

6.7. The b_2^+ ions of PH

Unlike the other b_2^+ ions, the nitrogen of the histidine protonated diketopiperazine (PH_dik_his_np) structure was the most stable in the b_2^+ ions of PH (Figure 6.8). It was 16.1 kcal/mol and 18.1 kcal/mol more stable than PH_dik_op1 and PH_dik_op2 isomers. Moreover, the protonated oxazolone structures have almost the same energies. They are competing to each other. The relative energy order of the protonated oxazolone isomers was 25.6 kcal/mol, 26.4 kcal/mol and 26.9 kcal/mol for the protonated nitrogen of the proline isomer (PH_oxa_pro_np), the protonated nitrogen of the histidine isomer (PH_oxa_his_np) and nitrogen of the oxazolone (PH_oxa_np) respectively. Similarly to others, the neutral diketopiperazine structure was 25.9 kcal/mol more stable than the neutral oxazolone isomer. This energy difference was 25.6 kcal/mol for the most stable protonated ones. When the neutral diketopiperazine was protonated from nitrogen of the His, the side chain of His was rotated about 180° and faced to the oxygen of the diketopiperazine structure. While the neutral oxazolone was protonated from nitrogen of Pro, the side chain of His was twisted to protonation site.

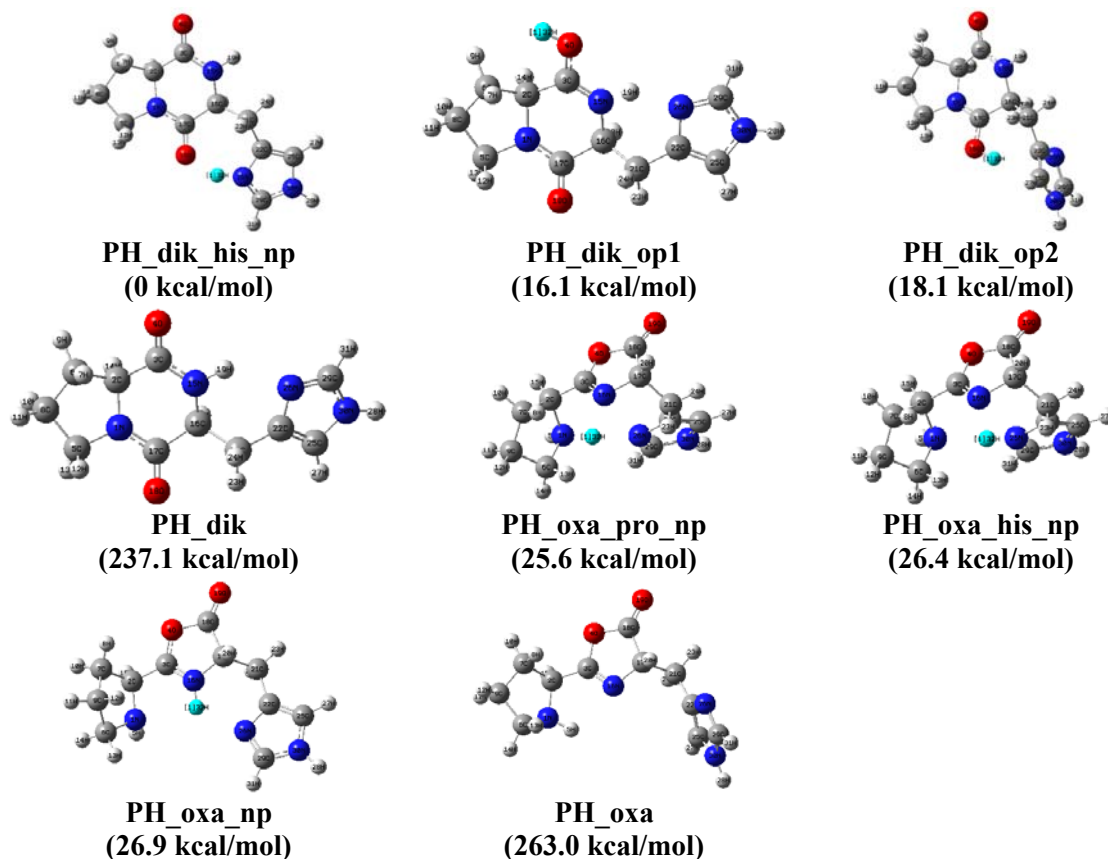


Figure 6.8. The favorable conformers of b_2 ion of PH

Table 6.2. The energies and zero point corrected energies (E+ZPE) of b ions of AAA, AAAA and PX

Structure	E (au)	E+ZPE (au)	Rel E kJ/mol	Rel (E+ZPE) kJ/mol
AAA_oxa_np	-742.372136	-742.111798	0.0	0.0
AAA_nterm_np	-742.368300	-742.106481	2.4	3.3
cyc_AAA_op	-742.355018	-742.091821	10.7	12.5
cyc_AAA	-742.009715	-741.759373	227.4	221.2
AAA_oxa	-742.000036	-741.752075	233.5	225.7
AAAA_oxa_np	-989.732896	-989.388180	0.0	0.0
AAAA_nterm_np	-989.732262	-989.385133	0.4	1.9
cyc_AAAA_op	-989.729447	-989.381620	2.2	4.1
cyc_AAAA	-989.373916	-989.037657	225.3	220.0
AAAA_oxa	-989.350542	-989.017583	239.9	232.6
PA_dik_op2	-572.451955	-572.237142	0	0
PA_dik_op1	-572.445975	-572.231131	3.8	3.8
PA_oxa_pro_np	-572.438850	-572.223201	8.2	8.7
PA_oxa_np	-572.434652	-572.220748	10.9	10.3
PA_dik_pro_np	-572.425539	-572.210445	16.6	16.8
PA_dik_np	-572.423590	-572.209023	17.8	17.6
PA_dik	-572.102672	-571.900734	219.2	211.1
PA_oxa	-572.064722	-571.863972	243.0	234.2
PF_dik_op2	-803.526205	-803.230000	0.0	0.0
PF_dik_op1	-803.516609	-803.220313	6.0	6.1
PF_oxa_pro_np	-803.505814	-803.208672	12.8	13.4
PF_oxa_np	-803.503818	-803.208480	14.0	13.5
PF_dik	-803.167555	-802.884226	225.1	217.0
PF_oxa	-803.127419	-802.845083	250.2	241.5
PD_dik_op2	-761.044200	-760.814068	0.0	0.0
PD_dik_op1	-761.032771	-760.802572	7.2	7.2
PD_oxa_pro_np	-761.022822	-760.791466	13.4	14.2
PD_dik_asp_op	-761.021497	-760.791157	14.2	14.4
PD_oxa_np	-761.015973	-760.786619	17.7	17.2
PD_oxa_asp_op	-760.958310	-760.729693	53.9	52.9
PD_dik	-760.684124	-760.466807	226.0	217.9
PD_oxa	-760.643657	-760.427503	251.3	242.6
PW_dik_op2	-935.111501	-934.786013	0.0	0.0
PW_dik_op1	-935.098903	-934.773361	7.9	7.9
PW_oxa_pro_np	-935.092829	-934.766008	11.7	12.6
PW_oxa_np	-935.087188	-934.762321	15.3	14.9
PW_dik_trp_np	-935.080896	-934.754644	19.2	19.7
PW_oxa_trp_np	-935.042491	-934.717333	43.3	43.1
PW_dik	-934.745938	-934.433384	229.4	221.3
PW_oxa	-934.706692	-934.395142	254.0	245.3
PH_dik_his_np	-797.533624	-797.265982	0.0	0.0
PH_dik_op1	-797.507421	-797.240344	16.4	16.1
PH_dik_op2	-797.504537	-797.237119	18.3	18.1
PH_oxa_pro_np	-797.493453	-797.225147	25.2	25.6
PH_oxa_his_np	-797.491571	-797.223953	26.4	26.4
PH_oxa_np	-797.489663	-797.223179	27.6	26.9
PH_dik	-797.142728	-796.888150	245.3	237.1
PH_oxa	-797.100041	-796.846869	272.1	263.0

6.8. The Conformational Analysis of the b₂ ions of PX

In all proline amino acid containing b₂⁺ ions (PX), the oxygen protonated diketopiperazine (PX_dik_op2) was the most favorable structure, where the proton was directed to the side chain (R) group of the X amino acids except PH. In the PH dipeptide, the nitrogen of the histidine protonated diketopiperazine (PH_dik_his_np) structure was the most stable one.

Furthermore, in the protonated oxazolone structures of PX, protonated nitrogen of the proline isomer (PX_oxa_pro_np) has the lowest energy isomer. And also the energy difference between PX_oxa_np and PX_oxa_pro_np were in the range of 0.1-2.3 kcal/mol. They are in competition.

In addition, the neutral diketopiperazine structures were on average 24.4 kcal/mol more stable than the neutral oxazolone isomer among the PX dipeptides. On the other hand, the relative energy difference between protonated diketopiperazine and oxazolone structures were 8.7 kcal/mol, 13.4 kcal/mol, 14.2 kcal/mol, 12.6 kcal/mol, 25.6 kcal/mol for PA, PF, PD, PW and PH respectively. Moreover, in the PH dipeptide the relative energy difference between protonated diketopiperazine and oxazolone (25.6 kcal/mol) were almost the same with the neutral diketopiperazine and oxazolone (25.9 kcal/mol) energy difference whereas, the others have more energy differences.

6.9. Proton Affinities of the b ions

The proton affinities of the diketopiperazine and oxazolone structures the b₂⁺ ions of PX have been calculated by using the DFT/B3LYP/6-31+G(d,p) level of theory via Gaussian09 program on the lowest energy conformers. The gas phase proton affinity of compound A in the reaction of A_(g) + H_(g)⁺ → AH_(g)⁺ were calculated computationally from the following equations [35, 53].

$$\text{Proton Affinity of (A)} = [E_{elec}(A) + ZPE(A)] - [E_{elec}(AH^+) + ZPE(AH^+)]$$

where; E_{elec} = Electronic energy and ZPE = Zero point energy

The proton affinity order was given in the ascending order in the following Table 6.3. The proton affinities of both diketopiperazine and oxazolone structures of PX have increased from PA to PH with increasing basicity of amino acids. Furthermore, the

calculated DFT proton affinities of diketopiperazine and oxazolone structures of b_2^+ ions of PX had similar trend and as shown in Figure 6.9.

In a previous study, Nold et al.[63] explored for the comparison the experimentally of the gas phase proton affinity of the diketopiperazine structures of AA, LG ,LA, LP and 2-phenyl-5 oxazolone. They showed that, the proton affinity of the diketopiperazine rises as the amino acids become more basic. In addition, they declared that, diketopiperazine structures had lower proton affinity than the oxazolone experimentally. Likewise, the calculated results in this study demonstrated that the proton affinities of the oxazolone structures were about 11 kcal/mol higher than the diketopiperazine structures, except the PH. In the PH, the proton affinities of the diketopiperazine and oxazolone structures were almost same; this difference was only 0.3 kcal/mol (Table 6.3).

Table 6.3. The DFT proton affinities of the diketopiperazine and oxazolone structures of b_2^+ ions of PX

b_2^+ ions of PX	oxazolone structure	diketopiperazine structure	$PA_{\text{oxa}}-PA_{\text{dik}}^*$
PA	225.4	211.1	14.3
PF	228.2	217.0	11.2
PD	228.4	217.9	10.5
PW	232.7	221.3	11.4
PH	237.4	237.1	0.3

The “ $PA_{\text{oxa}}-PA_{\text{dik}}$ ” refers the DFT proton affinity difference between diketopiperazine and oxazolone structures. The proton affinity values were given in kcal/mol.

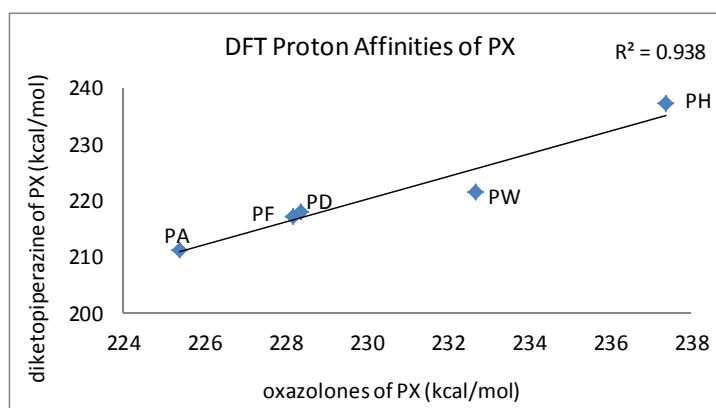


Figure 6.9. The calculated DFT proton affinities of diketopiperazine and oxazolone structures of b_2^+ ions of PX

The comparison of experimental proton affinity of single amino acids and calculated DFT proton affinity b_2^+ ions of PX were given in Figure 6.10. The experimental data of the proton affinity of single amino acids of A,F,D,W and H were taken from Harrison [45] and Hunter/Lias [52] respectively. On the other hand, DFT PX_oxa was referred to DFT calculation results of proton affinity of oxazolone structures of b_2^+ ions of PX (PA, PF, PD, PW and PH). The results showed that, when proline residue added to the single amino acid from the N-terminal side and formed b_2^+ ions of PX, than the proton affinity increased on average 7.2 kcal/mol and 9.2 kcal/mol for Hunter/Lias [52] and Harrison [45] respectively. Histidine containing b_2 ion behaved differently than the others, Hunter/Lias single amino acid value and calculated dipeptide values were almost coincide.

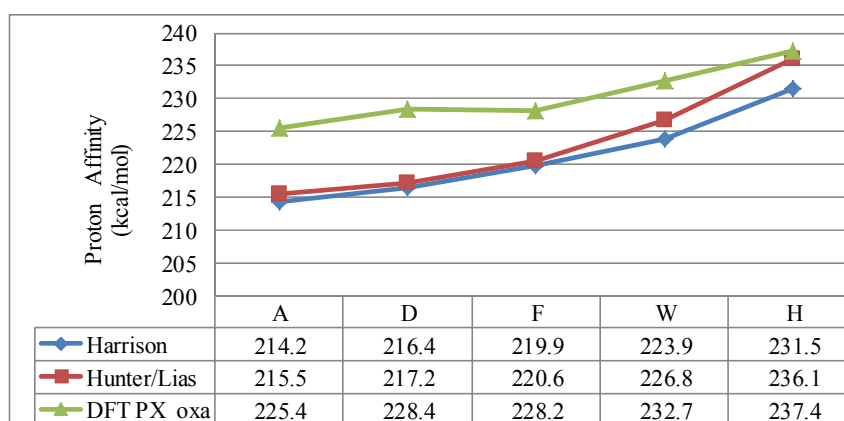


Figure 6.10. The experimental proton affinity of single amino acids and calculated DFT proton affinity b_2^+ ions of PX

The CID mass spectra of the b_6 ions obtained from the C-terminal amidated model peptides having a sequence of PAAAAAA-NH₂, PFAAAA-NH₂, PDAAAA-NH₂, PWAAAA-NH₂, and PHAAAA-NH₂ are shown in Figure 6.11. It has been observed that, the fragment intensities of PX and AAAA peaks in the b_6^+ ion mass spectra are influenced by altering the second amino acid residue; in some of them AAAA peak is dominant or vice versa. The relative intensities of PA (m/z 169), PF (m/z 245) and PD (m/z 213) have lower compared to the AAAA (m/z 285) fragment ion. On the contrary, the relative intensities of PW (m/z 284) and PH (m/z 235) ions are higher compared to the AAAA fragment ion.

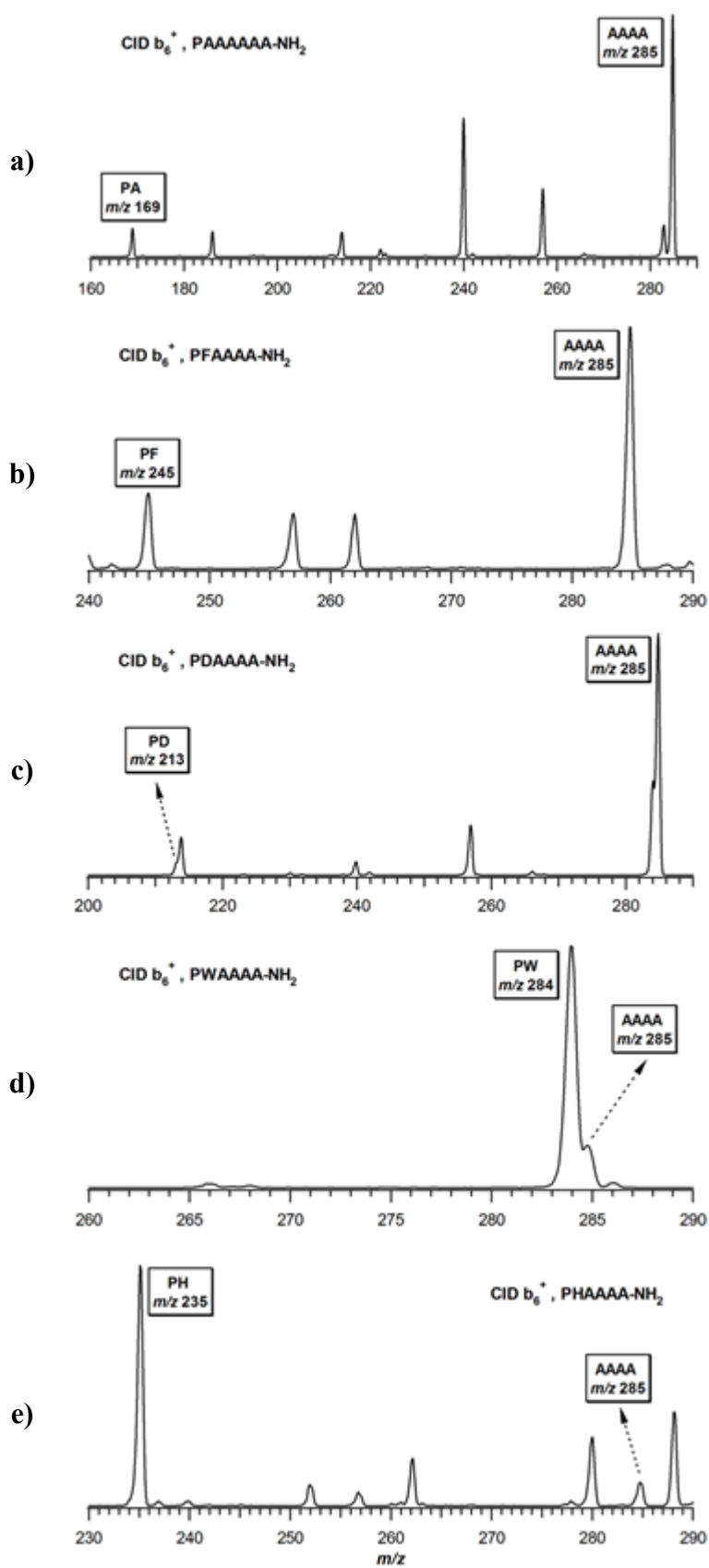


Figure 6.11. Comparison of the CID mass spectra of b_6 ions of PXAAAA-NH₂

To explain why these intensities are changing with the X; the peak intensity ratios (I) of PX and AAAA are compared with calculated proton affinities of PX. Figure 6.12 demonstrated that, the experimental mass spectra of peak intensities ratio $\ln(I_{PX}/I_{AAAA})$ of the ions were in correlation with the calculated DFT proton affinities of the PX ions.

Furthermore, the calculated proton affinities of oxazolone structures of PX and AAAA have been investigated. Proton affinity of AAAA was calculated as 232.6 kcal/mol in this work and there is perfect agreement with the one previously reported by Paizs et al [64] in the literature. The DFT results demonstrated that, the oxazolone structure of AAAA has higher proton affinity than the oxazolone structures of PA, PF, and PD. However, the proton affinity of AAAA was lower than the more basic containing residues of PW and PH (Table 6.3).

Consequently, the experimental results showed that, MS/MS spectrum consist of both PX and AAAA fragments were in competition with each other due to the their proton affinities. Moreover, the experimental results have been supported with DFT calculations.

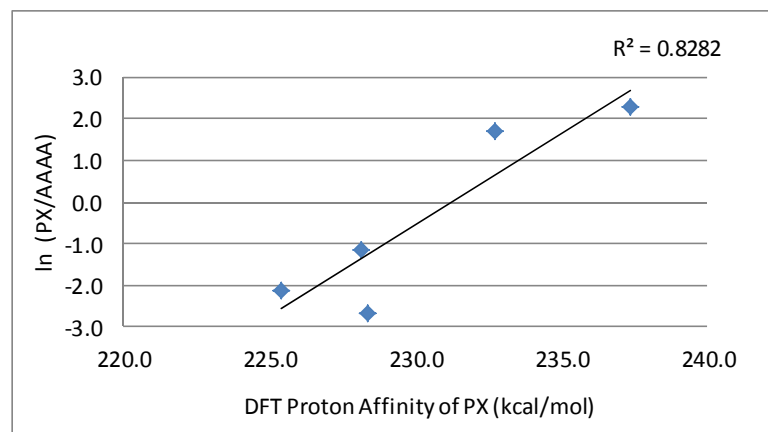


Figure 6.12. CID mass spectra of peak intensities ratio ($\ln (PX/AAAA)$) vs the calculated proton affinities of the PX ions

CHAPTER 7

CONCLUSION

In this thesis, the structures of peptide fragmentation ions; b_n ions, b_2^+ - b_7^+ , containing different type and size have been analyzed by using computational methods. The factors that affect the production of macrocycles for various b_n ions containing acidic, basic and neutral amino acids have been investigated. The following remarks have been obtained for the b ions studied under this thesis:

- The protonated diketopiperazine is always energetically more stable than the protonated oxazolone structures for the b_2 ions.
- The protonated site is very important for the b fragment of the peptides.
- The macrocyclic structures of b_5^+ ions have the lowest energies. The proton prefers to locate on the oxygen of the b_5^+ ions except histidine containing peptide where it likes to be on the nitrogen of the histidine.
- For the acyclic b_5^+ ions, the proton prefers to join nitrogen atom, mostly nitrogen in the oxazolone but sometimes in the N-terminal except His containing ones. The structures in which the proton located on the nitrogen of the histidine are the most stable one for the linear isomers of HA_4 and HA_6 .
- When the all macrocycle structures of b_5^+ ions including with different amino acids N, D, L, F, Y, C, have been compared, similar results have been observed. The bond distances on the macrocycle skeleton were almost the same. That means there is no significant amino acid effect on the bond lengths of macrocycle isomer. The bond lengths have been changed at the protonated part of the structure.
- It has been observed that, the small protonation cycle presents in the macrocycle structure for all amino acid types where the hydrogen bonded to the oxygen atom. All macrocycle structures of b_5^+ ions have almost the same bond lengths, bond angles (geometry) and charge distributions in the content of the proton cycle.
- In all Proline amino acid containing b_2^+ ions (PX), the oxygen protonated diketopiperazine was the most favorable structure. However, in the PH

dipeptide, the nitrogen of the histidine protonated diketopiperazine structure was the most stable one.

- In addition, the neutral diketopiperazine structures were more stable than the neutral oxazolone isomer among the PX dipeptides.
- The proton affinities of both diketopiperazine and oxazolone structures of PX have increased from PA to PH with increasing basicity of amino acids.
- The proton affinities of the oxazolone structures were about 11 kcal/mol higher than the diketopiperazine structures, except the PH. In the PH, the proton affinities of the diketopiperazine and oxazolone structures were almost same.
- The experimental results showed that, MS/MS spectrum consist of both PX and AAAA fragments were in competition with each other, this is explained by the proton affinity calculations.

We hoped that with the help of this study, the peptide MS/MS spectra can be understood more easily. The databases will be improved in order to obtain the more detailed and reliable results for the proteomic studies.

REFERENCES

1. Mader, S.S., *Concepts of Biology* 2008: McGraw Hill Higher Education.
2. Jeremy M Berg, J.L.T., and Lubert Stryer, *Biochemistry*. 5th edition ed. 2002: New York: W H Freeman.
3. Harrison, A.G., *TO b OR NOT TO b: THE ONGOING SAGA OF PEPTIDE b IONS*. *Mass Spectrometry Reviews*, 2009. 28(4): p. 640-654.
4. Roepstorff, P. and J. Fohlman, *Proposal for a Common Nomenclature for Sequence Ions in Mass-Spectra of Peptides*. *Biomedical Mass Spectrometry*, 1984. 11(11): p. 601-601.
5. Biemann, K., *Contributions of mass spectrometry to peptide and protein structure*. *Biological Mass Spectrometry*, 1988. 16(1-12): p. 99-111.
6. Mueller, D.R., M. Eckersley, and W.J. Richter, *Hydrogen Transfer-Reactions in the Formation of Y+2 Sequence Ions from Protonated Peptides*. *Organic Mass Spectrometry*, 1988. 23(3): p. 217-222.
7. Cordero, M.M., J.J. Houser, and C. Wesdemiotis, *The Neutral Products Formed during Backbone Fragmentations of Protonated Peptides in Tandem Mass-Spectrometry*. *Analytical Chemistry*, 1993. 65(11): p. 1594-1601.
8. Yalcin, T., I.G. Csizmadia, M.R. Peterson, and A.G. Harrison, *The structure and fragmentation of B-n (n>=3) ions in peptide spectra*. *Journal of the American Society for Mass Spectrometry*, 1996. 7(3): p. 233-242.
9. Yalcin, T., C. Khouw, I.G. Csizmadia, M.R. Peterson, and A.G. Harrison, *Why are B ions stable species in peptide spectra?* *Journal of the American Society for Mass Spectrometry*, 1995. 6(12): p. 1165-1174.
10. Paizs, B., G. Lendvay, K. Vekey, and S. Suhai, *Formation of b(2)(+) ions from protonated peptides: an ab initio study*. *Rapid Communications in Mass Spectrometry*, 1999. 13(6): p. 525-533.
11. Bleiholder, C., S. Osburn, T.D. Williams, S. Suhai, M. Van Stipdonk, A.G. Harrison, and B. Paizs, *Sequence-Scrambling Fragmentation Pathways of Protonated Peptides*. *Journal of the American Chemical Society*, 2008. 130(52): p. 17774-17789.
12. Harrison, A.G., A.B. Young, C. Bleiholder, S. Suhai, and B. Paizs, *Scrambling of sequence information in collision-induced dissociation of peptides*. *Journal of the American Chemical Society*, 2006. 128(32): p. 10364-10365.
13. Wesdemiotis, C., *The Neutral Products Formed during Backbone Fragmentations of Protonated Peptides in Tandem Mass Spectrometry*. *Journal of the American Society for Mass Spectrometry*, 1993. 65: p. 1594-1601.

14. Carrol, J.A.e.a., Proceedings of the 42nd ASMS Conference; Chicago, 1994: p. 475.
15. Eckart, K.S., J, Proceedings of the 42nd ASMS Conference Chicago, 1994: p. 474.
16. Rodriquez, C.F., T. Shoeib, I.K. Chu, K.W.M. Siu, and A.C. Hopkinson, *Comparison between protonation, lithiation, and argentination of 5-oxazolones: A study of a key intermediate in gas-phase peptide sequencing*. Journal of Physical Chemistry A, 2000. 104(22): p. 5335-5342.
17. Farrugia, J.M., R.A.J. O'Hair, and G.E. Reid, *Do all b(2) ions have oxazolone structures? Multistage mass spectrometry and ab initio studies on protonated N-acyl amino acid methyl ester model systems*. International Journal of Mass Spectrometry, 2001. 210(1-3): p. 71-87.
18. Farrugia, J.M., T. Taverner, and R.A.J. O'Hair, *Side-chain involvement in the fragmentation reactions of the protonated methyl esters of histidine and its peptides*. International Journal of Mass Spectrometry, 2001. 209(2-3): p. 99-112.
19. Perkins, B.R., J. Chamot-Rooke, S.H. Yoon, A.C. Gucinski, A. Somogyi, and V.H. Wysocki, *Evidence of Diketopiperazine and Oxazolone Structures for HA b(2)(+) Ion*. Journal of the American Chemical Society, 2009. 131(48): p. 17528-17529.
20. Chen, X., L. Yu, J.D. Steill, J. Oomens, and N.C. Polfer, *Effect of Peptide Fragment Size on the Propensity of Cyclization in Collision-Induced Dissociation: Oligoglycine b(2)-b(8)*. Journal of the American Chemical Society, 2009. 131(51): p. 18272-18282.
21. Oomens, J., S. Young, S. Molesworth, and M. van Stipdonk, *Spectroscopic Evidence for an Oxazolone Structure of the b(2) Fragment Ion from Protonated Tri-Alanine*. Journal of the American Society for Mass Spectrometry, 2009. 20(2): p. 334-339.
22. Yoon, S.H., J. Chamot-Rooke, B.R. Perkins, A.E. Hilderbrand, J.C. Poutsma, and V.H. Wysocki, *IRMPD Spectroscopy Shows That AGG Forms an Oxazolone b2+ Ion*. Journal of the American Chemical Society, 2008. 130(52): p. 17644-17645.
23. Sinha, R.K., U. Erlekam, B.J. Bythell, B. Paizs, and P. Maitre, *Diagnosing the Protonation Site of b (2) Peptide Fragment Ions using IRMPD in the X-H (X = O, N, and C) Stretching Region*. Journal of the American Society for Mass Spectrometry, 2011. 22(9): p. 1645-1650.
24. Gucinski, A.C., J. Chamot-Rooke, E. Nicol, A. Somogyi, and V.H. Wysocki, *Structural Influences on Preferential Oxazolone versus Diketopiperazine b(2)(+) Ion Formation for Histidine Analogue-Containing Peptides*. Journal of Physical Chemistry A, 2012. 116(17): p. 4296-4304.

25. Zou, S., J. Oomens, and N.C. Polfer, *Competition between diketopiperazine and oxazolone formation in water loss products from protonated ArgGly and GlyArg*. International Journal of Mass Spectrometry, 2012. 316: p. 12-17.
26. Polfer, N.C., J. Oomens, S. Suhai, and B. Paizs, *Spectroscopic and theoretical evidence for oxazolone ring formation in collision-induced dissociation of peptides*. Journal of the American Chemical Society, 2005. 127(49): p. 17154-17155.
27. Erlekam, U., B.J. Bythell, D. Scuderi, M. Van Stipdonk, B. Paizs, and P. Maitre, *Infrared Spectroscopy of Fragments of Protonated Peptides: Direct Evidence for Macrocyclic Structures of b(5) Ions*. Journal of the American Chemical Society, 2009. 131(32): p. 11503-11508.
28. Bythell, B.J., M. Knapp-Mohammady, B. Paizs, and A.G. Harrison, *Effect of the His Residue on the Cyclization of b Ions*. Journal of the American Society for Mass Spectrometry, 2010. 21(8): p. 1352-1363.
29. Becker, O.M., A.D. MacKerell, B. Roux, and M. Watanabe, *Computational Biochemistry and Biophysics*. 2001: Taylor & Francis.
30. Cramer, C.J., *Essentials of Computational Chemistry: Theories and Models*. 2005: Wiley.
31. Levine, I.N., *Quantum Chemistry*. 2000: Prentice Hall.
32. Lewars, E., *Computational Chemistry: Introduction to the Theory and Applications of Molecular and Quantum Mechanics*. 2010: Springer.
33. Tsai, C.S., *An Introduction to Computational Biochemistry*. 2003: Wiley.
34. Young, D., *Computational Chemistry: A Practical Guide for Applying Techniques to Real World Problems*. 2004: Wiley.
35. Foresman, J.B., A.E. Frisch, and I. Gaussian, *Exploring chemistry with electronic structure methods*. 1996: Gaussian, Inc.
36. Atkins, P.W., V. Walters, and J. De Paula, *Physical Chemistry*. 2006: Macmillan Higher Education.
37. Elmaci, N. and R.S. Berry, *Principal coordinate analysis on a protein model*. The Journal of Chemical Physics, 1999. 110(21): p. 10606-10622.
38. Panahi, N.S. and R.S. Berry, *Principal component analysis of potential energy surfaces of large clusters: allowing the practical calculation of the master equation*. Physical Chemistry Chemical Physics, 2009. 11(48): p. 11638-11646.
39. Wavefunction, I., *Spartan'10 (V 1.1.0)*.

40. Frisch, M.J., G.W. Trucks, H.B. Schlegel, G.E. Scuseria, M.A. Robb, J.R. Cheeseman, G. Scalmani, V. Barone, B. Mennucci, G.A. Petersson, H. Nakatsuji, M. Caricato, X. Li, H.P. Hratchian, A.F. Izmaylov, J. Bloino, G. Zheng, J.L. Sonnenberg, M. Hada, M. Ehara, K. Toyota, R. Fukuda, J. Hasegawa, M. Ishida, T. Nakajima, Y. Honda, O. Kitao, H. Nakai, T. Vreven, Jr, J.E. Peralta, F. Ogliaro, M. Bearpark, J.J. Heyd, E. Brothers, K.N. Kudin, V.N. Staroverov, R. Kobayashi, J. Normand, K. Raghavachari, A. Rendell, J.C. Burant, S.S. Iyengar, J. Tomasi, M. Cossi, N. Rega, J.M. Millam, M. Klene, J.E. Knox, J.B. Cross, V. Bakken, C. Adamo, J. Jaramillo, R. Gomperts, R.E. Stratmann, O. Yazyev, A.J. Austin, R. Cammi, C. Pomelli, J.W. Ochterski, R.L. Martin, K. Morokuma, V.G. Zakrzewski, G.A. Voth, P. Salvador, J.J. Dannenberg, S. Dapprich, A.D. Daniels, Farkas, J.B. Foresman, J.V. Ortiz, J. Cioslowski, and D.J. Fox, *Gaussian 09 Revision A.02*. 2009: Gaussian Inc. Wallingford CT 2009.
41. Jia, C., W. Qi, and Z. He, *Cyclization Reaction of Peptide Fragment Ions during Multistage Collisionally Activated Decomposition: An Inducement to Lose Internal Amino-Acid Residues*. Journal of the American Society for Mass Spectrometry, 2007. 18(4): p. 663-678.
42. Yague, J., A. Paradela, M. Ramos, S. Ogueta, A. Marina, F. Barahona, J.A.L. de Castro, and J. Vazquez, *Peptide rearrangement during quadrupole ion trap fragmentation: Added complexity to MS/MS spectra*. Analytical Chemistry, 2003. 75(6): p. 1524-1535.
43. Case, D., T.A. Darden, T.E. Cheatham, C. Simmerling, J. Wang, R. Duke, R. Luo, M. Crowley, R. Walker, W. Zhang, K.M. Merz, B. Wang, S. Hayik, A. Roitberg, G. Seabra, I. Kolossváry, K.F. Wong, F. Paesani, J. Vanicek, X. Wu, S. Brozell, T. Steinbrecher, H. Gohlke, L. Yang, C. Tan, J. Mongan, V. Hornak, G. Cui, D.H. Mathews, M.G. Seetin, C. Sagui, V. Babin, and P. Kollman, *Amber 11*.
44. Taşoğlu, Ç., *Phd. Thesis "Gas-phase fragmentation mechanisms of protonated peptides via tandem mass spectrometry"*. 2013, İzmir Institute of Technology.
45. Harrison, A.G., *The gas-phase basicities and proton affinities of amino acids and peptides*. Mass Spectrometry Reviews, 1997. 16(4): p. 201-217.
46. Bojesen, G., *The Order of Proton Affinities of the 20 Common 1-Alpha-Amino Acids*. Journal of the American Chemical Society, 1987. 109(18): p. 5557-5558.
47. Locke, M.J. and R.T. Mciver, *Effect of Solvation on the Acid-Base Properties of Glycine*. Journal of the American Chemical Society, 1983. 105(13): p. 4226-4232.
48. Carr, S.R. and C.J. Cassady, *Gas-phase basicities of histidine and lysine and their selected di- and tripeptides*. Journal of the American Society for Mass Spectrometry, 1996. 7(12): p. 1203-1210.

49. Gorman, G.S., J.P. Speir, C.A. Turner, and I.J. Amster, *Proton Affinities of the 20 Common Alpha-Amino-Acids*. Journal of the American Chemical Society, 1992. 114(10): p. 3986-3988.
50. Isa, K., T. Omote, and M. Amaya, *New Rules Concerning the Formation of Protonated Amino-Acids from Protonated Dipeptides Using the Proton Affinity Order Determined from Collisionally Activated Decomposition Spectra*. Organic Mass Spectrometry, 1990. 25(11): p. 620-628.
51. Wu, Z.C. and C. Fenselau, *Proton Affinity of Arginine Measured by the Kinetic Approach*. Rapid Communications in Mass Spectrometry, 1992. 6(6): p. 403-405.
52. Hunter, E.P.L. and S.G. Lias, *Evaluated gas phase basicities and proton affinities of molecules: An update*. Journal of Physical and Chemical Reference Data, 1998. 27(3): p. 413-656.
53. Maksic, Z.B. and B. Kovacevic, *Towards the absolute proton affinities of 20 alpha-amino acids*. Chemical Physics Letters, 1999. 307(5-6): p. 497-504.
54. Bleiholder, C., S. Suhai, and B. Paizs, *Revising the proton affinity scale of the naturally occurring α -amino acids*. Journal of the American Society for Mass Spectrometry, 2006. 17(9): p. 1275-1281.
55. Brechi, L.A., D.L. Tabb, J.R. Yates, and V.H. Wysocki, *Cleavage N-Terminal to Proline: Analysis of a Database of Peptide Tandem Mass Spectra*. Analytical Chemistry, 2003. 75(9): p. 1963-1971.
56. Loo, J.A., C.G. Edmonds, and R.D. Smith, *Tandem mass spectrometry of very large molecules. 2. Dissociation of multiply charged proline-containing proteins from electrospray ionization*. Analytical Chemistry, 1993. 65(4): p. 425-438.
57. Vaisar, T. and J. Urban, *Probing Proline Effect in CID of Protonated Peptides*. Journal of Mass Spectrometry, 1996. 31(10): p. 1185-1187.
58. Paizs, B., C. Bleiholder, S. Suhai, and A.G. Harrison, *Towards Understanding the Tandem Mass Spectra of Protonated Oligopeptides. 2: The Proline Effect in Collision-Induced Dissociation of Protonated Ala-Ala-Xxx-Pro-Ala (Xxx = Ala, Ser, Leu, Val, Phe, and Trp)*. Journal of the American Society for Mass Spectrometry, 2011. 22(6): p. 1032-1039.
59. Grewal, R.N., H. El Aribi, A.G. Harrison, K.W.M. Siu, and A.C. Hopkinson, *Fragmentation of Protonated Tripeptides: The Proline Effect Revisited*. The Journal of Physical Chemistry B, 2004. 108(15): p. 4899-4908.
60. Unnithan, A., M. Myer, C. Veale, and A. Danell, *MS/MS of protonated polyproline peptides: The influence of N-terminal protonation on dissociation*. Journal of the American Society for Mass Spectrometry, 2007. 18(12): p. 2198-2203.

61. Gucinski, A.C., J. Chamot-Rooke, V. Steinmetz, A. Somogyi, and V.H. Wysocki, *Influence of N-terminal Residue Composition on the Structure of Proline-Containing b(2)(+) Ions*. *Journal of Physical Chemistry A*, 2013. 117(6): p. 1291-1298.
62. Polfer, N.C., J. Oomens, S. Suhai, and B. Paizs, *Infrared spectroscopy and theoretical studies on gas-phase protonated leu-enkephalin and its fragments: Direct experimental evidence for the mobile proton*. *Journal of the American Chemical Society*, 2007. 129(18): p. 5887-5897.
63. Nold, M.J., B.A. Cerda, and C. Wesdemiotis, *Proton affinities of the N- and C-terminal segments arising upon the dissociation of the amide bond in protonated peptides*. *Journal of the American Society for Mass Spectrometry*, 1999. 10(1): p. 1-8.
64. Paizs, B. and S. Suhai, *Towards understanding the tandem mass spectra of protonated oligopeptides. 1: Mechanism of amide bond cleavage*. *Journal of the American Society for Mass Spectrometry*, 2004. 15(1): p. 103-113.

CURRICULUM VITAE

PERSONAL INFORMATION

Name-Surname : SILA KARACA
Date of Birth : 1980
Marital Status : Married
E-mail : karacasila@hotmail.com

EDUCATION

- Doctor of Philosophy (PhD) :** Izmir Institute of Technology, Department of Chemistry (2008-2014)
Dissertation Project: “A Computational Study on The Structures of Protonated Peptides”
- Master of Science (MSc) :** Izmir Institute of Technology, Department of Chemistry (2005-2008)
Dissertation Project: “The Study of Ground State and Excited State Properties of Cyanine Dyes by Using Computational Chemical Methods”
- Bachelor of Science (BSc) :** Izmir Institute of Technology, Department of Chemistry (1999-2005)
Dissertation Project: “The Structural and Electronic Properties of Non-Steroidal Anti inflammatory Drug Molecules”

WORK EXPERIENCES

Visiting Scientist: Eidgenössische Technische Hochschule Zürich (ETH Zürich), Switzerland, 04-25 June 2011
Research and Teaching Assistant: Izmir Institute of Technology, Department of Chemistry (2005-2014).

PUBLICATIONS

- 4) Ramsaywack, S.; **Karaca, S.**; Gholami, M.; McDonald, R.; Hampel, F.; Elmaci, N.; Lüthi, H.P.; Tykwinski, R.R.; “Donor and/or acceptor substituted expanded radialenes: Theory, synthesis, and properties” (Accepted, The Journal of Organic Chemistry)
- 3) Üçüncü, M.; Karakuş, E.; Kuş, M.; Akpınar, G. E.; Aksın-Artok, Ö.; Krause, N.; **Karaca, S.**; Elmacı, N.; Artok, L., “Rhodium- and Palladium-Catalyzed 1,5-Substitution Reactions of 2-En-4-yne Acetates and Carbonates with Organoboronic Acids”. The Journal of Organic Chemistry 76 (2011) 5959-5971.
- 2) **Karaca S.** and Elmaci N.; “A computational study on the excited state properties of a cationic cyanine dye: TTBC”: Computational and Theoretical Chemistry 964 (2011) 160–168.
- 1) **Karaca S.** and Elmaci N.; “A Theoretical Study on the Ground and Excited State Behaviors of TTBC Related Carbocyanine Dyes” Journal of Molecular Structure: THEOCHEM 915 (2009) 149–159.